AD-A175 410 BEHAVIOR OF SMOKES AND AGENTS DURING VARIABLE METEOROLOGICAL CONDITIONS OVER COMPLEX TERRAIN(U) SRI INTERNATIONAL MENLO PARK CA F L LUDWIG SEP 86 1/2

UNCLASSIFIED ARO-19630.8-GS DAAG29-83-K-0009 F/G 4/2 NL

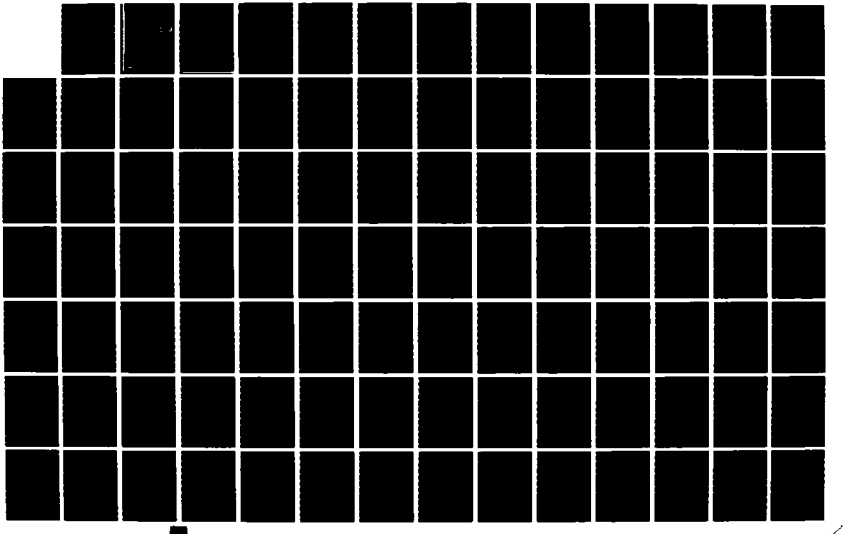

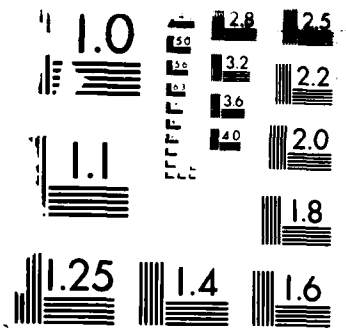

(2)

BEHAVIOR OF SMOKES AND AGENTS DURING VARIABLE METEOROLOGICAL CONDITIONS OVER COMPLEX TERRAIN

FINAL REPORT

September 1986

Prepared by:

F. L. Ludwig
Atmospheric Science Center

Prepared for:

U. S. Army Research Office
P. O. Box 12211
Research Triangle Park, NC 27709
Scientific Program Officer: Dr. Walter Bach

ARO Contract No. DAAG29-83-K-0009

SRI Project 5047

Approved by:

Robert S. Leonard, Executive Director
Radio Physics Laboratory
Engineering Research Group

SRI International
333 Ravenswood Avenue
Menlo Park, California 94025
415/859-6200

THE FINDINGS IN THIS REPORT ARE NOT TO BE CONSTRUED AS AN OFFICIAL DEPARTMENT OF THE ARMY POSITION, UNLESS SO DESIGNATED BY OTHER AUTHORIZED DOCUMENTS.

UNCLASSIFIED
SECURITY CLASSIFICATION OF THIS PAGE (When Data Entered)

AD-A175 410

REPORT DOCUMENTATION PAGE

READ INSTRUCTIONS BEFORE COMPLETING FORM

1. REPORT NUMBER	2. GOVT ACCESSION NO.	3. RECIPIENT'S CATALOG NUMBER
ARO 19630.8-GS	N/A	N/A

4. TITLE (and Subtitle)
BEHAVIOR OF SMOKES AND AGENTS DURING VARIABLE METEOROLOGICAL CONDITIONS OVER COMPLEX TERRAIN

5. TYPE OF REPORT & PERIOD COVERED
FINAL - 11/15/82 - 5/31/86

6. PERFORMING ORG. REPORT NUMBER
SRI Project 5047

7. AUTHOR(s)
F. L. Ludwig

8. CONTRACT OR GRANT NUMBER(s)
DAAG29-83-K-0009

9. PERFORMING ORGANIZATION NAME AND ADDRESS
SRI INTERNATIONAL
333 Ravenswood Avenue
Menlo Park, CA 94025

10. PROGRAM ELEMENT, PROJECT, TASK AREA & WORK UNIT NUMBERS
N/A

11. CONTROLLING OFFICE NAME AND ADDRESS
U. S. Army Research Office
Post Office Box 12211
Research Triangle Park, NC 27709

12. REPORT DATE
September 1986

13. NUMBER OF PAGES
133

14. MONITORING AGENCY NAME & ADDRESS (if different from Controlling Office)

15. SECURITY CLASS. (of this report)
Unclassified

15a. DECLASSIFICATION/DOWNGRADING SCHEDULE

16. DISTRIBUTION STATEMENT (of this Report)
Approved for public release; distribution unlimited.

17. DISTRIBUTION STATEMENT (of the abstract entered in Block 20, if different from Report)
NA

18. SUPPLEMENTARY NOTES
The view, opinions, and/or findings contained in this report are those of the author(s) and should not be construed as an official Department of the Army position, policy, or decision, unless so designated by other documentation.

19. KEY WORDS (Continue on reverse side if necessary and identify by block number)
wind field model
transport and diffusion model
fractals
smokes
lidar

20. ABSTRACT (Continue on reverse side if necessary and identify by block number)
A program was undertaken to develop a system of models for describing transport and diffusion of smokes and agents in complex terrain under time-varying meteorological conditions. The ultimate goal is to provide the probabilities for observing concentrations (point or path-integrated) above a specified threshold. The necessary components to achieve this goal are:

DD FORM 1 JAN 73 1473 EDITION OF 1 NOV 65 IS OBSOLETE

UNCLASSIFIED
SECURITY CLASSIFICATION OF THIS PAGE (When Data Entered)

(1) a wind model for describing airflow in complex terrain using minimal input data

(2) a transport and diffusion model capable of simulating transport and diffusion under non-steady, spatially-varying conditions

(3) a method for producing realistic small-scale variabilities in concentration distributions

(4) a method for estimating the required probabilities from the small-scale distributions.

The first two items have been completed and are described. The wind model FORTRAN source code is included in an appendix. The transport and diffusion model was previously described, and a Users' Guide has been issued separately.

Lidar cross-sections through smoke plumes were analyzed and a preliminary method for estimating the likelihood of finding a clear path through the plume is discussed.

The literature was reviewed to find a framework for generating the required small-scale concentration distributions. The concept of fractal dimension is shown to have considerable promise. An extensive literature review and bibliography on the subject of scaling, fractal dimension, and applications to atmospheric processes is included as an appendix. The report describes the research necessary to apply the identified concepts and to complete the desired system of models.

BEHAVIOR OF SMOKES AND AGENTS DURING VARIABLE METEOROLOGICAL CONDITIONS OVER COMPLEX TERRAIN

FINAL REPORT

September 1986

Prepared by:

F. L. Ludwig
Atmospheric Science Center
SRI International

Prepared for:

U. S. Army Research Office
P. O. Box 12211
Research Triangle Park, NC 27709
Scientific Program Officer: Dr. Walter Bach

ARO Contract No. DAAG29-83-K-0009

SRI Project 5047

Approved by:

Robert S. Leonard, Executive Director
Radio Physics Laboratory
Engineering Research Group

SRI International
333 Ravenswood Avenue, Menlo Park, California 94025
415/326-6299

ABSTRACT

A program was undertaken to develop a system of models for describing transport and diffusion of smokes and agents in complex terrain under time-varying meteorological conditions. The ultimate goal is to provide the probabilities for observing concentrations (point or path-integrated) above a specified threshold. The necessary components to achieve this goal are:

(1) a wind model for describing airflow in complex terrain using minimal input data

(2) a transport and diffusion model capable of simulating transport and diffusion under non-steady, spatially-varying conditions

(3) a method for producing realistic small-scale variabilities in concentration distributions

(4) a method for estimating the required probabilities from the small-scale distributions.

The first two items have been completed and are described. The wind model FORTRAN source code is included in an appendix. The transport and diffusion model was previously described, and a Users' Guide has been issued separately.

Lidar cross-sections through smoke plumes were analyzed and a preliminary method for estimating the likelihood of finding a clear path through the plume is discussed.

The literature was reviewed to find a framework for generating the required small-scale concentration distributions. The concept of fractal dimension is shown to have considerable promise. An extensive literature review and bibliography on the subject of scaling, fractal dimension, and applications to atmospheric processes is included as an appendix. The report describes the research necessary to apply the identified concepts and to complete the desired system of models.

CONTENTS

ILLUSTRATIONS

TABLES

I INTRODUCTION

This final report under ARO Contract No. DAAG29-83-K-0009 summarizes the most important results that have been obtained during the course of this project. Detailed information is provided about those research results that have not been described previously in detail, as was done in the publications listed in Appendix A. This is in accordance with the Army Research Office reporting instructions, which also require a statement of the problem that was studied, given in the following section. The required list of participants in the project is included as Appendix B; Appendices C and D present research accomplished on this project, but not previously reported in detail.

Although the complex terrain airflow model has been described in publications, no guide for users was published. Therefore, Appendix C has been included to provide an abbreviated set of instructions, and a listing of the source code for the wind model. Similarly, the review of the applications of fractals to the study of atmospheric processes, and the bibliography on the same topic that was compiled have not been published to date. For completeness, they appear here as Appendix D.

II STATEMENT OF THE PROBLEM STUDIED

This study has addressed the problem of modeling the behavior of smoke plumes or agents in complex terrain during temporally and spatially varying atmospheric conditions. In addition to the most probable concentration distributions, an analytical framework was sought which could be used to estimate the probabilities of encountering concentrations (point or path-integrated) exceeding some specified value. This is a large and difficult problem, and was divided into two major parts.

The first part of the problem was to develop a deterministic transport and diffusion model that could be used to describe the "average" or "most probable" concentration distribution. A non-steady-state Lagrangian model was developed that is very efficient and practical (Ludwig, 1984a,b, 1985a). However, it became apparent during the course of the project that transport and diffusion models were no better than the wind field and meteorological models used to provide inputs. Therefore, a wind model was developed to use minimal observational data, and to be efficient and practical enough for field use (Ludwig et al, 1985).

The more difficult part of the problem was to identify a framework that could be used to estimate concentration probabilities. Two complementary task efforts were undertaken to attack this problem. First, relevant data from past field tests and experiments were reviewed and analyzed in an attempt to develop a statistical framework that could be applied to real data to define the probability distributions that were sought. The existing data were not completely adequate for this purpose, but they were useful for developing promising approaches and determining what further information might be needed. This approach presumed that the spatial distribution of material could be known in considerable detail, a presumption that cannot in fact be met, except in the statistical sense. This leads to the second task where we sought methods to describe small scale variabilities and concentrations realistically and in a fashion consistent with the larger scale features determined by the general airflow and meteorological conditions.

In an effort to develop methods for defining relatively small-scale variabilities, the literature was reviewed, and a promising approach was identified. This approach is based on the use of fractals (e. g. Lovejoy and Schertzer, 1986). There is evidence that fractals can be used to provide the bridge between large-scale atmospheric features that can be modeled deterministically and the important statistical properties of the small-scale features that cannot. Although we have not been able to develop the complete statistical model, the information necessary to complete the work is clearly defined.

In summary, the complete system that we are seeking will include the following components:

(1) A wind field generator that can be used with limited inputs for generating 3-dimensional winds in complex terrain

(2) A deterministic transport and diffusion model that can define the general, most probable concentration distribution associated with the plume or cloud of material

(3) A statistical model for generating realistic small-scale concentration fluctuations within the plume

(4) A statistical model for calculating probability distributions for point or path-integrated concentrations given the small-scale concentration pattern.

Models were developed on this project that meet the requirements of the first two items in the above list. The problems associated with (4) were not completely solved, but enough progress was made so that it is believed that there will be no fundamental difficulties in arriving at such a model. The third item has proven to be by far the most difficult, but we feel that an approach involving the application of fractals can be successful in providing the necessary information.

The remainder of this report discusses significant research results. The findings with regard to the first two items above are more complete, and papers and reports have already been prepared describing results. The other, more preliminary findings, are described in somewhat more detail because papers have not yet been prepared. Although these findings are still preliminary and tentative, we believe them to be quite significant.

III SUMMARY OF IMPORTANT RESULTS

A. Wind Model Description

As noted before, transport and diffusion models require accurate specification of the wind fields. However, practical applications, especially those of greatest interest to the Army, will generally be restricted to the use of data from widely separated sites. Furthermore, applications in the field must usually make do with very restrictive computational facilities. The model described in Appendix C was developed to provide realistic wind fields using minimal input data, and calculations that do not require a mainframe computer.

The model is described completely (including a FORTRAN77 source code) in Appendix C. Very briefly, we attempted to devise a scheme that made maximum use of the available observations and theoretical and empirical relationships governing atmospheric processes. The result is essentially a wind interpolation scheme that is constrained to satisfy the principal of conservation of mass (nondivergence), and an empirical relationship based on conservation of energy. The latter constraint arises from the fact that there is a buoyant restoring force in a stably stratified atmosphere whenever air is displaced from its equilibrium position. Air displaced upward will be cooler (denser) than its surroundings and subjected to a downward force, while downward-moving air will have an upward restoring force. Work is required to move a volume of air from its equilibrium altitude, and this results in an increase in the potential energy of the displaced air. Hunt and Snyder (1980) reasoned that the potential energy was gained at the expense of the kinetic energy so that for a given wind speed and temperature stratification, there is some maximum upward displacement that can be induced by the underlying terrain. There will be a streamline for which this upward displacement causes the air to rise just to the height of a terrain obstacle. This is the "critical streamline." Air below this altitude passes around the obstacle. Air above the critical streamline flows over the obstacle. The validity of the critical streamline concept seems to be well supported by field experiments (Lavery et al, 1982; Egan, 1984).

In its original form, the critical streamline was used to determine whether or not a plume centerline would pass over a hill or around it. The model described in Appendix C has extended the concept to the definition of three-dimensional flow fields. It is used to define the shape of "flow surfaces" within which the streamlines lie. These surfaces may intersect a terrain feature or pass over it. If they intersect, the principle of mass conservation (nondivergence) forces the airflow to pass around the obstacle. This relatively simple concept has been implemented in the model described in Appendix C.

The model achieves the objectives of using minimal data. It uses a vertical profile of temperature. It is likely that data from my single Doppler acoustic sounder could be substituted for the temperature

profile, presuming that the vertical fluctuation in the wind can be related to the lapse rate. The model could be run with only a single wind input. However, much better results will be obtained if three or more surface observations are available so that estimates of upper-level winds can be obtained from the geostrophic and thermal wind relationships. Another alternative would be to have Doppler acoustic sounder, pilot-balloon, or other estimates of winds aloft. In summary, the model requires some estimate of stability stratification of the atmosphere and can use whatever wind observations are available. Obviously, its accuracy increases with more input data.

The objective of computational efficiency has been met. The samples given in Appendix C required only about 15 seconds of central processing unit (CPU) time on a VAX 11/782 computer. The practicality of the model is demonstrated by the fact that it has been incorporated into a larger code being developed at the U.S. Army's Atmospheric Sciences Laboratory at White Sands, New Mexico (Dr. R. Meyers, personal communication, 1986). It is understood that this latter application is on an IBM-AT computer.

B. Transport and Diffusion Model

The transport and diffusion models developed on this project have been described elsewhere. Two versions have been written. The first version was written in BASIC for use on an Apple-II or IBM-PC (Ludwig, 1984). That version was upgraded and converted to a second version in FORTRAN77. A complete users' guide was prepared for the FORTRAN77 version as a Technical Project Report (Ludwig, 1985).

The transport and diffusion models were developed before the wind model described in the preceding section. As a result, they were designed to use the outputs from models that invoked only the mass-consistency constraint. Small computers were slower and had more severe memory constraints at the time the models were developed than they do now, so attempts were made to reduce the computations required for the wind fields. The method described by Ludwig and Byrd (1980) for exploiting the linear properties of mass-consistent wind models was employed so that most of the calculations could be done ahead of time on a large machine, and then used to generate the winds from linear combinations of those precalculated solutions. The speed and available memory of small computers is now such that the transport and diffusion models developed earlier should probably be modified so that the winds are calculated online, using the model described in the preceding section. Time was not available to make this modification, although it should not be particularly difficult.

The models use a Lagrangian puff approach to describe a continuous emission. Each puff has a bivariate Gaussian concentration distribution. The puffs are moved according to the winds at their centers. They expand according to the atmospheric stability at the time they are

advected. As expansion causes the puffs to overlap, they are combined to reduce required computation.

Concentrations over a grid of points at the surface are calculated hourly by summing the contributions from all puffs within about three standard deviations of the point. The usual assumptions of "reflection" at the surface are used.

Details of the theory and its implementation can be found in two publications prepared during the course of this contract (Ludwig, 1984, 1985).

C. Probability Analysis Framework for Point and Path Integrated Concentrations

The framework that has evolved for assessing probabilities of encountering various concentration levels (or path-integrated concentrations) is a three step process:

(1) Average (or most probable) concentration patterns are calculated from the deterministic wind and dispersion models described above

(2) A subgrid scale spatial concentration pattern is superimposed on the smooth pattern from Step 1

(3) Point or line-of-sight concentration probabilities are estimated either from repeated realizations of Step 2, or from values at similar locations or along similar paths from a single subgrid-scale pattern.

The generation of realistic concentration patterns appears possible by adapting existing methods for generating fields of specified fractal dimension (Pentland, 1984; Lovejoy and Mandelbrot, 1985; Medler, Gelberg and Burkhart, 1986; Wilson et al, 1986). As noted by Medler et al (1986), this requires knowledge of the fractal dimension of the patterns of smoke concentration in a plume. Securing this missing information will be a major research effort. Section III-D describes the required research program that was developed during this contract.

The relevance of fractals to this problem is described in Appendix D which reviews recent developments in the use of fractals to describe spatially inhomogeneous scalar and vector atmospheric fields. Several methods are described for estimating fractal dimensions and generating the corresponding fields. Since that review was written, other methods have been identified which seem even more suitable for the anisotropic atmospheric distributions (e.g. Wilson et al, 1986; Schertzer and Lovejoy, 1986).

Figure 1 shows an example of one approach that has been taken to estimate clear lines-of-sight from observed lidar cross-section data.

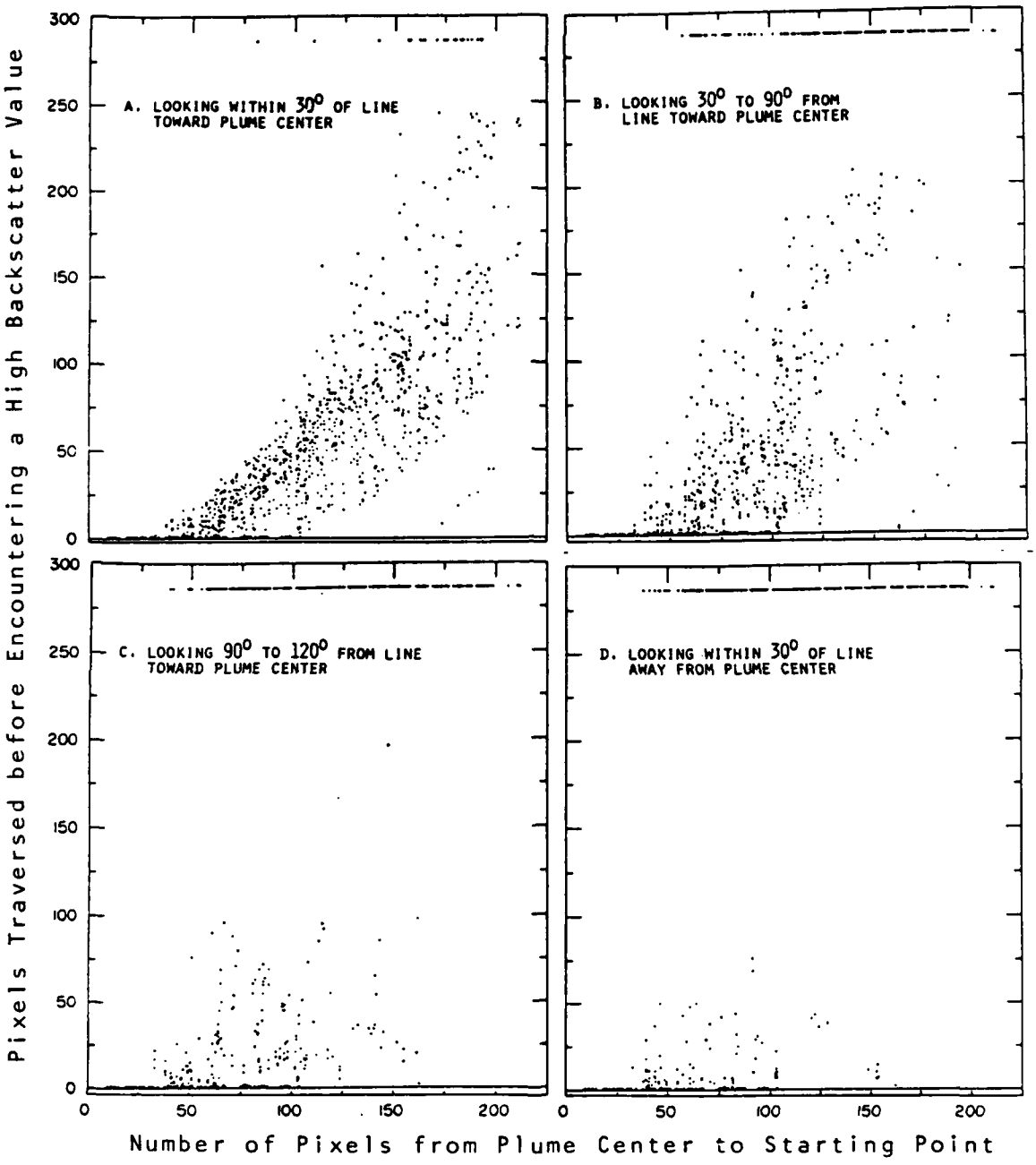

FIGURE 1 DISTANCES BEFORE ENCOUNTERING A HIGH-BACKSCATTER PIXEL AS A FUNCTION OF DISTANCE AND DIRECTION RELATIVE TO THE PLUME CENTER

Points have been plotted showing the distance from the center of mass of a smoke plume on the abcissa versus distance to the nearest pixel whose value (backscatter) is above a selected value. In Figure 1(a), only lines-of-sight that are within 30° of the direction toward the center of the plume have been included. The picture elements are nearly square, about 20 m on a side. The clustering of points at the top of the plot are those that pass unobstructed beyond the domain. As expected, the open paths are shorter near the center of the plume. Figures 1(b), 1(c), and 1(d) show that it is increasingly likely that a clear line-of-sight will be found in directions away from the plume center. The data in Figure 1 could be converted easily to a probability function. Backscatter values along the paths could also be summed to obtain path-integrated values whose probabilities of occurence could be estimated.

D. Description of Experimental and Theoretical Research Required to Implement a Fractal-Based Probabilistic Methodology

A research plan was developed during the course of this contract to provide a description of the effort needed to implement the probabilistic framework described above. Four main tasks are required:

(1) Acquisition of data

(2) Development or refinement of fractal analysis techniques

(3) Data analysis and interpretation using fractal methodology

(4) Adaptation of available techniques or development of new ones to generate fields with defined fractal and larger-scale characteristics.

These are discussed in more detail in the following sections.

1. Data Acquisition

Analysis techniques for digitized lidar cross-sections have been developed during the present effort. These techniques make use of a PDP 11/23 computer with a Peritech graphics package that facilitates visual interpretation of the results. The digitized lidar backscatter cross-sections have proven to be very amenable to automated analysis, but the currently available data have some shortcomings, namely:

- They have limited spatial resolution, about 15 to 30 m horizontal by 3 to 6 m vertical
- Most of the available data are for elevated, buoyant plumes and far downwind distances.

The first shortcoming is not fundamental and could be corrected by operating the equipment differently. It should be possible to achieve a resolution of about 3 x 3 m.

The second shortcoming requires appropriate field tests which meet the following criteria:

- Ground level release of smoke or other aerosol tracer material (not dense enough to be opaque to the lidar)
- Higher resolution backscatter cross sections measured at 2 or 3 distances closer (about 0.5 to 2.5 km) to the source than currently available data
- Several meteorological conditions represented, e.g. stable mornings, convective afternoons, neutral, transition periods, etc.

Airborne lidar systems are available that could collect digitized data with a resolution of a few meters as required (Uthe et al, 1980).

The availability and suitability of data from the stereo, multispectral imaging systems (formerly referred to as MIDAS) that are operated at some Smoke Week tests (e.g. Farmer et al, 1986) should also be explored. If these data could be used, they might obviate the need for the special tests described above, especially if it is possible to select planes through the smoke of different orientation so that the degree of isotropy of the patterns could be tested and some of the newer fractal analysis techniques (Schertzer and Lovejoy, 1986) could be applied.

The output velocity fields from large eddy computer simulations are another potential source of valuable information. However, there are some significant difficulties involved with using these data. Foremost among these is the problem of storing and retrieving the massive volume of results that are generated, i.e. literally millions of numbers for every few seconds of simulated time. Although this approach seems attractive because of the ability to generate true ensembles of cases, it is not clear that the problems are surmountable. If the data were usable, "experiments" could be conducted to cover a variety of conditions, e.g.:

- Different sizes and shapes of initial particle clouds
- Continuous releases in a field with mean transport
- Different locations if an inhomogeneous field is used.

Such computer experiments have the potential to identify relationships between observable patterns of smoke diffusion and the characteristics of atmospheric turbulence. Chorin's (1982) analysis of the evolution of the vorticity field associated with a bent vortex tube provides considerable encouragement for this kind of analysis.

2. Develop Fractal Analysis Methods for Inhomogeneous and Anisotropic Fields

Only two of several available fractal estimation methods have been developed and used during the current research effort, and those two methods were used under the assumption that the processes were isotropic. Lovejoy and Schertzer (1986) have recently pointed out the importance of anisotropy in the atmosphere. Some of the methods available for estimating fractal dimensions are:

(1) A subcell counting method (e.g. Mandelbrot, 1975; Ludwig and Nitz, 1986)

(2) An average power spectrum method (e.g. Pentland, 1984)

(3) A method based on the probability distribution of the differences in the variable versus separation distance (e.g. Schertzer and Lovejoy, 1983)

(4) A method based on the relationship between the area and the perimeter of regions enclosed by isopleths (Lovejoy and Mandelbrot, 1985)

(5) A method for estimating "elliptical fractal dimension" (Lovejoy and Schertzer, 1986) using a variation of the subcell counting method (Schertzer and Lovejoy, 1986).

This is a rapidly evolving area of research and it will be essential that new methods be examined for applicability as they are developed. The fifth method listed above shows considerable promise because of its ability to describe anisotropic features. It appears to be particularly applicable to 3-d data like those from the stereo imaging systems.

3. Data Analysis and Interpretation with Fractal Methods

Although several of the methods discussed above should be mathematically equivalent, there are some differences that arise from the way that they are applied, so a comparison of results is warranted. The most important of the differences is between the cell counting method and the others. In the isotropic case, the cell counting method defines a fractal dimension for a topologically one-dimensional surface, the isopleth. It is thought that the intersection of a surface and a plane has a fractal dimension one less than that of the surface itself (Mandelbrot, 1975) so it would be easy to reconcile the two approaches except that isopleths tend to be arranged in concentric patterns about the plume center. Therefore, the fractal dimensions of high-valued isopleths will be more representative of the interior of the plume than are the fractal dimensions of the lower value isopleths. The other methods will have to be applied to fairly large subregions of the plume in order to have samples that are sufficiently large to characterize the

probability functions or spectral densities. These subregions are likely to cut across a range of isopleth "rings".

The discussion of possible methodological differences in the preceding section points out the potential for differences from one part of a plume to another. Without systematic examination, it is not clear whether or not these differences will be found. At first, it seems as though clean air entrainment at the edge of a plume might lead to a different pattern than in the interior. However, this may only cause differences in the amplitude of fluctuations, but their spatial pattern may be the same. Stated differently, the slope of the spectral density function may be the same although the amplitudes may be larger at the edge than in the middle.

During periods of fumigation or lofting, part of the plume will be in a stable layer and part in a more turbulent zone. Differences, especially in the nature of any anisotropic effects are quite likely and should be investigated.

The overall dimension of the plume almost certainly will set some upper limit on the range over which scaling occurs. As noted earlier, there are apt to be differences between the vertical and the horizontal. The relationships between scaling range and plume dimension should be examined.

Lidar cross sections taken through the widely dispersed plumes in convective boundary layers have a very different appearance from the more compact plumes found when there is less convective activity. It is not certain whether or not these cases have a different fractal dimension, but at the very least, it seems reasonable to assume that the "spheroscale"* will be changed by the presence or absence of convection.

If one assumes that the eddy scales affect the patterns of smoke distribution within a plume, then there is reason to believe that there will be variations with vertical position in the mixed layer. Near the upper and lower boundaries of the convective mixing layer, vertical motions are inhibited, so local patterns may be vertically compressed. One obvious objective of an analysis of the vertical changes in fractal dimension within the mixing layer would be to see if the spheroscale is a function of the mixing height. An even more important objective would be to relate the properties of smoke patterns to the statistics of the eddy motions from large eddy simulation and field experiments.

---

*"Spheroscale" is the term used by Lovejoy and Schertzer (1986) for the scale at which the characteristic vertical and horizontal dimensions of the pattern are equal.

From the practical standpoint, an ability to relate the fractal properties of smoke distributions to the prevailing meteorology would be most important. It is doubtful that this could be done for the complete range of meteorological conditions because of limitations on the conditions under which lidar data can be collected. However, there already exists a body of data covering a broad range of atmospheric stability, wind speed and surface heating conditions. Future experiments should extend these to other conditions and various positions within the mixed layer.

If recent studies of turbulent diffusion modeling can serve as a guide, then mixing depth (H), Monin-Obhukov length (L), convective scaling velocity (w_*), friction velocity (u_*), wind fluctuations (σ_θ and σ_w) and eddy heat flux are good candidate parameters for characterizing the meteorological conditions. For this reason, it would be preferable to use data sets for which the appropriate special corollary meteorological measurements were available. However, such is not always the case, so it will often be necessary to estimate the appropriate parameters from more conventional observations by following quidelines such as those suggested by Holtslag et al (1985) or Hanna (1984).

4. Develop Appropriate Fractal Simulation Methods

The next step in the process will be to take the relationships gleaned from the analysis described in the preceding section and use it as the basis for specific fractal generation algorithms. It is not necessary to develop entirely new approaches, but rather to use the fractal characteristics derived from analysis and interpretation with existing methods (e.g. Lovejoy and Mandelbrot, 1985; Norton, 1982; Voss, 1982; Wilson et al, 1986). It will be necessary to superimpose the fractal patterns on the general distributions of concentration, such as the frequently used Gaussian distribution.

A problem may be encountered if fractal characteristics vary over the area of a plume, as preliminary analysis suggests may be the case. Most existing image generation algorithms have only to deal with patterns and textures that have reasonably well defined edges rather than smooth transitions from one to another. The random cylinder method of Lovejoy and Mandelbrot (1985) appears promising if modified to use elliptical cross-sections to account for anisotropy. The parameters of the random generating function would be functions of location allowing for the desired smooth transitions.

Once the appropriate spatial patterns can be generated, it will be possible to combine them with the results from more conventional models (e.g. complex terrain airflow and nonsteady state transport and diffusion models) to generate more realistic spatial distributions of concentration. These distributions can, in turn, serve as a basis for estimates of the probability of exceeding specified point or path integrated concentrations. Under the assumption that patterns remain "frozen" for

time periods of a few seconds, estimates could be derived for the probability that a given path integrated concentration would not be exceeded over some short time interval.

REFERENCES

Chorin, A. J., 1982: "The Evolution of a Turbulent Vortex," Commun. Math. Phys., 83, 517-535.

Egan, B., 1984: "Transport and Diffusion in Complex Terrain (Review)," Bound. Lay. Meteorol., 30, 3-28.

Farmer, W. M., V. E. Bowman, and J. Steedman, 1986: "Evaluation of System Performance in Smoke and Obscurant Environments (Smoke Week VIII Test Plan)," Sci. Tech. Corp., Los Cruces, NM 88005, 23 pp.

Hanna, S., 1984: "Concentration Fluctuations in a Smoke Plume," Atmos. Environ., 18, 1091-1106.

Holtslag, A. A. M., S. E. Gryning, J. S. Irwin, and B. Silvertsen, 1985: "Parameterization of the Atmospheric Boundary Layer for Air Pollution Dispersion Models," preprint 15th International Tech. Meeting on Air Pollution Modeling and Its Applications (sponsored by NATO), St. Louis, Missouri, April.

Lavery, T. F., A. Bass, D. G. Strimaitis, A. Venkatram, B. R. Greene, P. J. Drivas, and B. A. Egan, 1982: "EPA Complex Terrain Model Development, First Milestone Report--1981," U.S. Environmental Protection Agency Report 600/3-82-036, 331 pp.

Lovejoy, S. and B. B. Mandelbrot, 1985: "Fractal Properties of Rain, and a Fractal Model," Tellus, 37A, 209-232.

Lovejoy, S. and D. Schertzer, 1986: "Scale Invariance, Symmetries, Fractals, and Stochastic Simulations of Atmospheric Phenomena," Bull. Amer. Meteorol. Soc., 67, 21-32.

Ludwig, F. L., 1984a: "Transport and Diffusion Calculations During Time- and Space-Varying Meteorological Conditions Using a Microcomputer," J. Air Poll. Cont. Assoc., 34, 227-237.

Ludwig, F. L., 1984b: "Efficient Models of Smoke Behavior During Varying Meteorological Conditions," EOSAEL/TWI Conference, Las Cruces, NM (November).

Ludwig, F. L., 1985: "User's Guide for a Model of Airflow and Diffusion In Complex Terrain (MADICT)," Tech. Report 1, Army Research Office Contract DAAG29-83-K-0009, SRI International, Menlo Park, CA, 163 pp.

Ludwig, F. L., and G. Byrd, 1980: "A Very Efficient Method for Deriving Mass Consistent Flow Fields from Wind Observations in Rough Terrain," Atmos. Environ., 14, 585-587.

Ludwig, F. L., R. M. Endlich, and K. C. Nitz, 1985: "Use of Mass and Energy Conservation Principles for Wind Interpolation in Complex Terrain," Proc. 6th EOSAEL/TWI Conference, Las Cruces, NM, 3-5 December.

Ludwig, F. L. and K. C. Nitz, 1986: "Analysis of Lidar Cross-Sections to Determine Spatial Structure of Material in Smoke Plumes," Smoke/Obscurants Symposium X, Harry Diamond Labs, Adelphi, MD (April).

Ludwig, F. L., K. C. Nitz, and A. J. Valdes, 1984: "Techniques for Studying the Spatial Distribution of Clear Patches in Smoke Plumes," Smoke/Obscurants Symposium VIII, Vol. 1, Smoke PM, Aberdeen MD, 231-241.

Mandelbrot, B. B., 1975: "On the Geometry of Homogeneous Turbulence, with Stress on the Fractal Dimension of the Iso-Surfaces of Scalars," J. Fluid Mech., 72(part 2), 401-416.

Medler, C. L., L. M. Gelberg, and R. P. Burkhart, 1986: "Graphical Realization of Turbulent Smoke Plumes on the Pixar," Smoke/Obscurants Symposium X, Harry Diamond Lab, Adelphi, MD (April).

Norton, A., 1982: "Generation and Display of Geometric Fractals in 3-D," Computer Graphics, 16, 61-67.

Pentland, A. P., 1984: "Fractal-Based Description of Natural Scenes," IEEE Trans on Pattern Anal. and Mach. Intell., PAMI-6, 661-674.

Schertzer, D. and S. Lovejoy, 1986: "Rain and Clouds as Anisotropic, Scaling, and Turbulent Cascade Processes," Submitted to J. Geophys. Res.

Uthe, E. E., N. B. Nielsen, and W. L. Jimison, 1980: "Airborne Lidar Plume and Haze Analyzer (ALPHA-1)," Bull. Amer. Meteorol. Soc., 61, 1035-1043.

Voss, R. F., 1982: "Fourier Synthesis of Gaussian Fractals 1/f Noises, Landscapes, and Flakes," Manuscript IBM Thomas J. Watson Research Center, Yorktown Heights, NY 10598, 21 pp.

Wilson, J., S. Lovejoy, and D. Schertzer, 1986: "Physically Based Cloud Modelling by Scaling Multiplicative Cascade Processes," paper presented at Workshop on Scaling, Fractals and Nonlinear Variability in Geophysics, McGill University, Montreal, Quebec, Canada, 25-29 August 1986.

Appendix A

LIST OF PUBLICATIONS
RESULTING FROM THIS PROJECT

LIST OF PUBLICATIONS RESULTING FROM THIS PROJECT

Ludwig, F. L., 1983: "Microcomputer Modeling of Transport and Diffusion for Chemical Defense Applications," Proc. 1983 Chemical Research and Development Center Scientific Conference on Chemical Defense Research.

Ludwig, F. L., 1983: "Modeling Concepts Suitable for Use with Small Computers in the Field to Obtain Descriptions of Transport and Diffusion During Time- and Space-Varying Meteorological Conditions," Proc. Smoke/Obscurants Symposium VII, Vol. I, 255-267.

Ludwig, F. L., 1984: "Transport and Diffusion Calculations During Time- and Space-Varying Meteorological Conditions Using a Microcomputer," J. Air Poll. Cont. Assoc., 34, 227-232.

Ludwig, F. L., K. C. Nitz, and A. D. Valdes, 1984: "Techniques for Studying the Spatial Distribution of Clear Patches in Smoke Plumes," Proc. Smoke/Obscurants Symposium VIII, Vol. 1, C.A. Deepak, editor, PM Smoke/Obscurants Report DRCPM-SMK-T-001-84, 231-241.

Ludwig, F. L., K. C. Nitz, and A. D. Valdes, 1984: "Spatial Fluctuations of Concentration in Smoke Plume Cross-Sections," Preprints Fourth Joint Conf. on Applications of Air Pollution Meteorology (Portland, OR, 15-19 October), American Meteorological Society, Boston, MA, 51-59.

Ludwig, F. L., 1984: "Two Efficient Models of Smoke Behavior in Uneven Terrain During Temporally Varying Meteorological Conditions," Proc. 5th Annual EOSAEL/TWI Conference, Las Cruces, NM, 27-29 November.

Ludwig, F. L., 1985: "Users' Guide for a Model of Airflow and Diffusion in Complex Terrain," Technical Report 1, ARO Contract DAAG29-83-K-0009, SRI International, Menlo Park, CA, November, 163 pp.

Ludwig, F. L., 1985: "Inclusion of Buoyancy Forces and Energy Considerations in Mass-Consistent Wind Interpolation Schemes," Presented at Seventh Symposium on Atmospheric Turbulence and Diffusion, Boulder, CO, November.

Ludwig, F. L., R. M. Endlich, and K. C. Nitz, 1985: "Use of Mass and Energy Conservation Principles for Wind Interpolation in Complex Terrain," Proc. for 6th EOSAEL/TWI Conference, Las Cruces, NM, 3-5 December.

Ludwig, F. L. and K. C. Nitz, 1986: "Analysis of Cross-Sections to Determine Spatial Structure of Material in Smoke Plumes," Proc. Smoke/Obscurants Symposium X, Harry Diamond Laboratories, Adelphi, MD 22-24 April.

Ludwig, F. L., 1986: "Incorporation of the Critical Streamline and Mass Conservation Principles in an Efficient 3-D Wind Interpolation Model," to appear in the Summary Volume of Joint Interagency Propulsion Committee Flow Modeling Workshop to be held 29-30 September at Vandenberg Air Force Base.

Appendix B

LIST OF PARTICIPATING SCIENTIFIC PERSONNEL

PARTICIPATING SCIENTIFIC PERSONNEL

F. L. Ludwig, Staff Scientist (meteorologist)

H. S. Javitz, Director, Statistical Information Management Department

C. M. Ablow, Staff Scientist (mathematician)

R. M. Endlich, Senior Research Meteorologist

B. P. Eynon, Statistician

D. H. Kleiner, Senior Information Specialist

J. D. Lee, Scientific Programmer

C. Maxwell, Statistical Analyst

B. M. Morley, Atmospheric Physicist

K. C. Nitz, Scientific Programmer/Analyst

G. A. Pierce, Senior Research Engineer

R. M. Redmond, Research Analyst

A. D. Valdes, Senior Operations Analyst

Appendix C

WIND MODEL INCORPORATING THE CRITICAL STREAMLINE CONCEPT

I INTRODUCTION

As a general rule, sites from which wind observations are available are widely separated. If the atmosphere is reasonably well mixed and the terrain is flat, simple interpolation techniques can be used to estimate winds at any given location between the observing sites. There are many applications for which wind fields obtained by simple interpolation techniques are not adequate. Any application that involves the calculation of fluxes and concentrations will suffer if the wind field has appreciable divergence. The most common of such applications is in the modeling of transport and diffusion. A divergent wind field can completely obliterate the effects of turbulent diffusion, chemical reactions, and even transport in such models.

When complex terrain and stable atmospheric stratifications are introduced, simple interpolation schemes can be quite misleading. Some improvements can be achieved by invoking the principle of conservation of mass to produce nondivergent wind fields, but there still remains the question of whether air will flow over, or around an obstacle. The result obtained by a transport and diffusion model is very dependent upon the choice that is made. The effects extend beyond determining which areas are affected by a plume; the magnitude of the effects is also determined by the wind field. For example, a plume that impacts a hill will produce much greater ground level concentrations than one that passes to one side and stays well above the surface. There is an obvious need for wind interpolation schemes that can estimate winds on a three-dimensional grid, especially objective methods with few "adjustable constants" and modest computational requirements.

An ideal approach would invoke all the laws of thermodynamics and fluid motion in the interpolation process. In essence, this would be a planetary boundary layer model that incorporated all the available observations. It is likely that it would be at least as complicated as existing planetary boundary layer models, so that it could not be widely used with inexpensive machines. This paper limits itself to a more modest approach. The principle of conservation of mass (nondivergence) has been invoked in several wind interpolation schemes (e.g., Sherman, 1978; Dickerson, 1978; Bhumralkar et al., 1980; Goodin et al., 1980; and Endlich et al , 1982). The next logical step seems to be the incorporation of conservation of energy to account for the changes in potential energy with vertical motion when the atmosphere is stably stratified.

Current approaches to wind field interpolation involve two steps. First, winds are estimated at the points in a 2- or 3-dimensional grid by some standard, unconstrained interpolation technique. The second step is to adjust this initial wind field so that it satisfies some specified constraints. The initial wind field is typically obtained by linear interpolation, inverse distance (or inverse distance squared) weighting or a Gaussian weighting scheme. Most commonly, the constraints involve conservation of mass. Sherman (1978) and Bhumralkar et al (1980) both further constrain the adjustment so that it represents a

"minimum" change in the initial field required to reduce the divergence (and convergence) below some specified level. Endlich (1967) has a more general technique where the initial wind fields can be adjusted to satisfy some specified fields of divergence and vertical vorticity component. These approaches provide a useful starting point. Effects of stable stratification on air flow are discussed in the next section to provide the rationale for the method described later.

II BUOYANCY EFFECTS

The following discussion deals with those cases where potential temperature increases with height, i.e., $\partial\theta/\partial z>0$. Furthermore, we shall only deal with the situations where the atmospheric processes are approximately adiabatic. Thus, the following discussion assumes that no condensation or evaporation takes place and the time scales are of the order of a few hours or less, so that there will be a buoyant restoring force whenever the air is displaced from its equilibrium position. Air displaced upward will be cooler (denser) than its surroundings and subjected to a downward force. Downward moving air will be warmer with an upward restoring force. In either case, work is required to move a volume of air from its equilibrium altitude, so there is a positive change in the potential energy of the displaced air.

If we assume that the displacements are small enough so that the higher order effects can be ignored (i.e., that the lapse rate is constant over the displacement distance), then the restoring force is proportional to the temperature difference between the displaced parcel and its environment, which in turn is proportional to the displacement distance (Δz) and the difference between the ambient lapse rate (γ) and the adiabatic (γ_d). The corresponding acceleration (force per unit mass) can be written as follows (e.g., Holmboe et al , 1948).

$$\frac{d^2z}{dt^2} = \frac{g}{T}(\gamma - \gamma_d)\,\Delta z = \frac{g\,\Delta z}{T}\frac{\partial\theta}{\partial z} \tag{1}$$

The change in potential energy is obtained by integrating the above expression with respect to z over the complete displacement distance. This results in the following expression for the acquired potential energy per unit mass (E):

$$E = \frac{2g}{\bar{T}}(\gamma - \gamma_d)(\Delta z)^2 = \frac{2g}{\bar{T}}(\Delta z)^2\frac{\partial\theta}{\partial\theta} \tag{2}$$

where g is the acceleration due to gravity and $\bar{T}$ is the average temperature (°K) through the layer encompassed by Δz .

Steady-state Lagrangian plume models have invoked energy considerations in the concept of a critical dividing streamline height in order to develop simple descriptions of plume behavior around terrain obstacles in a stably stratified atmosphere (e.g., Lavery et al , 1982). McNider et al (1984) attribute this concept to Hunt and Snyder (1980). The critical streamline height (H_c) is the height at which the kinetic energy of the flow exactly matches the potential energy gained by raising the air to the top of the obstacle. Air above this height goes over the obstacle. Below the critical streamline height, the air goes around the obstacle, providing that wind speed increases with height. The governing relationship can be written

$$\frac{1}{2} U_c^2 = \frac{g}{\bar{T}} \int_{H_c}^{Z} (Z - z) \frac{\partial \theta}{\partial z} dz \tag{3}$$

The left side is the kinetic energy (per unit mass) of the flow at the height of the critical streamline. The right side is the potential energy (per unit mass) gained in lifting the air from the critical streamline height to the height of the top of the obstacle (Z). If the vertical temperature gradient is constant between H_c and Z, then H_c can be expressed in terms of the bulk Froude number:

$$H_c = Z(1 - Fr) \tag{4}$$

where

$$Fr = \frac{U_c}{Z} \left(\frac{g}{\bar{T}} \frac{\partial \theta}{\partial z} \right)^{-1/2} \tag{5}$$

For our purposes, it is more useful to restate this equivalence of potential and kinetic energy in terms of a critical height, Z_{max}, the highest height to which the air at height z could be propelled by the local wind speed (u) against the local $\partial\theta/\partial z$. That critical height is given by

$$Z_{max} - z = u \left(\frac{g}{\bar{T}} \frac{\partial \theta}{\partial z} \right)^{-1/2} \tag{6}$$

III MASS CONSERVATION

As noted earlier, mass-conserving wind interpolation schemes obtain an "initial guess" and then adjust that guess to remove the divergence. An initial guess for the winds above the surface are more difficult to

An initial guess for the winds above the surface are more difficult to obtain. Sherman (1978) used the shape of any measured wind profile (when available) to extrapolate upward throughout the region. When no observed profile was available, Sherman assumed a linear variation of wind with height. Endlich et al. (1982) assumed a uniform wind at the top of the domain. They derived that wind from the surface pressure field, using the geostrophic wind relationship (see e.g., Holmboe, 1948). More recent versions of the model (Endlich and Lee, 1983) use both surface temperature and pressure observations with both the geostrophic and thermal wind relationships to provide upper level wind estimates. The most recent version of this work is designed to use Doppler acoustic sounder wind profiles with the geostrophic/thermal wind estimate to obtain a spatially varying wind field at the top of the domain (Nitz et al., 1985). Winds at intermediate levels are derived from a log-linear interpolation between the surface wind estimate and that for the top of the domain.

In addition to the differences in the way in which the initial wind field estimate is obtained, there are also major differences in the coordinate systems that are used. For example, Sherman (1978) uses standard rectangular coordinates while Endlich et al. (1982) use a curvilinear coordinate system that depends on the shape of the upper and lower boundaries of the domain. Ludwig (1985) has reviewed the main features of these two modeling approaches and discussed some of the difficulties of incorporating energy conservation schemes into the rectangular coordinate system. The following discussion is limited to curvilinear coordinates.

Bhumralkar et al. (1980) used a curvilinear coordinate system to simplify the treatment of the lower boundary in their mass-consistent wind interpolation scheme. That work was modified by Endlich et al. (1982) and later by Nitz et al. (1985). This latter version (Nitz et al., 1985) forms the basis for the mass conservation aspects of the model described here. In this model, the flow is assumed to take place within specified surfaces. We will refer to these as "flow" surfaces. They are similar in many respects to the "sigma" surfaces used by others (e.g. Bhumralkar et al, 1980), but they differ in at least one important respect. The flow surfaces can intersect the underlying terrain. Wherever they intersect the terrain, the wind will be zero, and mass conservation will require that there be flow around the obstacle. The computational scheme allows for these internal boundaries.

Before proceeding to discuss how the topography of the flow surfaces is determined, we will review the methods by which non-divergence is achieved and vertical velocity is calculated. Inasmuch as the surfaces are assumed to conform with the streamlines, vertical velocity (in a rectangular system) is given by

$$w = \vec{V} \cdot \nabla z_{sfc} \tag{7}$$

where $\vec{V}$ is the horizontal velocity and ∇z_{sfc} is the slope of the flow surface. If the slope is not too great, then the velocity in the flow surface can be used.

Nitz et al (1982) replaced the wind component variables with the following

$$u^* = u\Delta z$$
$$v^* = v\Delta z \tag{8}$$

where Δz is the average separation between the surface and the next higher and next lower ones. At the bottom and top of the domain, Δz is half the distance to the adjacent surface. If the vertical motions caused by the slope of the flow surfaces are small compared to the horizontal motions, the continuity equation can be written

$$\frac{\partial u^*}{\partial x} + \frac{\partial v^*}{\partial y} = 0 \quad . \tag{9}$$

The iterative scheme for producing nondivergence has been described by Endlich (1984) and Nitz et al (1985).

IV DEFINING FLOW SURFACES

In essence, the objective is to define a coordinate system that is more-or-less flow following. Once this is done, then there is no reason why the coordinate surfaces may not intersect the terrain in areas where there is flow around an obstacle. The winds are set to zero for any grid points that lie below the local terrain height. As noted before, this approach has been implemented in a recent version of the model (Nitz et al., 1985). In order to make the method work properly, there must be some way to determine where a given sigma surface intersects the terrain. Nitz et al. (1985) provide only subjective guidance. The critical streamline concept, as stated in Equation (6) seems to provide a basis for an objective approach to the determination of sigma surface shapes. That equation can be rewritten

$$\left[z_{max} - z_o\right]_{\sigma=const.} = \bar{V}_o \left(\frac{g}{\bar{T}_o} \frac{\partial \theta}{\partial z_o}\right)^{-1/2} \tag{10}$$

where the subscript "o" refers to conditions at the lowest geometric altitudes found on a particular flow surface. These conditions are then used in Equation (10) to determine z_{max}, the highest altitude that that particular flow surface will reach. In order to implement a system based on this approach, the following steps are used:

(1) The lowest and highest surface elevations within the model domain are identified.

(2) The top of the domain (i.e. the top of the boundary layer) over the lowest terrain elevation is defined and the vertical extent of the domain at that point is divided into uniformly separated layers.

(3) A value of $\bar{V}_o$ is estimated from the initially interpolated wind field for each flow level; the estimate is derived from an average of the interpolated winds at the appropriate levels above each of the five lowest grid points. Other parameters in Equation (10) are estimated from a temperature sounding, although Doppler acoustic sounder observations of σ_w or climatological information could probably be used.

(4) Equation (10) is solved for z_{max} for each flow surface; these define the heights of the flow surfaces at the x,y coordinates of the highest topographical point.

(5) The value z_{max} calculated for each flow surface is adjusted (beginning at the second from topmost level) so that the lower surfaces do not approach too close to the surfaces above them; surfaces are currently, restricted from being closer than half their separation above the lowest terrain elevations.

(6) A second, upward pass is made through the z_{max} list to insure that each upper surface is parallel to the lower surfaces, or approaches closer to them over the high terrain; this prevents the effects of the underlying terrain from penetrating upward through stable layers.

(7) The heights of flow surfaces above the remaining grid points are interpolated linearly according to the surface terrain height.

(8) Mass-consistent wind field adjustments are made using a model like that of Nitz et al. (1985).

The procedure outlined above assumes a positive (stable) vertical potential temperature gradient throughout the depth of the modeling domain. If this is not the case, then the flow surfaces will be terrain following, i.e. z_{max} is equal to the difference in elevation between highest and lowest surface points. A standard interpolation scheme in rectangular coordinates is applied to obtain a "first-guess" wind field that is used for the flow surface definition procedure just described.

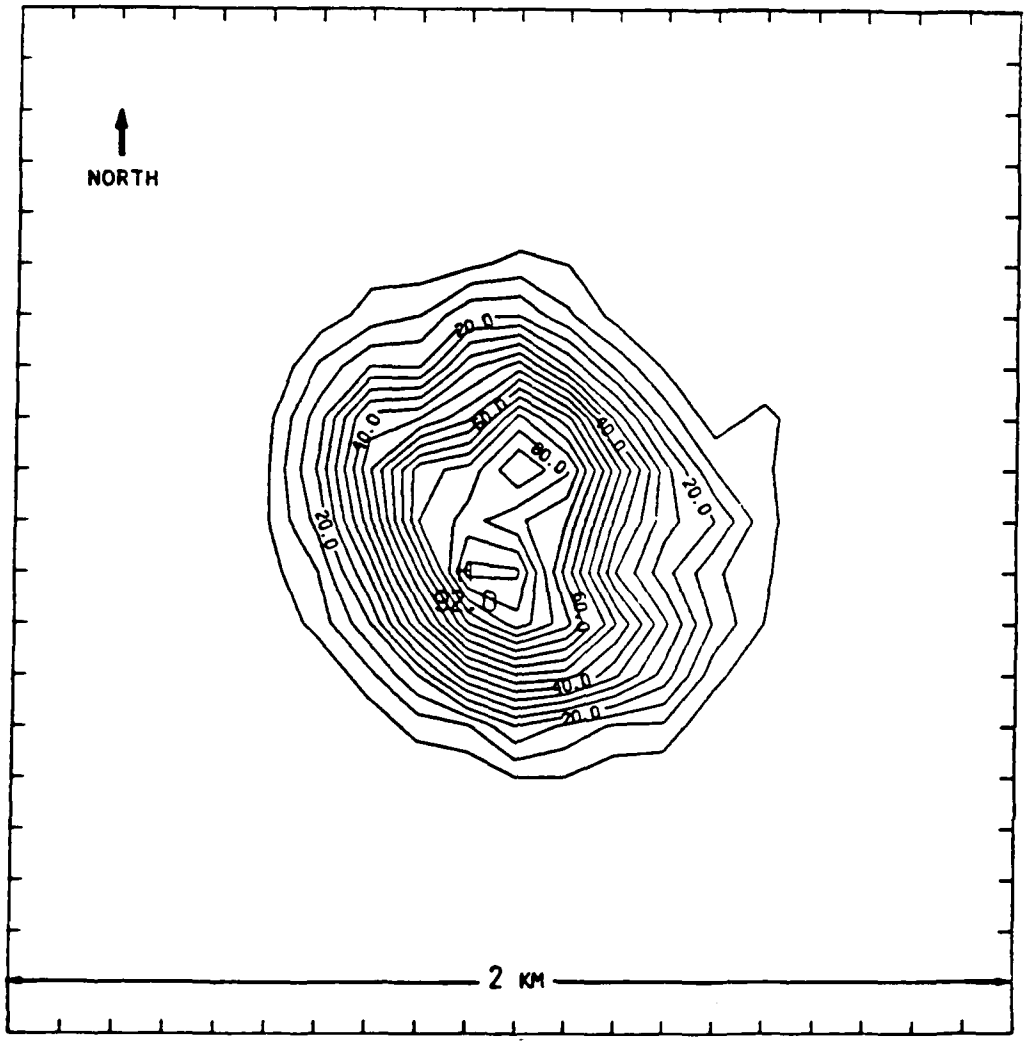

FIGURE C-1. Terrain used for wind model test.
(Contour interval is 5 meters)

V TEST RUNS

The above procedure has been implemented and preliminary tests have been completed. A 21 x 21 x 6 grid, extending from the surface to about 200 m was superimposed on the terrain shown in Figure C-1. Two cases were studied. In both cases, a steady south wind was used with wind speeds of 1 m s^{-1} near the surface and 2 m s^{-1} at an altitude of 300 m above the plain on which the 92 m hill is located. This wind profile was used with a neutral, adiabatic lapse rate and with a stable, inversion rate of 3.6 x 10^{-2}°C m^{-1}.

Figure C-2 shows the shape of lowest flow surface for the two tests. The upper part of the figure shows that the flow surface parallels the topography throughout the region for the neutral case. The stable stratification has a modest rise as the terrain is approached, but the surface does not pass over it. This forces a flow around the hill as can be seen in Figure C-3. For the neutral case, the vectors are all parallel, indicating flow over the hill. Some slowing of the wind arises over the elevations near 40 m because of the logarithmic interpolation upward from the zero wind speed at the surface. The flow around the hill is clearly evident in the stable case at this altitude.

Figure C-4 shows the results at the level 80 m above the terrain surrounding the hill. Again, the neutral case shows wind directions to be unaltered by the hill. The speed reductions are less pronounced than at the lower altitude. The next highest flow surface (at 80 m above the flat terrain) just barely clears the top of the hill for the stable case and causes deviations in the flow so that it is nearly parallel to the topographical contours in some places. There is even some flow through the small col at the crest of the hill.

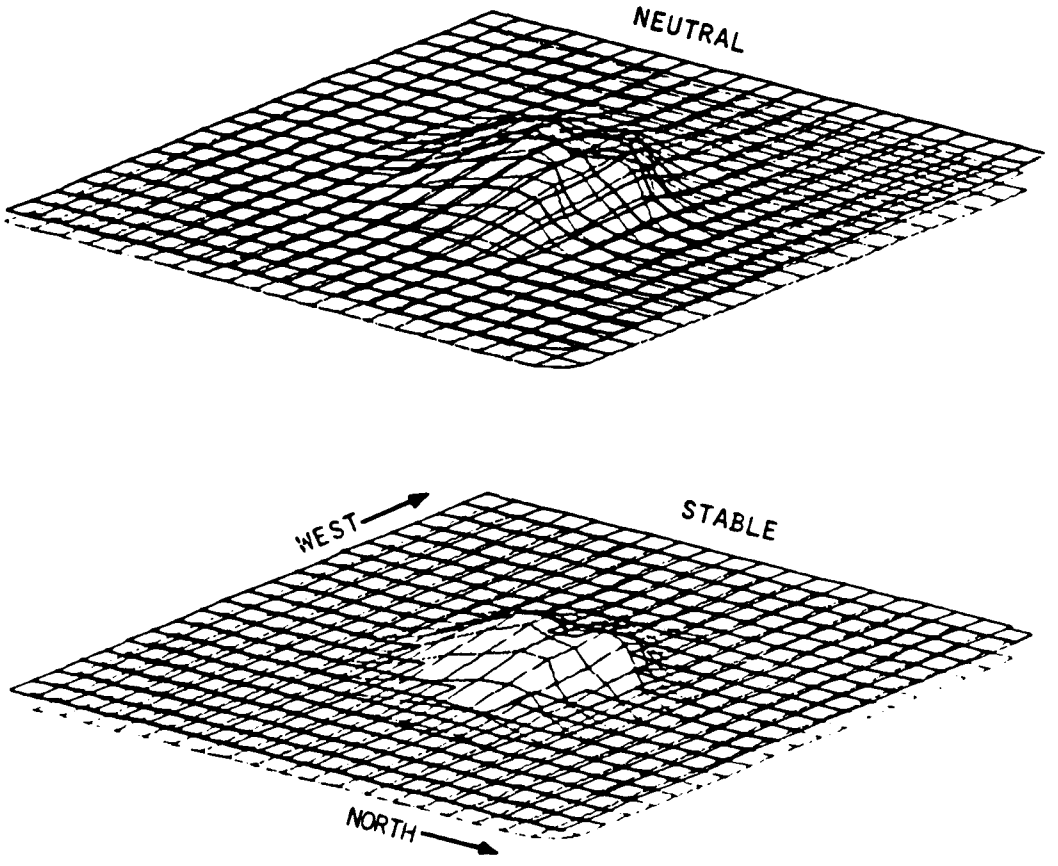

FIGURE C-2. Schematic representation of the terrain and lowest flow surface for neutral and stable test cases.

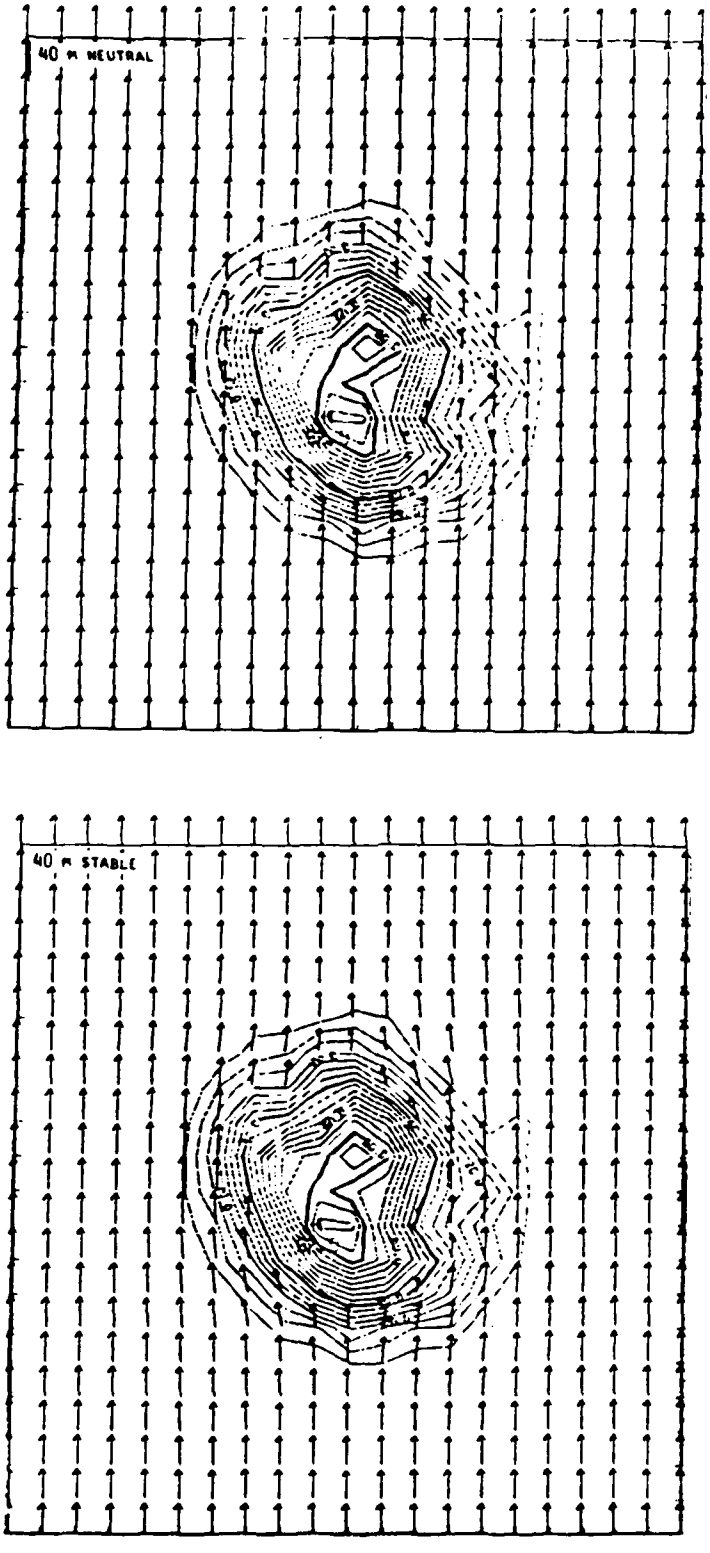

FIGURE C-3. Flow at 40 m above the surrounding terrain for neutral and stable test cases.

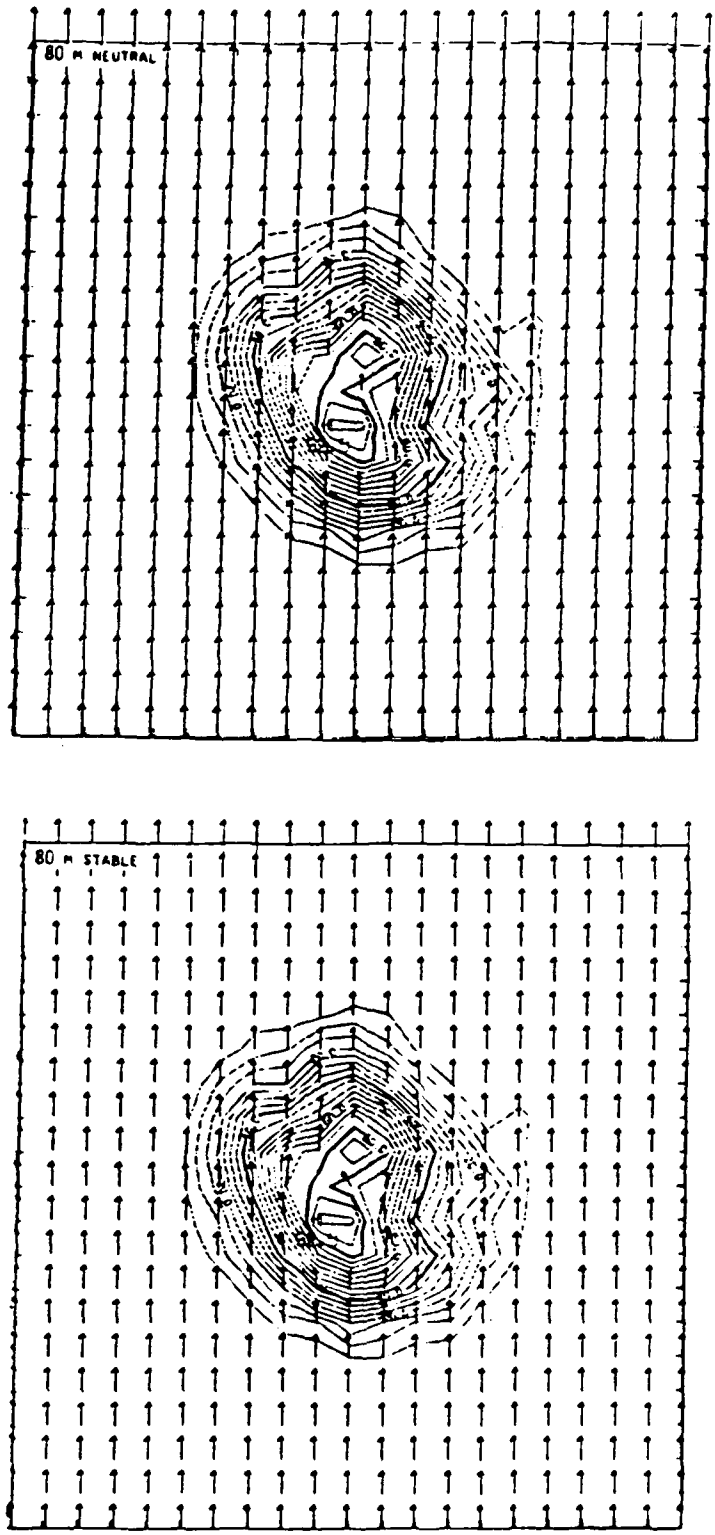

FIGURE C-4. Flow at 80 m above the surrounding terrain for neutral and stable test cases.

Figure C-5 shows two cross sections through the center of the hill from south to north. The vertical scale is magnified by a factor of 3 relative to the horizontal, the same difference in scale is used for the w (vertical) and v (northward) components of the plotted vectors. The terrain following streamlines are clearly evident in the neutral test results. However, the stable test shows streamlines rising only slightly.

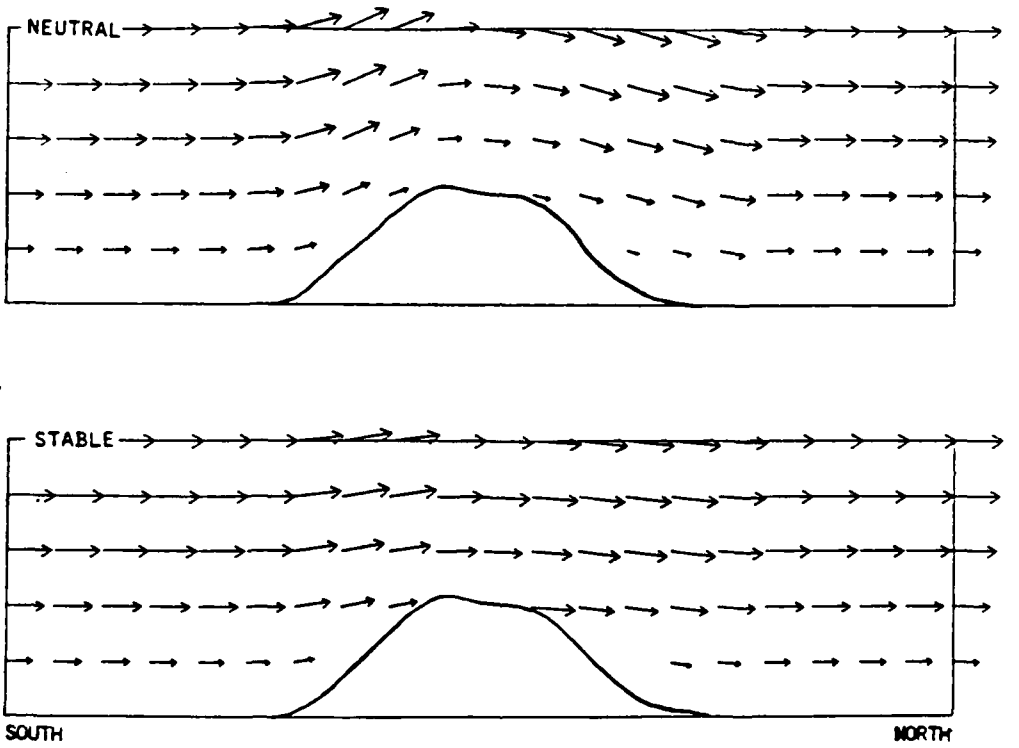

FIGURE C-5. Flow in cross-sections through the center of the hill for neutral and stable test cases.

The results obtained here required only about 15 seconds cpu time on a VAX 11/782 computer. The storage requirements are mostly accounted for by 7 floating point arrays that must be at least as large as the grid used (21 x 21 x 6 in this case), and 4 two-dimensional arrays (21 x 21 for these tests). There are also numerous smaller arrays, but overall the computational requirements are limited enough that the technique should be usable in real time on machines that are small enough for routine field use.

The model discussed has not been fully tested. We hope to compare model outputs with observations from regions of varying topographical

complexity, and to use the results to refine the model. The model already shows considerable promise for practical applications. The early results are certainly qualitatively realistic. The data requirements are modest, and it is likely that a single Doppler acoustic sounder could provide the information necessary to run the model, although more inputs would improve the results.

The FORTRAN77 source code for this model follows the references. Tables C-1 through C-3 summarize the input data file requirements. They also show the logical unit designations from which the various inputs are read. Outputs (and the corresponding logical units for the output files) are summarized in Tables C-4 and C-5. Grid sizes are defined in data statements in the code.

Most of the input variable requirements are self-explanatory. However, if the critical streamline feature is not invoked, the user should be familiar with the parameters that are used to set the shape of the flow surfaces.

The thickness of the boundary layer and the shape of the top (whether curved or flat) are important factors in producing the characteristics of the nondivergent flow. In many instances, radiosonde data that describe the boundary layer top (BLT) are not available. In such cases, average thickness over the grid (taken from experience or climatological values) and a slope factor are used to specify the height of the BLT at each grid point. The height of the BLT at a particular grid point is denoted by H; the average thickness of the boundary layer in the area of interest is denoted by $\bar{H}$; h_g is the terrain height at the grid point; h_o is the terrain height at a reference point where $H = \bar{H} + h_o$; and k is the slope factor. Then the basic equation is

$$H = \bar{H} + kh_g + (1 - k)h_o$$

If $k = 0$, the boundary layer top is flat; if $k = 1$, the top parallels the terrain. Values between zero and one give intermediate slopes, and values greater than one give slopes steeper than the terrain slope. Negative values give slopes opposite to the terrain slopes. Figure C-6 shows typical boundary layer tops for a nighttime case ($\bar{H} = 500$ m, $k = 0.2$) and a daytime case ($\bar{H} = 1500$ m, $k = 0.8$). The parameters $\bar{H}$ and k can be treated as functions of time of day and season.

In the vicinity of coastlines the BLT usually has a general slope from ocean to higher values over land in the daytime, with the reverse situation at night. To account for this, two additional parameters are used to specify a tilt to the BLT. One parameter specifies the west-to-east difference in the thickness of the boundary layer across the grid, and the other parameter specifies the south-to-north difference. There is also a parameter for the minimum thickness of the boundary layer over isolated mountain peaks. These five parameters are used in an iterative solution for the height of the BLT (Endlich and Lee, 1983).

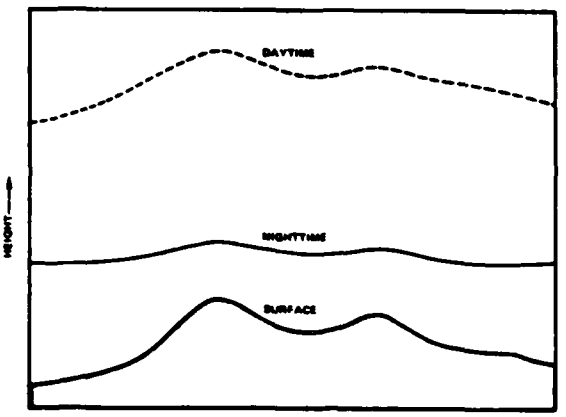

FIGURE C-6. Typical configurations of the boundary-layer top for daytime and nighttime.

Table C-1

TOPOGRAPHIC ELEVATION INPUTS
(Logical Unit 11)

Format	Variables
8F10.2	((HTCRS(I,JR), I=1,MCRS), JR=NCRS,1,-1)
8F10.2	((HTMED(I,JR), I=1,MMED), JR=NMED,1,-1)
8F10.2	((HTFIN(I,JR), I=1,MFIN), JR=NFIN,1,-1)

HTCRS,HTMED,HTFIN--elevations of points in coarse, medium and fine grids. HTMED read only if more than one grid used. HTFIN read only if more than two grids used.

MCRS,NCRS--number of coarse grid points in x,y directions (=21 x 21).

MMED,NMED--number of medium grid points (21 x 21).

MFIN,NFIN--number of fine grid points (21 x 21).

Table C-2

VARIABLES READ BY WIND MODEL FROM LOGICAL UNIT 12

Format	Variables	Subroutine
*	AUTHK, SLFAC, STNK, DNI, BLGRX, BLGRY	MAIN
*	TERLIM, IDATE, IHOUR	MAIN
*	(LPRNT(K), K=1, NLVL	MAIN
*	NUMDOP	DOPSIG
*	(STAID(IT), STLT(IT), STLN(IT), IT=1,NUMDOP)	DOPSIG
*	(NHTS, continued	
*	(DPHT(IT,LL), DPWD(IT,LL), DPWS(IT,LL), LL=1,NHTS), ISITE=1,NUMDOP)	DOPSIG
*	NUMNWS	WXANAL
*	(STAID(IT), STLT(IT), STLN(IT), PRESS(IT), TEMP(IT), WD(IT), WS(IT), IT=1,NUMNWS)	GEOSIG
*	NTSOND	WXANAL

AVTHK = average boundary layer thickness (m)
SLFAC = degree to which terrain is followed 0=flat, 1=follow
BLGRX, BLGRY = boundary layer gradient
TERLIM = intersection height with terrain

The above parameters used primarily when the stability option is not used. AVTHK defines heights of surfaces over low terrain, otherwise the values are overridden by stability method.

IDATE, IHOUR = date and hour for identification
LPRNT = levels to be printed have LPRNT=1
NUMDOP = number of Doppler sodars
STAID = Doppler station ID numbers (not used)
STLT, STLN = Doppler station latitude and longitude (decimal degree)
NHTS = number of elevations for Doppler input
DPHT, DPWD, DPWS = height (m), wind direction (deg), speed (m s^{-1})
NUMWS = number of sfc wx inputs
STAID = sfc station identification number (not used)
STLT, STLN = sfc station latitude and longitude
NTSOND = indicates if stability option used (=1) or not used (=0)

Note Units:

PRESS, TEMP = sfc station pressure ("Hg) and temperature (°F)
WD,WS = sfc station wind direction (decimal deg) and speed (m s^{-1})

Table C-3

TEMPERATURE SOUNDING INPUTS
(LOGICAL UNIT 13)

Format	Variables*	Subroutine
*	NHITES, ITYP	STRAT
*	(Z(I), T(I), P(I), I=1,NHIES)	STRAT

NHITES -- number elevations for inputs

ITYP -- type of inputs (see below)

Z,T,P -- height (m), temperature (°C), dθ/dz for ITYP=1

Z,T,P -- height (m), temperature (°C), pressure (mb) for ITYP=0

*Read only if NTSOND (Table C-2) is 1.

Table C-4

WIND COMPONENT OUTPUTS
(LOGICAL UNIT 33)

Format	Variables
1X,21I6	((U(I,J,L), I=1, NCOL), J=NROW,1,1-1)
1X,21I6	((V(I,J,L), I=1, NCOL), J=NROW,1,-1)
1X,21I6	((W(I,J,L), I=1, NCOL), J=NROW,1,-1)
	REPEATED FOR L=2,NLVL

U,V,W = wind components ($cm\ s^{-1}$)

NROW, NCOL, NLVL = number of rows, columns, and levels

Winds are for flat surfaces, at heights determined by flow surface heights above the lowest terrain.

Table C-5

FLOW SURFACE TOPOGRAPHY OUTPUTS
(LOGICAL UNIT 15)

Format	Variables
(1X,25F5.0)	(((RHS(IX,IY,L) + SFCHT(IX,IY), IX=1,21), IY-21,1,-1), L=1, 6)

RHS = height of flow surface relative to underlying terrain (m)

SFCHT = height of underlying terrain (m)

REFERENCES

Bhumralkar, C.M., R.L. Mancuso, F.L. Ludwig, and D.S. Renne', 1980: "A Practical and Economic Method for Estimating Wind Characteristics at Potential Wind Energy Conversion Sites," Solar Energy, 25, 55-65.

Dickerson, M.H., 1978: "MASCON--A Mass Consistent Atmospheric Flux Model for Regions with Complex Terrain," J. Appl. Meteorol., 17, 241-253.

Endlich, R.M., 1967: "An Iterative Method for Altering the Kinematic Properties of Wind Fields," J. Appl. Meteorol., 6, 837-844.

Endlich, R.M., 1984: "Wind Energy Estimates by Use of a Diagnostic Model", Boundary Layer Meteorol., 30, 375-386

Endlich, R.M. and J.D. Lee, 1983: "An Improved Diagnostic Model for Estimating Wind Energy," Final Report to Pacific Northwest Laboratory, Subcontract B-D5789-A-E, SRI International, Menlo Park, California 94025.

Endlich, R.M., F.L. Ludwig, C.M. Bhumralkar, and M.A. Estoque, 1982: "A Diagnostic Model for Estimating Wind at Potential Sites for Wind Turbines," J. Appl. Meteorol., 21, 1441-1454.

Goodin, W.R., G.J. McRae, and J.H. Seinfeld, 1980: "An Objective Analysis Technique for Constructing Three-Dimensional Urban-Scale Wind Fields," J. Appl. Meteorol., 19, 98-108.

Holmboe, J., G.E. Forsythe, and W. Gustin, 1948: "Dynamic Meteorology," John Wiley and Sons, New York, 378 pp.

Hunt, J.C.R. and W.H. Snyder, 1980: "Experiments on Stably and Neutrally Stratified Flow Over a Three-Dimensional Hill," J. Fluid Mech., 96, (Part 4), 671-704.

Lavery, T.F., A. Bass, D.G. Strimaitis, A. Venkatram, B.R. Greene, P.J. Drivas, and B.A. Egan, 1982: "EPA Complex Terrain Model Development, First Milestone Report--1981," U.S. Environmental Protection Agency Report 600/3-82-036, 331 pp.

Ludwig, F.L., 1985: "Inclusion of Buoyancy Forces and Energy Considerations in Mass-Consistent Interpolation Schemes," prepared for Stanford University Civil Engineering 299, (Prof. Robert Street), Stanford, CA (available from author), 26 pp.

McNider, R.T., K.E. Johnson, and R.W. Arritt, 1984: "Transferability of Critical Dividing Streamline Models to Larger Scale Terrain," Conference Volume--4th Joint Conference on Applications of Air Pollution Meteorology, American Meteorological Society, Boston, MA, J25-J27.

Nitz, K.C., R.M. Endlich, and F.L. Ludwig, 1985: "User's Guide for On-Line Software for Wind Field Analysis and Display," prepared for Pacific Gas and Electric Co., SRI International Project 7688, Menlo Park, CA 94025.

Sherman, C.A., 1978: "A Mass-Consistent Model for Wind Fields Over Complex Terrain," J. Appl. Meteorol., 17, 312-319.

FORTRAN SOURCE CODE

```
      PROGRAM     WND
C
C*************************************************************************
C
C**THIS FORM OF PROGRAM COMPLEX COMPUTES TOPOGRAPHICALLY INDUCED
C* WINDS BY MAKING THE ORIGINALLY ANALYZED WINDS NONDIVERGENT.
C       SIGMA SURFACES ARE DEFINED USING A CONCEPT ANALAGOUS TO
C       THE CRITICAL STREAMLINE WHEN THE ATMOS IS STABLY STRATIFIED.
C       THESE MODIFICATIONS ARE PRIMARILY CONTAINED IN SUBROUTINES
C       XTREM,STRAT,RESIG. SIGMA SURFACES CAN INTERSECT THE TERRAIN
C       RESULTING IN ZERO WINDS IN THE "UNDERGROUND CELLS"
C  THIS FORM ALSO REPLACES INWND WITH WXANAL WHICH READS IN WIND
C  SOUNDINGS AND NWS DATA  AND MAKES THE INITIAL WIND ANALYSIS.
C* THIS FORM USES DIRECT VECTOR ALTERATIONS IN SUBROUTINE BAL5.
C   OTHER NEW FEATURES INTRODUCED IN '84-'85 ARE:
C         WIND COMPONENTS AT SPECIFIED POINTS CAN BE HELD CONSTANT IN BAL5.
C                 BY R. ENDLICH,   F. LUDWIG, K. NITZ, C. MAXWELL
C                 SRI INTERNATIONAL
C                 333 RAVENSWOOD AVE MENLO PARK, CALIF 94025.
C                 PHONE (415) 859-3395 OR (415) 859-2915
      INTEGER DNI
      LOGICAL DBUG(15), KEY, UTMUSE
      DIMENSION B(25,25),LPRNT(10),IB(25,25),ZFLAT(6)
      COMMON/RARS/RHS(25,25,6)
      COMMON/CSFC/SFCHT(25,25),SIGMA(6)
      COMMON/UARS/U(25,25,6),UA(25,25,6),V(25,25,6),VA(25,25,6)
      COMMON/WARS/W(25,25,6),WA(25,25,6)
      COMMON/PARMS/ZTOP,DS,DSIGMA,NLVLM1,XHT1,XHT2,X1,Y1,
     1  X2,Y2,UG,VG,RATIO,TDSI
      COMMON /CVOS/ RCM,RMF,IV,DSCRS,IXCRS,JYCRS,IXMED,JYMED,
     +  IXFIN,JYFIN
      COMMON/CTOP/ MCRS,NCRS,MMED,NMED,MFIN,NFIN,NGRID
      COMMON /LIMITS/NCOL,NROW,NLVL,NCOLM1,NROWM1,
     $                LOWIX(5,3),LOWIY(5,3),SFCMAX
      COMMON /BLHT/ BLT(25,25),HSITE, AVTHK, SLFAC,STHK,BLGRX,BLGRY
      COMMON /SITE/ IXS, JYS, THSITE, IGRID
      COMMON /ANCHOR/ SLAT, SLNG ,UTMUSE
      COMMON /GROUND/ TERLIM
      COMMON /PRLIM/, I1, I2
C  SET LIMIT ON NO. OF ITERATIONS IN SUBR. BAL5
      DATA NIT/15/
C  SET NUMBER OF VERTICAL LEVELS
      DATA NLVL/6/
C  SET SIGMA LEVELS (VERTICAL COORDINATES)
      DATA SIGMA/0.0, 0.2, 0.4, 0.6, 0.8, 1.0/
C  SET NO. OF GRIDS TO BE USED
      DATA NGRID/1/
C  SET NO. COLS,ROWS FOR COARSE,MED,FINE GRIDS
      DATA MCRS/17/,NCRS/13/,MMED/21/,NMED/21/
      DATA MFIN/21/,NFIN/21/
C SET GRID INTERVALS IN KM
      DATA DSCRS/0.5/, DSMED/0.25/, DSFIN/0.1/
C SET RATIOS OF GRID INTERVALS, COARSE TO MED. , MED. TO FINE
      DATA RCM/2.0/, RMF/2.5/
C  SET HEIGHT (METERS) OF ANCHOR POINT (REFERENCE POINT)
      DATA HSITE/838.0/
C  SET LATITUDE, LONGITUDE OF ANCHOR POINT (UTMUSE=.FALSE), OR
C  UTM COORDINATES OF ANCHOR PT (UTMUSE=.TRUE.)
      DATA SLAT/4290.0/, SLNG/522.0/ ,UTMUSE/.TRUE./
C  SET ANCHOR POINT LOCATION (IX,JY) IN EACH GRID
      DATA IXCRS/ 1/,JYCRS/ 1/,IXMED/7/,JYMED/ 5/
      DATA IXFIN/7/,JYFIN/5/
C  SET LIMITS FOR PRINTING COLUMNS
      DATA I1/1/, I2/17/  ,KEY/.TRUE./
C
C   DBUG CALLS PRINTS IN  BAL5    DOPSIG  GEOSIG    GPAN    RESIG
```

```
      DATA DBUG     /.FALSE.,    .FALSE., .FALSE., .FALSE., .FALSE.,
C
C                        SETBLT   SETMAT   STRAT    TOPO     WXANAL
     $                  .FALSE., .FALSE., .FALSE.,  .FALSE.,  .FALSE.,
C
C                         XTREM    MAIN PROG  REINT    LEVWND 1ST ESTIMATES
     $                   .FALSE.,  .TRUE.,    .FALSE.,  .FALSE., .TRUE./
C
C*  IN ALL ARRAYS POINT (1,1) IS AT SW CORNER.  X INCREASES TO EAST, Y
C    TO N. INDICES ARE I,J,K -(COL,ROW,LYR) WITH LIMITS NCOL,NROW,NLVL
C  UNITS USED IN COMPUTATIONS ARE M, G, SECONDS
      IF(DBUG(12)) PRINT 9013, MCRS,NCRS,MMED,NMED
      IF(DBUG(12)) PRINT 9014, DSCRS, DSMED, DSFIN
C  READ BOUNDARY LAYER VARIABLES (USED IN SETBLT)
C           READ(12,9022) AVTHK, SLFAC, STHK, DNI, BLGRX, BLGRY
      READ(12,*) AVTHK, SLFAC, STHK, DNI, BLGRX, BLGRY
      IF(DBUG(12)) PRINT 9025, AVTHK, SLFAC, STHK, DNI, BLGRX, BLGRY
C  UNITS ARE METERS
C  READ TERRAIN INTERSECTION (USED IN TOPO), DATE, HOUR
C           READ (12,9023) TERLIM, IDATE, IHOUR
      READ (12,*) TERLIM, IDATE, IHOUR
      IF(DBUG(12)) PRINT 9026, TERLIM
      IF(DBUG(12)) PRINT 9027, IDATE, IHOUR
C* READ PRINT INDICATORS. TO PRINT LEVEL K USE LPRNT(K)=1.
C           READ(12,9030) (LPRNT(K),K=1,NLVL)
      READ(12,*) (LPRNT(K),K=1,NLVL)
      IF(DBUG(12)) PRINT 9035
      IF(DBUG(12)) PRINT 9030, (LPRNT(K),K=1,NLVL)
C  LOOP THRU NGRID SYSTEMS.
      DO 1040 IGRID=1,NGRID
        IF(DBUG(12)) THEN
              IF (IGRID .EQ. 2) PRINT 9005
              IF (IGRID .EQ. 3) PRINT 9006
        END IF
C   SET CONTROLS FOR PROPER GRID
      IF (IGRID .NE. 1) GO TO 11
      IXS=IXCRS
      JYS=JYCRS
      NCOL=MCRS
      NROW=NCRS
      DS=DSCRS
   11 CONTINUE
      IF (IGRID .NE. 2) GO TO 14
      IXS=IXMED
      JYS=JYMED
      NCOL=MMED
      NROW=NMED
      DS=DSMED
   14 CONTINUE
      IF (IGRID .NE. 3) GO TO 15
      IXS=IXFIN
      JYS=JYFIN
      NCOL=MFIN
      NROW=NFIN
      DS=DSFIN
   15 CONTINUE
C  READ TERRAIN HEIGHTS FOR ALL GRIDS USING TOPO
      NUM1=0
      IF (IGRID .EQ. 1) CALL TOPO(NUM1,DBUG)
      DS=DS*1.0E3
      NCOLM1=NCOL-1
      NROWM1=NROW-1
      NLVLM1=NLVL-1
      TDSI=1./(2.0*DS)
C SET BL TOP AND SIGMA SURFACES
      CALL TOPO(IGRID,DBUG)
```

```
C PRINT + PLOT SURFACE HEIGHT
      IF(DBUG(15)) PRINT 171
        DO 53 JP=1,NROW
        DO 53 IP=1,NCOL
              B(IP,JP)= SFCHT(IP,JP)
            IB(IP,JP)=JNINT(B(IP,JP))
  53  CONTINUE
      IF (DBUG(15)) THEN
        DO 54 JP=1,NROW
              JR=NROW+ 1-JP
  54          PRINT 9105, (IB(IP,JR),IP=I1,I2)
      END IF
C * * * *PLOT GEOMETRIC HEIGHTS OF  SELECTED SIGMA SURFACES
      DO 511  K=1,NLVL
      IF (LPRNT(K) .NE. 1) GO TO 511
      DO  627  JP=1,NROW
      DO 627 IP=1,NCOL
              B(IP,JP)= RHS(IP,JP,K)
            IB(IP,JP)=JNINT(B(IP,JP))
  627 CONTINUE
      IF(DBUG(15)) PRINT 571,K
      DO 628 JP=1,NROW
      JR=NROW+ 1-JP
  628 PRINT 9105, (IB(IP,JR),IP=I1,I2)
  511 CONTINUE
C* READ AND ANALYZE WIND DATA USING WXANAL
C* MAKE INITIAL WIND ANALYSIS ON MESH
      CALL WXANAL(IGRID,DBUG)
C * * * * * * *PLOT  OBSERVED VELOCITY COMPONENTS AT SELECTED LEVELS * *
      DO 211  K=1,NLVL
      IF (LPRNT(K) .NE. 1) GO TO 211
      DO 46 J=1,NROW
      DO 46 I=1,NCOL
        IB(I,J)=JNINT(U(I,J,K)*10.)
  46  CONTINUE
      IF(DBUG(15)) PRINT 271,K
      DO 56 JP=1,NROW
      JR=NROW+ 1-JP
   56 IF(DBUG(15)) PRINT 9105, (IB(I,JR),I=I1,I2)
   211 CONTINUE
      DO 212  K=1,NLVL
      IF (LPRNT(K) .NE. 1) GO TO 212
      DO 48 J=1,NROW
      DO 48 I=1,NCOL
        IB(I,J)=JNINT(V(I,J,K)*10.)
  48  CONTINUE
      IF(DBUG(15)) PRINT 272,K
      DO 58 JP=1,NROW
      JR=NROW+ 1-JP
   58 IF(DBUG(15)) PRINT 9105, (IB(I,JR),I=I1,I2)
   212 CONTINUE
      IF (IGRID.GT.1)  GO TO 226
C  COMPUTE VERTICAL MOTION W ALONG SIGMA SURFACES
      DO 220  K=2,NLVL
      DO 220  I=2,NCOLM1
      DO 220  J=2,NROWM1
      W(I,J,K)=0.0
      IF (RHS(I,J,K).LE.0.0) GO TO 220  !  FOR TERRAIN LIMIT
       HSIGE=SFCHT(I+1,J)+RHS(I+1,J,K)
       HSIGW=SFCHT(I-1,J)+RHS(I-1,J,K)
       HSIGN=SFCHT(I,J+1)+RHS(I,J+1,K)
       HSIGS=SFCHT(I,J-1)+RHS(I,J-1,K)
       DHDX=(HSIGE-HSIGW)*TDSI
       DHDY=(HSIGN-HSIGS)*TDSI
       W(I,J,K)=U(I,J,K)*DHDX+V(I,J,K)*DHDY
   220 CONTINUE
```

```
 226   CONTINUE
       IF (IGRID .EQ. 1) PRINT 9050
       IF (IGRID .EQ. 2) PRINT 9055
       IF (IGRID .EQ. 3) PRINT 9056
       IF(DBUG(15)) PRINT 9020
       IF(DBUG(15)) PRINT 3,(K, U(IXS,JYS,K), V(IXS,JYS,K),
     $              W(IXS,JYS,K),RHS(IXS,JYS,K),K=1,NLVL)
       DO 213  K=1,NLVL
       IF (LPRNT(K) .NE. 1) GO TO 213
       IF(DBUG(15)) PRINT 273,K
       DO 60  JP=1,NROW
       DO 60  IP=1,NCOL
        IB(IP,JP)=JNINT(W(IP,JP,K)*100.)
 60    CONTINUE
       IF(DBUG(15)) THEN
         DO 65  JP=1,NROW
         JR=NROW+ 1-JP
 65      PRINT 9105, (IB(IP,JR),IP=I1,I2)
       END IF
 213   CONTINUE
C
C CALL SUBROUTINE TO MAKE WINDS NONDIVERGENT
C
       CALL BAL5(NIT,DBUG)
       CALL LEVWND(DBUG,IGRID,ZFLAT)
C
C PLOT ADJUSTED VELOCITY COMPONENTS INTERPOLATED TO SELECTED LEVELS
C
       DO 611  K=1,NLVL
       IF (LPRNT(K) .NE. 1) GO TO 611
       DO 615 J=1,NROW
       DO 615 I=1,NCOL
         IB(I,J)=JNINT(UA(I,J,K)*10.)
 615   CONTINUE
       IF(DBUG(12))THEN
          PRINT 671,K
          DO 622 JP=1,NROW
               JR=NROW+ 1-JP
 622           PRINT 9105, (IB(I,JR),I=I1,I2)
       END IF
 611   CONTINUE
       DO 612  K=1,NLVL
       IF (LPRNT(K) .NE. 1) GO TO 612
       DO 616 J=1,NROW
       DO 616 I=1,NCOL
         IB(I,J)=JNINT(VA(I,J,K)*10.)
 616   CONTINUE
       IF(DBUG(12))THEN
          PRINT 672,K
          DO 624 JP=1,NROW
            JR=NROW+ 1-JP
 624        PRINT 9105, (IB(I,JR),I=I1,I2)
       END IF
 612   CONTINUE
       DO 641  K=1,NLVL
       IF (LPRNT(K) .NE. 1) GO TO 641
       DO 645 J=1,NROW
       DO 645 I=1,NCOL
         IB(I,J)=JNINT(WA(I,J,K)*10.)
 645   CONTINUE
       IF(DBUG(12))THEN
          PRINT 675,K
          DO 652 JP=1,NROW
               JR=NROW+ 1-JP
 652           PRINT 9105, (IB(I,JR),I=I1,I2)
       END IF
```

```
 641    CONTINUE
        IF (IGRID .EQ. 1) PRINT 9050
        IF (IGRID .EQ. 2) PRINT 9055
        IF (IGRID .EQ. 3) PRINT 9056
        IF(DBUG(12)) PRINT 2
        IF(DBUG(12)) PRINT 10,(K,UA(IXS,JYS,K),VA(IXS,JYS,K),
     $                 RHS(IXS,JYS,K),K=1,NLVL)
C
C--WRITE WNDS INTERPOLATED TO FLAT SFCS (OR 10M ABOVE TERRAIN FOR 1ST LVL)----
C
         DO 700 K=1, NLVL
           DO 690 J=1, NROW
            JR=NROW+1-J
 690       WRITE (3,9065) (NINT(100.*UA(I,JR,K)),I=1,NCOL)
           DO 695 J=1, NROW
             JR=NROW+1-J
 695       WRITE (3,9065) (NINT(100.0*VA(I,JR,K)),I=1,NCOL)
            DO 697 J=1, NROW
              JR=NROW+1-J
 697       WRITE (3,9065) (NINT(100.0*WA(I,JR,K)),I=1,NCOL)
 700    CONTINUE
C
C----------WRITE WINDS ON SIGMA SFCS-----------------------
C
C         DO 750 K=2, NLVL
C          DO 990 J=1, NROW
C            JR=NROW+1-J
C990       WRITE (3,9065) (NINT(100.*U(I,JR,K)),I=1,NCOL)
C          DO 995 J=1, NROW
C            JR=NROW+1-J
C995       WRITE (3,9065) (NINT(100.0*V(I,JR,K)),I=1,NCOL)
C          DO 997 J=1, NROW
C            JR=NROW+1-J
C997       WRITE (3,9065) (NINT(100.0*W(I,JR,K)),I=1,NCOL)
C750    CONTINUE
C-------------------------------------------------------------------------
 1040   CONTINUE
    2   FORMAT  (/'  FINAL RESULTS AT ANCHOR PT'/2X,'K       UA        VA        W
     +        REL. HTS.'/)
    3   FORMAT(1X,I2,2X,2F10.2,F11.3,F10.1)
   10   FORMAT (1X,I2,2X,2F10.2,F10.1)
  171   FORMAT (1H1,'    TERRAIN HEIGHT,  METERS,  NORTH ROW FIRST'/)
  271   FORMAT(1H1,'  U COMPONENT DECIMETERS/SEC, LVL = 'I4/)
  272   FORMAT(1H1,'  V COMPONENT DECIMETERS/SEC, LVL = 'I4/)
  273   FORMAT(1H1,'  W, CM/SEC , LVL ='I3/)
  571   FORMAT (1H1,'   HEIGHT ABOVE TERRAIN, M,  LVL='I3/)
  671   FORMAT (1H1,'   ADJUSTED U COMPONENT, ',
     $             'DECIMETERS/SEC,  LVL='I3/)
  672   FORMAT (1H1,'   ADJUSTED V COMPONENT,',
     $             ' DECIMETERS/SEC,  LVL='I3/)
  675   FORMAT (1H1,'   ADJUSTED W COMPONENT,',
     $             ' DECIMETERS/SEC,  LVL='I3/)
 9005   FORMAT (1H1,' **BEGIN COMPUTATIONS FOR MEDIUM GRID**'/)
 9006   FORMAT (1H1,' **BEGIN COMPUTATIONS FOR FINE GRID**'/)
 9013   FORMAT (/' COARSE GRID E-W'I5,' S-N'I5,'  MEDIUM GRID E-W'I4,'  S-N
     +  'I4/)
 9014   FORMAT (/' GRID INCREMENTS IN KM, COARSE='F4.1,' MED.='F4.1,'
     +  FINE='F4.1/)
 9020   FORMAT (/'  ORIGINAL U, V, W, REL. HTS AT ANCHOR PT.'/)
 9022   FORMAT (F10.1,F10.2,F10.1,I5,2F7.1)
 9023   FORMAT (F10.1,2I8)
 9025   FORMAT (//'   AVER. BNDY. THICKNESS IN M ='F8.1,
     +  'SLOPE FACTOR FOR BL TOP='F4.1,' MIN. THICKNESS='F7.1,
     +  /' DAY1 NITE2 INDICATOR='I3,' B LYR GRADIENT TO EAST, M='F7.1
     +  ' TO NORTH =' F7.1/)
 9026   FORMAT (/'    TERRAIN INTERSECTION WILL OCCUR FOR HTS
```

```
     +  ABOVE'F6.1,' METERS'/)
 9027   FORMAT (/'   DATE ='I8,'    HOUR ='I4/)
 9030   FORMAT (12I5)
 9035   FORMAT (/'   INDICATORS, LPRNT(K),FOR PRINTING FIELDS'/)
 9046   FORMAT (1H1,'    V COMP. AT LEVEL 3  '/)
 9050   FORMAT (1H1,'    COARSE GRID')
 9055   FORMAT (1H1,'     MEDIUM GRID')
 9056   FORMAT (1H1,'   FINE GRID')
 9060   FORMAT (I5,E10.1,I5)
 9065   FORMAT (1X,21I6)
 9100   FORMAT (/5X,22F5.0)
 9105   FORMAT (/1X,25I5)
        STOP
          END
C
C*******************************************************************************
C
      SUBROUTINE BAL5(NITER,DBUG)
C*****THIS IS VERSION 11, OCTOBER '84.
C  THIS ROUTINE BALANCES DIVERGENCE TO VALUES IN ARRAY DD (OR
C  TO DDIJ=0) AND VORTICITY TO ARRAY VT(I,J).
C  FOR WIND SPEED IN MPS. DIV AND VORT ARE SCALED TO UNITS
C  10 -6 SEC-1. THE METHOD USES DIRECT VECTOR ALTERATIONS.
C  THIS FORM FOR RECTANG GRID OMITS TRIG FUNCTIONS.
C  THE FLUX FORMULATION IS USED FOR FINITE DIFFERENCES. FOR SIGMA LAYERS
C  COMPUTE NON-DIV WINDS FOR WINDS WEIGHTED BY THICKNESS OF LAYER.
C  ASSUME SIGMADOT=0. INDICES IN ARRAYS (I,J,K) ARE I=COLUMN,
C  J=ROW, K=LEVEL; PT (1,1,1) IS AT SW CORNER AT GROUND.
C  FOR COMPUTATION BOXES, INDICES REFER TO SW CORNER OF BOX.
C  IVORT CONTROLS USE OF VORTICITY. IF=2 VORT IS NOT HELD
C  CONSTANT.
C  BY R.M. ENDLICH, SRI INTN'L, 1ST VERSION FOR LAYERS JUNE '82.
C
      LOGICAL DBUG(15),RYT3
      DIMENSION VT(25,25),DI(25,25),VO(25,25),U1(25,25),V1(25,25)
      DIMENSION UN(25,25),VN(25,25),THK(25,25),NEWLVL(5)
      DIMENSION IFXPT(25,25)
      COMMON /UARS/U(25,25,6),UA(25,25,6),V(25,25,6),VA(25,25,6)
      COMMON/PARMS/ZTOP,DS,DSIGMA,NLVLM1,XHT1,XHT2,X1,Y1,
     +             X2,Y2,UG,VG,RATIO,TDSI
      COMMON /LIMITS/NCOL,NROW,NLVL,NCOLM1,NROWM1,
     $               LOWIX(5,3),LOWIY(5,3),SFCMAX
      COMMON /SITE/ IXS, JYS, THSITE, IGRID
      COMMON /RARS/RHS(25,25,6)
      COMMON /PRLIM/ I1,I2
      DATA NEWLVL/2,6,3,4,5/
      DATA RYT3/.FALSE./
       IVORT=2    !  IGNORE VORTICITY
      IF(DBUG(1)) PRINT 9002
      GS=DS*1.0E-05
C  USE GRID SPACING IN 100'S OF KM.  DS IS IN M.
      GSI=10.0/GS        ! FOR PROPER SCALING
C  FOR RECTANGULAR GRID OMIT TRIG FUNCTIONS USED PREVIOUSLY
C  ASSIGN PTS WHERE INITIAL WIND ANALYSIS IS HELD FIXED
      IF (IGRID .NE. 1) GO TO 10   ! FOR COARSE GRID
      CALL SETMAT(0, IFXPT, NCOL, NROW)
C
C-----------IDENTIFY PTS NOT TO BE CHANGED---------------------
C       IFXPT(11,8)=1
  10  CONTINUE
      IF (IGRID .NE. 2) GO TO 15   ! FOR MEDIUM GRID
      CALL SETMAT(0, IFXPT, NCOL, NROW)
C       IFXPT(   ,   )= 1
  15  CONTINUE
C-------------------------------------------------------------------
C  PRINT POINTS WITH FIXED WINDS
```

```
C       DO 25 J=1,NROW
C       DO 25 I=1,NCOL
C         IF (IFXPT(I,J) .EQ. 1)  PRINT 9582, I,J
C 25    CONTINUE
C-----------------------------------------------------------------------
C  ARRAYS U,V,RHS ARE WRITTEN (COLS,ROWS,LEVELS)
C  TRANSFER WINDS TO 2D ARRAYS IN ORDER BOTTOM(LEV2), TOP,3,4,5
C
C       DO 800 NORDR=1,NLVL-1
C
C  INTERPOLATING IN VERTICAL TO GET 1ST GUESS FIELDS FOR LEVELS 3,4,5
C
C               L=NEWLVL(NORDR)
C               IF (NORDR.GE.3) CALL REINT(DBUG,L)
C-----------------------------------------------------------------------
C  NOT REINTERPOLATING FROM PREVIOUSLY BALANCED LEVELS
C
       DO 800 L=2,NLVL
C-----------------------------------------------------------------------
               DO 35 J=1,NROW
               DO 35 I=1,NCOL
                       UN(I,J)=U(I,J,L)
                       VN(I,J)=V(I,J,L)
  35           CONTINUE
       CALL SETMAT(0.0,DI ,NCOL,NROW)
       CALL SETMAT(0.0,VT ,NCOL,NROW)
       CALL SETMAT(0.0,VO ,NCOL,NROW)
C COMPUTE LAYER THICKNESS AND MULTIPLY WIND COMPONENTS
      DO 40 J=1,NROW
      DO 40 I=1,NCOL
        LA=L +1
        IF (LA.GT.NLVL) LA=NLVL
        HTA=RHS(I,J,LA)
        LB=L-1
        IF (LB.LT.1) LB=1
        HTB=RHS(I,J,LB)
        IF (HTB.LT.-1.0) HTB=-1.0
        THK(I,J)=0.5*(HTA-HTB)*0.01
C-------------------------------------------------------
       IF (THK(I,J).LE.0.) THK(I,J)=1.0  ! FOR NEG. RHS
C-------------------------------------------------------
C UNITS OF THICKNESS ARE HUNDREDS OF M FOR CONVENIENCE
C  SET INITIAL WINDS BEFORE ALTERATIONS
        U1(I,J)=UN(I,J)
        V1(I,J)=VN(I,J)
C  WEIGHT WINDS WITH THICKNESS OF LAYER
       UN(I,J)=U1(I,J)*THK(I,J)
       VN(I,J)=V1(I,J)*THK(I,J)
 40    CONTINUE
C       IF(DBUG(1)) PRINT 9520
C       DO 45 J=1,NROW
        JP=NROW+1-J
C 45    IF(DBUG(1)) PRINT 9102, (THK(I,JP),I=I1,I2)
C       COMPUTE ORIGINAL DIVERGENCE AND VORTICITY
       DO 170 J=1,NROWM1
       DO 170 I=1,NCOLM1
        UE=0.5*(UN(I+1,J)+UN(I+1,J+1))
        UW=0.5*(UN(I,J)  +UN(I,J+1))
        VSO=0.5*(VN(I+1,J)+VN(I,J))
        VNO=0.5*(VN(I,J+1)+VN(I+1,J+1))
        DUE=GSI*(UE-UW)
        DVN=GSI*(VNO-VSO)
        DI(I,J)=DUE+DVN    !  DIV, UNITS ARE 10-6 SEC-1
        IF (IVORT .EQ. 2) GO TO 170
        VE=0.5*(VN(I+1,J)+VN(I+1,J+1))
        VW=0.5*(VN(I,J)  +VN(I,J+1))
```

```
          USO=0.5*(UN(I+1,J)+UN(I,J))
          UNO=0.5*(UN(I,J+1)+UN(I+1,J+1))
          DVE=GSI*(VE-VW)
          DUN=GSI*(UNO-USO)
          VT(I,J)=DVE-DUN       !  VORTICITY
 170   CONTINUE
C        IF(DBUG(1)) PRINT 9570
C       DO 173 J=1,NROW
         JP=NROW+1-J
C 173   IF(DBUG(1)) PRINT 9100, (VT(I,JP),I=I1,I2)
C       IF(DBUG(1)) PRINT 9571
C       DO 172 J=1,NROW
         JP=NROW+1-J
C 172   IF(DBUG(1)) PRINT 9100, (DI(I,JP),I=I1,I2)
C   FOR NONDIVERGENCE SET DDIJ=0.0
         DDIJ=0.0
          LG=0
       RA=0.4    !  RELAXATION FACTOR
 210   LG=LG+1
       DO 500 J=1,NROWM1
       DO 500 I=1,NCOLM1
         UE=0.5*(UN(I+1,J)+UN(I+1,J+1))
         UW=0.5*(UN(I,J)  +UN(I,J+1))
         VSO=0.5*(VN(I+1,J)+VN(I,J))
         VNO=0.5*(VN(I,J+1)+VN(I+1,J+1))
         DUE=GSI*(UE-UW)
         DVN=GSI*(VNO-VSO)
         DI(I,J)=DUE+DVN
         CUIJ=.05*GS *(DDIJ-DI(I,J))*RA
         CVIJ=.05*GS*(DDIJ-DI(I,J))*RA
         IF (CUIJ .LT.-1.0) CUIJ=-1.0  !  LIMIT CHANGES
         IF (CUIJ.GT. 1.0) CUIJ=1.0
         IF (CVIJ .LT.-1.0) CVIJ=-1.0
         IF (CVIJ.GT. 1.0) CVIJ=1.0
         UN(I+1,J)=UN(I+1,J)+CUIJ
         UN(I+1,J+1)=UN(I+1,J+1) +CUIJ
         UN(I,J)=UN(I,J) -CUIJ
         UN(I,J+1)=UN(I,J+1) -CUIJ
         VN(I+1,J)=VN(I+1,J)-CVIJ
         VN(I,J)=VN(I,J)-CVIJ
         VN(I,J+1)=VN(I,J+1)+CVIJ
         VN(I+1,J+1)=VN(I+1,J+1)+CVIJ
         IF (IVORT .EQ. 2) GO TO 490
         VE=0.5*(VN(I+1,J)+VN(I+1,J+1))
         VW=0.5*(VN(I,J)+VN(I,J+1))
         USO=0.5*(UN(I+1,J)+UN(I,J))
        UNO=0.5*(UN(I,J+1)+UN(I+1,J+1))
        DVE=GSI*(VE-VW)
        DUN=GSI*(UNO-USO)
        VO(I,J)=DVE-DUN
        CVIJ=.05*GS *(VT(I,J)-VO(I,J))*RA
        CUIJ=.05*GS*(VT(I,J)-VO(I,J))*RA
         IF (CUIJ .LT.-1.0)  CUIJ=-1.0  ! LIMIT CHANGES
         IF (CUIJ.GT. 1.0) CUIJ=1.0
         IF (CVIJ .LT.-1.0) CVIJ=-1.0
         IF (CVIJ.GT. 1.0) CVIJ=1.0
        UN(I,J)=UN(I,J) +CUIJ
        UN(I+1,J)=UN(I+1,J)+CUIJ
        UN(I,J+1)=UN(I,J+1)-CUIJ
        UN(I+1,J+1)=UN(I+1,J+1)-CUIJ
        VN(I+1,J)=VN(I+1,J)+CVIJ
        VN(I+1,J+1)=VN(I+1,J+1) +CVIJ
        VN(I,J)=VN(I,J)-CVIJ
        VN(I,J+1)=VN(I,J+1)-CVIJ
 490    CONTINUE
C  TO KEEP WINDS 0.0 WHERE RHS IS NEGATIVE
```

```
      IF (RHS(I,J,L).LE.0.0) THEN
       UN(I,J)=0.0
       VN(I,J)=0.0
      END IF
C  HOLD ANALYZED WIND COMPONENTS FIXED AT PTS WHERE IFXPT=1
      IF (IFXPT(I,J)  .NE. 1) GO TO 500
       UN(I,J)=U1(I,J)*THK(I,J)
       VN(I,J)=V1(I,J)*THK(I,J)
 500   CONTINUE
       IF (LG.GT.NITER) GO TO 540
      DO 530 J=2,NROWM1
      DO 530 I=2,NCOLM1
         IF (ABS(DDIJ-DI(I,J)).GT.50.0) GO TO 210
C        IF (ABS(VT(I,J)-VO(I,J)).GT.50.0) GO TO 210
 530  CONTINUE
 540  CONTINUE
C                IF(DBUG(1)) PRINT 9570
C       IF(DBUG(1)) PRINT 9580
C      DO 510 J=1,NROW
        JP=NROW+1-J
C 510   IF(DBUG(1)) PRINT 9100,    (VO(I,JP),I=I1,I2)
C       IF(DBUG(1)) PRINT 9200, LG
C        IF(DBUG(1)) PRINT 9571
C       IF(DBUG(1)) PRINT 9580
C      DO 520 J=1,NROW
        JP=NROW+1-J
C 520   IF(DBUG(1)) PRINT 9100,    (DI(I,JP),I=I1,I2)
        SUM1=0.0
        SUM2=0.0
        Q1=0.0
       DO 1040 J=1,NROW
       DO 1040 I=1,NCOL
       IF (RHS(I,J,L).LE.0.0) GO TO 1040  !  OMIT THESE PTS
         Q1=Q1+1.0
         UN(I,J)=UN(I,J)/THK(I,J)
         VN(I,J)=VN(I,J)/THK(I,J)
         U1(I,J)=U1(I,J)-UN(I,J)
         V1(I,J)=V1(I,J)-VN(I,J)
         SUM1=SUM1+U1(I,J)
         SUM2=SUM2+V1(I,J)
 1040 CONTINUE
        SUM1=SUM1/Q1
        SUM2=SUM2/Q1
C NORMALIZE ORIG. AVERAGE VALUES
C      DO 1045 J=1,NROW
C      DO 1045 I=1,NCOL
C         UN(I,J)=UN(I,J)+SUM1
C         VN(I,J)=VN(I,J) +SUM2
        IF(DBUG(1)) PRINT 1145, L
        DO 1160 J=1,NROW
        JP=NROW+1-J
 1160   IF(DBUG(1)) PRINT 9150, (U1(I,JP),I=I1,I2)
        IF(DBUG(1)) PRINT 1155
        DO 1170 J=1,NROW
        JP=NROW+1-J
 1170   IF(DBUG(1)) PRINT 9150, (V1(I,JP),I=I1,I2)
C  WRITE LEVEL 4 DIV WINDS TO OUTPUT FILE
       IF (L .NE. 4) GO TO 700
        IF(.NOT.RYT3) GO TO 700
          DO 690 J=1, NROW
            JR=NROW+1-J
 690        WRITE (3,9065) (U1(I,JR),I=1,NCOL)
          DO 695 J=1, NROW
            JR=NROW+1-J
 695        WRITE (3,9065) (V1(I,JR),I=1,NCOL)
 700    CONTINUE
```

```
C
C  CHANGE BACK TO 3D ARRAYS
C
        DO 580 J=1,NROW
        DO 580 I=1,NCOL
                U(I,J,L)=UN(I,J)
                V(I,J,L)=VN(I,J)
  580   CONTINUE
  800   CONTINUE
       IF(DBUG(1)) PRINT 9003
 1145 FORMAT(' U COMP. DIVERGENT, LEVEL ='I3)
 1155 FORMAT(' V COMP. DIVERGENT ')
 9002 FORMAT (//'  BEGIN SUBROUTINE BAL5 '/)
 9003 FORMAT (//'  END OF SUBROUTINE BAL5 '/)
 9065 FORMAT (10F8.1)
 9150 FORMAT(' ',33F4.1)
 9582 FORMAT (/' POINT WITH FIXED WIND IS COL ='I3,'ROW ='I3/)
      RETURN
      END
C
C*******************************************************************************
C
       SUBROUTINE DOPSIG(DBUG,KEY)
C  ASSIGN DOPPLER WIND PROFILES TO SIGMA SURFACES.
C  MISSING WINDS ARE DENOTED BY -999.
C  IF SOUNDING IS NOT COMPLETE THE LAST REPORTED WIND
C  IS USED AT THE HIGHEST ALTITUDES.
C  WIND DATA START AT 40 M AND CONTINUE AT 30-M INTERVALS
C  TO 610 M.  THERE ARE 20 POINTS IN A PROFILE.
C  FILL IN MISSING DATA WITH NEAREST POINT UP OR DOWN.
C  FOR PROGRAM DIABWND, JAN  '85.
C  BY R.M. ENDLICH, SRI INTN'L, MENLO PARK CA 94025.
C       MODIFIED BY FLLUDWIG--12/85
C
        LOGICAL KEY,DBUG(15),UTMUSE
      DIMENSION  DPHT(5,50), DPUC(5,50), DPVC(5,50),RHS1(5,6)
      DIMENSION DPWD(5,50),DPWS(5,50),XS(5),YS(5),STLT(5),STLN(5)
      COMMON /STALOC/ XG(50), YG(50)
      COMMON /WINDS/ USIG(50,6), VSIG(50,6)
      COMMON /LIMITS/NCOL,NROW,NLVL,NCOLM1,NROWM1,
     $              LOWIX(5,3),LOWIY(5,3),SFCMAX
       COMMON/RARS/RHS(25,25,6)
       COMMON/PARMS/ZTOP,DS,DSIGMA,NLVLM1,XHT1,XHT2,X1,Y1,
     1 X2,Y2,UG,VG,RATIO,TDSI
       COMMON /SITE/ IXS, JYS, THSITE, IGRID
       COMMON /ANCHOR/ SLAT, SLNG ,UTMUSE
       COMMON /NUMOBS/ NUMDOP, NUMNWS, NUMTOT
       COMMON /UPWIND/ UTOP, VTOP
        INTEGER STAID(5)
C  VARIABLES ARE:
C    DPUC=U COMPONENT OF DOPPLER WIND IN MPS
C    DPVC=V COMPONENT OF DOPPLER WIND IN MPS
C    NHTS=NUMBER OF POINTS IN VERTICAL WIND PROFILE
C    NLVL=NUMBER OF SIGMA LEVELS
C    RHS=HT OF SIGMA SURFACES ABOVE TERRAIN (M)
C    XG,YG=STA. DIST IN X,Y IN GRID UNITS FROM SW CORNER
       IF(DBUG(2)) PRINT 9001
C  FILL IN HEIGHTS OF DOPPLER DATA POINTS
C -------------------------------
C  PRINT LAT,LONG OF ANCHOR POINT (UTMUSE=F) OR UTM COORDS (UTMUSE=T)
       IF(DBUG(2)) PRINT 9007, SLAT, SLNG
C* READ LAT , LONG  OF STATIONS (DEG) AND CONVERT TO  XS,YS (KM)--UTMUSE=F--
C  OR READ IN UTM COORDINATES (KM) DIRECTLY--UTMUSE=TRUE--FROM SW CORNER
C
        IF (KEY) THEN
C                       READ(12,9014) NUMDOP
```

```
              READ(12,*) NUMDOP
              IF(DBUG(2)) PRINT 9027, NUMDOP
              READ(12,*) (STAID(IT),STLT(IT), STLN(IT),IT=1,NUMDOP)
              IF(DBUG(2)) PRINT 9004
              IF(DBUG(2)) PRINT 9014,
     $           (STAID(IT),STLT(IT), STLN(IT),IT=1,NUMDOP)
             DO 15 IT=1,NUMDOP
               IF (UTMUSE) THEN
                  XS(IT)=STLN(IT)-SLNG
                  YS(IT)=STLT(IT)-SLAT
               ELSE
                  XS(IT)=(STLN(IT)-SLNG)*(111.2*COS(SLAT/57.295))
                  YS(IT)=(STLT(IT)-SLAT)*111.2
               END IF
               XS(IT)=XS(IT)+IXS*(DS*.001)
               YS(IT)=YS(IT)+JYS*(DS*.001)
               XG(IT)=XS(IT)/(DS*.001)
               YG(IT)=YS(IT)/(DS*.001)
  15          CONTINUE
              IF(DBUG(2)) PRINT 9008
              IF(DBUG(2)) PRINT 9011,
     $           (XS(IT), YS(IT),XG(IT),YG(IT),IT=1,NUMDOP)
          END IF
C  ASSIGN HTS OF SIGMA SFC FOR EACH SOUNDING
            DO 25 IT=1,NUMDOP
              DO 20 K=1,NLVL
                IX=JNINT(XG(IT))
                JY=JNINT(YG(IT))
                IF (IX.LT.1) IX=1
                IF (IX.GT.NCOL) IX=NCOL
                IF (JY.LT.1) JY=1
                IF (JY.GT.NROW) JY=NROW
                RHS1(IT,K)=RHS(IX,JY,K)
  20          CONTINUE
            IF(DBUG(2)) PRINT 9024
            IF(DBUG(2)) PRINT 9015, IT, (RHS1(IT,K),K=1,NLVL)
  25        CONTINUE
C  READ DOPPLER SOUNDINGS FOR NUMDOP STATIONS
          DO 450 IT=1,NUMDOP
            IF (KEY) THEN
C                READ (12,9014) NHTS
              READ (12,*) NHTS
              IF(DBUG(2)) PRINT 9003, IT, NHTS
C                READ (12,9009) (DPHT(IT,LL),DPWD(IT,LL), DPWS(IT,LL),
C     $                           LL=1,NHTS)
              READ (12,*) (DPHT(IT,LL),DPWD(IT,LL), DPWS(IT,LL),
     $                     LL=1,NHTS)
              IF(DBUG(2)) PRINT 9009,
     $           (DPHT(IT,LL),DPWD(IT,LL), DPWS(IT,LL),LL=1,NHTS)
C  CHANGE DIRECTION AND SPEED (MPS) TO U AND V
            DO 40 LL=1,NHTS
               IF (DPWD(IT,LL) .EQ.-999.0) THEN
                    DPUC(IT,LL)=-999.0
                    DPVC(IT,LL)=-999.0
               ELSE
                    DPUC(IT,LL)=-DPWS(IT,LL)*SIN(DPWD(IT,LL)/57.295)
                    DPVC(IT,LL)=-DPWS(IT,LL)*COS(DPWD(IT,LL)/57.295)
               END IF
  40          CONTINUE
              IF(DBUG(2)) PRINT 9010,(DPUC(IT,LL),
     $                          DPVC(IT,LL),LL=1,NHTS)
C  FILL IN MISSING DATA IF NEEDED
C  START FROM BOTTOM AND GO UPWARD
              LL=0
  60          LL=LL +1
              IF (LL .EQ. NHTS) GO TO 100
```

```
            IF (DPUC(IT,LL) .EQ.-999.0) THEN
              GO TO 70
            ELSE
              GO TO 60
            END IF
 70         LL1=LL
 75         LL1=LL1+1
            IF (DPUC(IT,LL1) .EQ.-999.0 .AND. LL1 .EQ. NHTS)
     +        GO TO 100
            IF (DPUC(IT,LL1) .EQ.-999.0) THEN
              GO TO 75
            ELSE
              DPUC(IT,LL)=DPUC(IT,LL1)
              DPVC(IT,LL)=DPVC(IT,LL1)
              IF(DBUG(2)) PRINT 9015, LL, DPUC(IT,LL), DPVC(IT,LL)
              GO TO 60
            END IF
 100        CONTINUE
            IF(DBUG(2)) PRINT 9010,(DPUC(IT,LL),DPVC(IT,LL),LL=1,NHTS)
C  START FROM TOP AND GO DOWN
            LL=NHTS+1
 110        LL=LL-1
            IF (LL .EQ. 1) GO TO 140
            IF (DPUC(IT,LL) .EQ.-999.0) THEN
              GO TO 120
            ELSE
              GO TO 110
            END IF
 120        LL1=LL
 125        LL1=LL1-1
            IF (DPUC(IT,LL1) .EQ.-999.0) THEN
              GO TO 125
            ELSE
              DPUC(IT,LL)=DPUC(IT,LL1)
              DPVC(IT,LL)=DPVC(IT,LL1)
              IF(DBUG(2)) PRINT 9015, LL, DPUC(IT,LL), DPVC(IT,LL)
              GO TO 110
            END IF
 140      CONTINUE
          IF(DBUG(2)) PRINT 9012
          IF(DBUG(2)) PRINT 9010,(DPUC(IT,LL),DPVC(IT,LL),LL=1,NHTS)
         END IF
C  BEGIN INTERPOLATION SCHEME
         DO 400 K=2, NLVL  ! COUNTER FOR SIGMA LEVELS
            LL=0
 200        LL=LL+1
            IF (RHS1(IT,K).GT.0.0) GO TO 365
            USIG(IT,K)=0.0
            VSIG(IT,K)=0.0
            GO TO 400
 365        IF (RHS1(IT,K).LE.DPHT(IT,LL)) GO TO 320
            IF (RHS1(IT,K).GE.DPHT(IT,NHTS)) GO TO 380
            IF (RHS1(IT,K).GE.DPHT(IT,LL) .AND. RHS1(IT,K).LE.
     +      DPHT(IT,LL+1))  GO TO 360
            GO TO 200
C  FOR LEVELS BELOW 1ST MEASURED WINDS (ASSUME SPEED=0 AT 1M
C  AND AT GROUND WHERE RHS=0)
 320       USIG(IT,K)=(DPUC(IT,LL))*(ALOG10(RHS1(IT,K)))/
     +     ALOG10(DPHT(IT,LL))
           VSIG(IT,K)=(DPVC(IT,LL))*(ALOG10(RHS1(IT,K)))/
     +      ALOG10(DPHT(IT,LL))
           GO TO 400
C FOR SIGMA LEVELS BETWEEN DOPPLER WIND POINTS
 360     RATIO=(ALOG10(RHS1(IT,K))-ALOG10(DPHT(IT,LL)))/
     +    (ALOG10(DPHT(IT,LL+1))- ALOG10(DPHT(IT,LL)))
          USIG(IT,K)=DPUC(IT,LL) +(DPUC(IT,LL+1)-DPUC(IT,LL))
```

```
     +      *RATIO
            VSIG(IT,K)=DPVC(IT,LL) +(DPVC(IT,LL+1)-DPVC(IT,LL))
     +      *RATIO
            GO TO 400
C  FOR SIGMA LEVELS ABOVE LAST DOPPLER POINT
  380       USIG(IT,K)=DPUC(IT,NHTS)
            VSIG(IT,K)=DPVC(IT,NHTS)
  400    CONTINUE
         IF(DBUG(2)) PRINT 9020, IT
         IF(DBUG(2)) PRINT 9010, (USIG(IT,K), VSIG(IT,K), K=1,NLVL)
  450  CONTINUE
C  GET AVER UPPER WIND FOR POSSIBLE USE IN GEOSIG IF GEOS WIND
C  IS NOT AVAILABLE
            UTOP=0
            VTOP=0
         DO 460 IT=1, NUMDOP
            UTOP=UTOP+USIG(IT,NLVL)
            VTOP=VTOP+VSIG(IT,NLVL)
  460    CONTINUE
            UTOP=UTOP/(FLOAT(NUMDOP))
            VTOP=VTOP/(FLOAT(NUMDOP))
         IF(DBUG(2)) PRINT 9026, UTOP, VTOP
         IF(DBUG(2)) PRINT 9002
 9001    FORMAT (/'     BEGIN SUBROUTINE DOPSIG  '/)
 9002    FORMAT (/'         END OF SUBROUTINE DOPSIG  '/)
 9003    FORMAT (/'   STA. ='I3,'  NO. OF POINTS IN PROFILE='I3/)
 9004    FORMAT (//'  LATITUDE AND LONGITUDE OF STATIONS'/)
 9007    FORMAT (//'  THE ANCHOR PT. IS AT LAT ='F9.3,'  AND LONG='F9.3)
 9008    FORMAT (//'  X AND Y OF STATIONS IN KM AND IN COLS,ROWS FROM SW
     +  CORNER OF COARSE GRID'/)
 9009    FORMAT (3X,3F7.1)
 9010    FORMAT (3X,8F6.1)
 9011    FORMAT (/4X,2F11.3,8X,2F10.2)
 9012    FORMAT (/' SOUNDING WITH FILLED IN DATA '/)
 9014    FORMAT (3X,I5,2F8.2)
 9015    FORMAT (3X,I5,6F8.2)
 9020    FORMAT (/' STATION NUMBER ='I6/)
 9024    FORMAT (/'  HEIGHTS OF SIGMA SURFACES '/)
 9026    FORMAT (/'   AVER. UPPER WIND, U ='F6.1,'    V='F6.1/)
 9027    FORMAT (/'  NUMBER OF WIND SOUNDINGS ='I3/)
         RETURN
         END
C
C*********************************************************************
C
         SUBROUTINE GEOSIG(DBUG)
C
C  PREPARE NWS HOURLY REPORTS OF WIND DIRECTION, WIND SPEED
C  (KNOTS), SEA LEVEL PRESSURE (MB), AND TEMPERATURE (DEG F)
C  FOR INPUT TO WIND ANALYSIS FOR DIABLO PGE SITE.
C  COMPUTE GEOS WIND FROM PRESSURE AT THREE STATIONS AND
C  CORRECT IT FOR THERMAL WIND COMPONENT (IF DESIRED).
C  ASSUME THAT WIND COMPONENTS VARY WITH LOG(HEIGHT) BETWEEN
C  ANEMOMETER HT AND GEOS WIND AT HT GEOSHT(ABOUT 500M).
C  AT EACH NWS STATION INTERPOLATE WINDS TO SIGMA SURFACES.
C  BY RM ENDLICH, SRI INTN'L, MENLO PARK CA 94025 DEC '84.
C  VARIABLES
C    NUMNWS = NUMBER OF NWS REPORTS
C    NWSID = IDENTIFICATION ID OF NWS STATION
C    WD = WIND DIRECTION
C    SP = WIND SPEED
C    STLT = STATION LATITUDE IN DEGS AND HUNDREDTHS
C    STLN = STATION LONGITUDE
C    PRESS = STATION SEA LEVEL PRESSURE IN INCHES HG
C    TEMP = STATION TEMP IN DEG F
       LOGICAL DBUG(15), UTMUSE
```

```
      INTEGER STAID(50)
      DIMENSION   STLT(50), STLN(50), PRESS(50)
      DIMENSION TEMP(50)
      DIMENSION RHS1(50,6), UNWS(50,6), VNWS(50,6)
      DIMENSION UCOMP(50), VCOMP(50), WD(50), WS(50)
      DIMENSION XS(50), YS(50)
      DIMENSION XG1(50), YG1(50), USIG1(50,6), VSIG1(50,6)
      COMMON /LIMITS/NCOL,NROW,NLVL,NCOLM1,NROWM1,
     $                  LOWIX(5,3),LOWIY(5,3),SFCMAX
      COMMON/RARS/RHS(25,25,6)
      COMMON/PARMS/ZTOP,DS,DSIGMA,NLVLM1,XHT1,XHT2,X1,Y1,
     1             X2,Y2,UG,VG,RATIO,TDSI
      COMMON /SITE/ IXS, JYS, THSITE, IGRID
      COMMON /STALOC/ XG(50), YG(50)
      COMMON /WINDS/ USIG(50,6), VSIG(50,6)
      COMMON /ANCHOR/ SLAT, SLNG ,UTMUSE
      COMMON /NUMOBS/ NUMDOP, NUMNWS, NUMTOT
      COMMON /UPWIND/ UTOP, VTOP
      IF(DBUG(3)) PRINT 9001
C
C  READ INPUT OF HOURLY DATA: STATION ID, LATITUDE, LONGITUDE (UTMUSE=F) OR
C  UTM COORDS (KM,UTMUSE=T) PRESSURE, TEMPERATURE, WIND DIR., WIND SPEED (MPS)
C
      DO  70 IT=1,NUMNWS
C           READ (12, 10) STAID(IT), STLT(IT), STLN(IT),
C          +   PRESS(IT), TEMP(IT), WD(IT), WS(IT)
        READ (12,*) STAID(IT), STLT(IT), STLN(IT),
     +         PRESS(IT), TEMP(IT), WD(IT), WS(IT)
        IF(DBUG(3)) PRINT 20, IT,  STAID(IT),STLT(IT),STLN(IT),
     +       PRESS(IT),TEMP(IT)
        IF(DBUG(3)) PRINT 25, WD(IT), WS(IT)
 70   CONTINUE
C
C  CONVERT LAT,LONG (UTMUSE=F) OR UTM COORDS(KM,UTMUSE=T) TO XS,YS (KM)
C  MEASURED FROM SW CORNER OF COARSE GRID
C
      DO 15 J=1,NUMNWS
        IF (UTMUSE) THEN
           XS(J)=STLN(J)-SLNG
           YS(J)=STLT(J)-SLAT
        ELSE
           XS(J)=(STLN(J)-SLNG)*(111.0*COS(SLAT/57.295))
           YS(J)=(STLT(J)-SLAT)*111.0
        END IF
        XS(J)=XS(J) + IXS*(DS*.001)
        YS(J)=YS(J)+JYS*(DS*.001)
        XG1(J)=XS(J)/(DS*.001)
        YG1(J)=YS(J)/(DS*.001)
 15   CONTINUE
      IF(DBUG(3)) PRINT 9008
      IF(DBUG(3)) PRINT 9011, (XS(J), YS(J),XG1(J),YG1(J),
     $                         J=1,NUMNWS)
C  CHANGE DIRECTION AND SPEED (MPS) TO U AND V
      DO 80 IT=1,NUMNWS
         UCOMP(IT)=-WS(IT)*SIN(WD(IT)/57.295)
         VCOMP(IT)=-WS(IT)*COS(WD(IT)/57.295)
      IF(DBUG(3)) PRINT 9002
      IF(DBUG(3)) PRINT 9013, IT, UCOMP(IT), VCOMP(IT)
 80    CONTINUE
C  ASSIGN HEIGHTS TO SIGMA SURFACES
      DO 125  J=1,NUMNWS
      DO 120 K=1,NLVL
        IX=JNINT (XG1(J))
        JY=JNINT (YG1(J))
        IF (IX.LT.1) IX=1
        IF (IX.GT.NCOL) IX=NCOL
```

```
          IF (JY.LT.1) JY=1
          IF (JY.GT.NROW) JY=NROW
          RHS1(J,K)=RHS(IX,JY,K)
  120   CONTINUE
        IF(DBUG(3)) PRINT 9024
        IF(DBUG(3)) PRINT 9015, J, (RHS1(J,K),K=1,NLVL)
  125   CONTINUE
C   IF LESS THAN 3 NWS STATIONS CANT COMPUTE GEOS WIND.  INSTEAD
C   USE UTOP, VTOP FROM DOPPLER.
        IF (NUMNWS.LT.3) UGEOS=UTOP
        IF (NUMNWS.LT.3) VGEOS=VTOP
        IF (NUMNWS.LT.3) GO TO 200
C
C**THIS SECTION COMPUTES GEOSTROPHIC WINDS AND IT ALSO CORRECTS
C   THEM FOR THERMAL WINDS IF NTHERM=1.
C
          IS1=NUMNWS-2
          IS2=NUMNWS-1
          IS3=NUMNWS
C   SET NTHERM
        NTHERM=1
        PR1=PRESS(IS1)*(1013.3/29.92)
        PR2=PRESS(IS2)*(1013.3/29.92)
        PR3=PRESS(IS3)*(1013.3/29.92)
        STLT1=STLT(IS1)
        STLT2=STLT(IS2)
        STLT3=STLT(IS3)
        STLN1=STLN(IS1)
        STLN2=STLN(IS2)
        STLN3=STLN(IS3)
        TMP1=TEMP(IS1)
        TMP2=TEMP(IS2)
        TMP3=TEMP(IS3)
C   DEFINE CONSTANTS
        AVLAT=.333* (STLT1+STLT2+STLT3)/57.295
        FC=14.584*SIN (AVLAT)
C     CORIOLIS FORCE IN UNITS 10-5 SEC-1
        COSLAT=COS (AVLAT)
        DENOM=(STLT2-STLT1)*(STLN3-STLN1)-(STLT3-STLT1) *
     +          (STLN2-STLN1)
        RHO=1.1
C   DENSITY IN UNITS 10-3 G/CM3
         C2=100.0/(RHO*1.112)
C   COMPUTE GEOSTROPHIC WINDS
        DPDLT=((STLN2-STLN1)*(PR3-PR1)-(STLN3-STLN1) *
     +          (PR2-PR1))/(-DENOM)
        DPDLN=((STLT2-STLT1)*(PR3-PR1)-(STLT3-STLT1) *
     +          (PR2-PR1))/DENOM
        UGEOS=(-C2/FC)*DPDLT
        VGEOS=(C2/FC)*(DPDLN/COSLAT)
C   SPEED UNITS ARE M SEC-1
        IF(DBUG(3)) PRINT 30, UGEOS, VGEOS
C   THIS PART MAKES THERMAL WIND CORRECTION TO UGEOS, VGEOS
C   NTHERM IS INDICATOR FOR USE (WHEN=1)
        IF (NTHERM .NE. 1) GO TO 200
        FVNIN=5.0/9.0
        TMP1=(TMP1-32.0)*FVNIN
        TMP2=(TMP2-32.0)*FVNIN
        TMP3=(TMP3-32.0)*FVNIN
        AVTMP=273.0+.333*(TMP1+TMP2+TMP3)
C   GRAVITY=9.8 M SEC-2, TEMP IN DEG K
        C3=9.8/(FC*1.112)
        DTDLT=((STLN2-STLN1)* (TMP3-TMP1)-(STLN3-STLN1)
     +     *(TMP2-TMP1))/(-DENOM)
        DTDLN=((STLT2-STLT1)* (TMP3-TMP1)-(STLT3-STLT1)
     +     *(TMP2-TMP1))/DENOM
```

```
      UTHERM=-(C3/AVTMP)*DTDLT
      VTHERM=(C3/AVTMP)*(DTDLN/COSLAT)
C  ASSUME SHEAR ACTS OVER LAYER OF DEPTH DEPL (IN M)
       DEPL=200    !  TIE THIS IN TO AVTHK FOR B LYR TOP
      USHEAR=UTHERM*DEPL
      VSHEAR=VTHERM*DEPL
       IF(DBUG(3)) PRINT 40, USHEAR, VSHEAR, DEPL
      UGEOS=UGEOS+USHEAR
      VGEOS=VGEOS+VSHEAR
       IF(DBUG(3)) PRINT 50
       IF(DBUG(3)) PRINT 30, UGEOS, VGEOS
 200  CONTINUE
C**END OF GEOSTROPHIC WIND SECTION
C INTERPOLATE WINDS BETWEEN SFC AND GEOSHT
      DO 450 IT=1, NUMNWS
      DO 400 K=2, NLVL  ! COUNTER FOR SIGMA LEVELS
        IF (RHSl(IT,K).GT.0.0) GO TO 370
          UNWS(IT,K)=0.0
          VNWS(IT,K)=0.0
          GO TO 400
 370    IF (RHSl(IT,NLVL).GE.800.) GEOSHT=800.
        IF (RHSl(IT,NLVL).LT.800.) GEOSHT=RHSl(IT,NLVL)
       IF (RHSl(IT,K).GT.GEOSHT) GO TO 380
C  FOR SIGMA LEVELS BETWEEN SURFACE OBS AND GEOSHT
       RATIO=(ALOG10(RHSl(IT,K))-1.0)/(ALOG10(GEOSHT)-1.0)
       UNWS(IT,K)=UCOMP(IT) +(UGEOS-UCOMP(IT))*RATIO
       VNWS(IT,K)=VCOMP(IT) +(VGEOS-VCOMP(IT))*RATIO
       GO TO 400
C  FOR SIGMA LEVELS ABOVE  GEOSHT
 380   UNWS(IT,K)=UGEOS
       VNWS(IT,K)=VGEOS
 400  CONTINUE
      IF(DBUG(3)) PRINT 9020, IT
      IF(DBUG(3)) PRINT 9010, (UNWS(IT,K), VNWS(IT,K), K=1,NLVL)
 450  CONTINUE
C  INCLUDE NWS DATA WITH DOPPLER DATA IN ARRAYS NEEDED
C   FOR OBJECTIVE ANALYSIS.
      DO 460 N=1, NUMNWS
         M=N+NUMDOP
        XG(M)=XG1(N)'
        YG(M)=YG1(N)
      DO 460  K=1, NLVL
         USIG(M,K)=UNWS(N,K)
         VSIG(M,K)=VNWS(N,K)
 460  CONTINUE
      NUMTOT=NUMDOP+NUMNWS
      DO 480 M=1, NUMTOT
      IF(DBUG(3)) PRINT 9020,M
      IF(DBUG(3)) PRINT 9010, (USIG(M,K), VSIG(M,K), K=1,NLVL)
 480  CONTINUE
      IF(DBUG(3)) PRINT 9003
  10  FORMAT (I5,2F8.2,4F7.1)
  20  FORMAT (/' NO.='I3,'  STA ID='I5,'  LAT='F7.2,'  LONG.
     + ='F7.2,'  PRESS='F7.2,'  TEMP='F6.1/)
  25  FORMAT ('    WIND DIR='F6.1,'  WIND SPEED='F5.1/)
  30  FORMAT ('   GEOSTROPHIC WIND COMPONENTS, MPS, U ='F5.1,
     + '   V ='F5.1/)
  40  FORMAT (//'    THERMAL WIND SHEAR COMPONENTS, MPS, U ='
     + F5.1,'    V ='F5.1,'  LAYER DEPTH ='F6.1,' M'/)
  50  FORMAT (//'  GEOSTROPHIC WIND CORRECTED FOR THERMAL WIND')
 9001 FORMAT (/'     BEGIN SUBROUTINE GEOSIG  '/)
 9002 FORMAT (//'  STA. NO.    U COMP    V COMP '/)
 9003 FORMAT (/'    END OF SUBROUTINE GEOSIG  '/)
 9008 FORMAT (//'  X AND Y OF STATIONS IN KM AND IN COLS,ROWS
     + FROM SW CORNER OF COARSE GRID'/)
 9010 FORMAT (3X,8F6.1)
```

```
 9011   FORMAT (/4X,2F11.0,8X,2F10.1)
 9013   FORMAT (/' STA. ='I5,' UCOMP='F8.1,'    VCOMP='F8.1/)
 9015   FORMAT (3X,I5,8F8.1)
 9020   FORMAT (/' STATION NUMBER ='I6/)
 9024   FORMAT (/'  HEIGHTS OF SIGMA SURFACES '/)
        RETURN
         END
C
C*******************************************************************************
C
        SUBROUTINE GPAN(DBUG)
C
C  THIS ROUTINE MAKES A GRID PT ANALYSIS FROM AVAILABLE
C  WIND OBSERVATIONS.  THE OBSERVATIONS HAVE BEEN INTERPO-
C  LATED TO SIGMA SURFACES.  THE WEIGHTING GIVEN TO EACH
C  STATION IS INVERSELY PROPORTIONAL TO ITS DISTANCE FROM
C  THE GRID POINT.
C  FOR SUBROUTINE DIABWND, JAN  '85.
C  BY R.M. ENDLICH, SRI INTN'L, MENLO PARK CA 94025.
C
        LOGICAL DBUG(15)
        INTEGER STAID(6)
        DIMENSION WT(50)
        COMMON /WINDS/ USIG(50,6), VSIG(50,6)
        COMMON /STALOC/ XG(50), YG(50)
        COMMON /LIMITS/NCOL,NROW,NLVL,NCOLM1,NROWM1,
     $                    LOWIX(5,3),LOWIY(5,3),SFCMAX
        COMMON/UARS/U(25,25,6),UA(25,25,6),V(25,25,6),VA(25,25,6)
        COMMON /NUMOBS/ NUMDOP, NUMNWS, NUMTOT
        COMMON /PRLIM/ I1, I2
C  VARIABLES ARE:
C     USIG=U COMP OF WIND ON A SIGMA SFC
C    VSIG=V COMP OF WIND ON A SIGMA SFC
C    WT=WEIGHT ASSIGNED TO A GIVEN STATION
C    U(I,J,K) AND V(I,J,K) ARE FINAL WIND COMPONENTS
C    NLVL=NUMBER OF SIGMA LEVELS
C    XG,YG ARE DISTANCES OF STATIONS FROM SW CORNER OF COARSE
C    GRID AND ARE MEASURED IN GRID UNITS (DSCRS)
C    IN ARRAYS (IT,K) IT DENOTES STATIONS, K DENOTES LEVELS
C    IN 3-D ARRAYS I,J,K DENOTE COLS, ROWS, LEVELS FROM SW CORNER
C -------------------------------
        IF(DBUG(4)) PRINT 9001
C  SET MINIMUM DISTANCE (GRID UNITS) TO AVOID INFINITE WTS
         DISMIN=0.15
         DO 400 I=1, NCOL
         DO 400 J=1, NROW
            SUMWT=0.0
              DO 100 IT=1, NUMTOT
                 DIST=(FLOAT(I)-XG(IT))**2+(FLOAT(J)-YG(IT))**2
                 DIST=SQRT(DIST)
                 IF (DIST.LE.DISMIN) DIST=DISMIN
                 WT(IT)=1.0/(DIST*DIST)
                 SUMWT=SUMWT+WT(IT)
  100         CONTINUE
C  NORMALIZE WEIGHTS
              DO 120 IT=1, NUMTOT
                 WT (IT)=WT(IT)/SUMWT
  120         CONTINUE
              IF (J .EQ. 11) THEN
                 IF(DBUG(4)) PRINT 9030, I, J
                 IF(DBUG(4)) PRINT 9010, (WT(IT),IT=1,NUMTOT)
              END IF
C  MAKE GRID POINT ANALYSIS USING WTS AND STA DATA
              DO 350 K=1, NLVL
                U(I,J,K)=0.0
                V(I,J,K)=0.0
```

```
            DO 300 IT=1, NUMTOT
                U(I,J,K)=U(I,J,K)+WT(IT)*USIG(IT,K)
                V(I,J,K)=V(I,J,K)+WT(IT)*VSIG(IT,K)
300         CONTINUE
350       CONTINUE
400     CONTINUE
        IF (DBUG(4)) THEN
           DO 430 K=2, NLVL
              PRINT 9035, K
              DO 420 JR=1, NROW
                 JP=NROW+1-JR
420           PRINT 9031, (U(IP,JP,K),IP=I1,I2)
              PRINT 9038, K
              DO 425 JR=1, NROW
                 JP=NROW+1-JR
425           PRINT 9031, (V(IP,JP,K),IP=I1,I2)
430       CONTINUE
          PRINT 9002
        END IF
9001   FORMAT (/ ' BEGIN SUBROUTINE GPAN  '/)
9002   FORMAT (//'  END OF SUBROUTINE GPAN '/,
9010   FORMAT (3X,8F6.1)
9030   FORMAT (/'   WTS FOR STATIONS FOR GRID POINT X,Y='2I3)
9031   FORMAT (1X,21F5.1)
9035   FORMAT (/'  U COMPONENT AT LEVEL ='I3/)
9038   FORMAT ('   V COMPONENT AT LEVEL ='I3/)
        RETURN
          END
C
C*************************************************************************
C
        SUBROUTINE LEVWND(DBUG,IG,ZFLAT)
C
C  LINEARLY INTERPOLATES WINDS FROM SIGMA SURFACES TO HORIZONTAL PLANES OR
C  TO A HEIGHT OF 10 M ABOVE THE LOCAL TERRAIN FOR THE 1ST LEVEL
C       --F.LUDWIG, 12/23/85
C
        LOGICAL DBUG(15)
        DIMENSION ZFLAT(6)
        COMMON /BLHT/ BLT(25,25),HSITE, AVTHK, SLFAC,STHK,BLGRX,BLGRY
        COMMON/RARS/RHS(25,25,6)
        COMMON/CSFC/SFCHT(25,25),SIGMA(6)
        COMMON/UARS/U(25,25,6),UA(25,25,6),V(25,25,6),VA(25,25,6)
        COMMON/WARS/W(25,25,6),WA(25,25,6)
        COMMON /LIMITS/NCOL,NROW,NLVL,NCOLM1,NROWM1,
     $                 LOWIX(5,3),LOWIY(5,3),SFCMAX
C
C  STATEMENT FUNCTION FOR LINEAR INTERPOLATION.
C
        VALINT(A1,A2,X)=A1+(A2-A1)*X
        IF (DBUG(15)) PRINT*, 'START LEVWND'
C
C  GET LOWEST PTS AT SFC & TOP OF BOUNDARY LAYER, THEN DEFINE LAYER HTS.
C
           SFCMIN=SFCHT(LOWIX(1,IG),LOWIY(1,IG))
           THICK=RHS(LOWIX(1,IG),LOWIY(1,IG),NLVL)
           DO 25 L=1,NLVL
              ZFLAT(L)=SFCMIN+THICK*SIGMA(L)
              IF (DBUG(14)) PRINT *, ZFLAT(L),'HT AT LEV',L
 25        CONTINUE
        DO 100 IX=1,NCOL
        DO 100 IY=1,NROW
C
C  1ST LEVEL IS NOT FLAT; IT IS SET AT 10 M ABOVE THE LOCAL TERRAIN.
C
           ZFLAT(1)=SFCHT(IX,IY)+10.0
```

```
          DO 75 IFLAT=1,NLVL
C
C  IS THIS LEVEL MORE THAN 1/2 METER ABOVE GROUND?
C
              IF(ZFLAT(IFLAT)-SFCHT(IX,IY).GT.0.5) THEN
                DO 50 IZ=2,NLVL
C
C  FIND THE FLOW SFCS BETWEEN WHICH THIS FLAT SFC LIES & DO LOG INTERPOL.
C
                  IF(RHS(IX,IY,IZ)+SFCHT(IX,IY).GE.ZFLAT(IFLAT))
     $               THEN
                     ZBLO=RHS(IX,IY,IZ-1)
                     IF (ZBLO.LT.1.)ZBLO=1.0
                     DZT=ALOG10(RHS(IX,IY,IZ)/ZBLO)
                     ZFLT=ZFLAT(IFLAT)-SFCHT(IX,IY)
                     IF (ZFLT .LT. 1.0) ZFLT=1.0
                     DZF=ALOG10(ZFLT/ZBLO)
                     RATIO=DZF/DZT
                     IF(RATIO.GT.1.001)STOP 'BAD RATIO IN LEVWND'
                     UA(IX,IY,IFLAT)=VALINT(U(IX,IY,IZ-1),U(IX,IY,IZ),
     $                                      RATIO)
                     VA(IX,IY,IFLAT)=VALINT(V(IX,IY,IZ-1),V(IX,IY,IZ),
     $                                      RATIO)
                     WA(IX,IY,IFLAT)=VALINT(W(IX,IY,IZ-1),W(IX,IY,IZ),
     $                                      RATIO)
                     GO TO 75
                  END IF
 50             CONTINUE
              ELSE
                UA(IX,IY,IFLAT)=0.0
                VA(IX,IY,IFLAT)=0.0
                WA(IX,IY,IFLAT)=0.0
              END IF
 75         CONTINUE
 100     CONTINUE
         IF(DBUG(14)) PRINT *, 'END LEVWND'
         RETURN
         END
C
C*************************************************************************
C
         SUBROUTINE REINT(DBUG,L)
C
C  INTERPOLATES LOG-LINEARLY TO GET U&V FOR LEVEL L USING NEXT LOWER LEVEL
C  & THE TOP LEVEL. LOWEST & HIGHEST LAYERS ARE DETERMINED 1ST,THEN 3,4 ETC
C
         LOGICAL DBUG(15)
         COMMON /LIMITS/NCOL,NROW,NLVL,NCOLM1,NROWM1,
     $                  LOWIX(5,3),LOWIY(5,3),SFCMAX
         COMMON /RARS/RHS(25,25,6)
         COMMON /UARS/U(25,25,6),UA(25,25,6),V(25,25,6),VA(25,25,6)
C
C  STATEMENT FUNCTION FOR INTERPOLATING
C
         VALU(X1,X2,DT,D1)=X1+(X2-X1)*D1/DT
         ZERO=0.0
         IF (DBUG(13)) PRINT*,'START REINT'
         DO 100 I=1,NCOL
         DO 100 J=1,NROW
            IF(RHS(I,J,L-1).GT.0.0) THEN
                 ZB=RHS(I,J,L-1)
                 IF(ZB.LT.10.)ZB=10.0
                 DLT=ALOG10(RHS(I,J,NLVL)/ZB)
                 DL1=ALOG10(RHS(I,J,L)/ZB)
                 U(I,J,L)=VALU(U(I,J,L-1),U(I,J,NLVL),DLT,DL1)
                 V(I,J,L)=VALU(V(I,J,L-1),V(I,J,NLVL),DLT,DL1)
```

```
            ELSE
                 IF(RHS(I,J,L).GT.0.5) THEN
C
C  ASSUME WIND=0 BELOW 0.5 METER
C
                    DLT=ALOG10(RHS(I,J,NLVL)/0.5)
                    DL1=ALOG10(RHS(I,J,L)/0.5)
                    U(I,J,L)=VALU(ZERO,U(I,J,NLVL),DLT,DL1)
                    V(I,J,L)=VALU(ZERO,V(I,J,NLVL),DLT,DL1)
                 ELSE
                    U(I,J,L)=0.0
                    V(I,J,L)=0.0
                 END IF
              END IF
  100      CONTINUE
           IF(DBUG(13)) PRINT*,'END REINT'
           RETURN
           END
C
C*******************************************************************************
C
           SUBROUTINE RESIG(DBUG,IG)
C
C  REDEFINES THE HEIGHTS OF THE SIGMA SURFACES BASED ON WIND SPEED OVER
C  THE LOWEST TERRRAIN HEIGHTS & LAPSE RATES AT THE VARIOUS SIGMA LEVELS
C  --THE UNDERLYING CONCEPT IS SIMILAR TO THAT OF THE "CRITICAL STREAMLINE."
C
           LOGICAL DBUG(15)
           DIMENSION RHSLO(6),DZMAX(6),COMPDZ(5)
           COMMON /SOUND/ PTLAPS(6),TO(6)
           COMMON /LIMITS/NCOL,NROW,NLVL,NCOLM1,NROWM1,
       $                  LOWIX(5,3),LOWIY(5,3),SFCMAX
           COMMON /RARS/RHS(25,25,6)
           COMMON /BLHT/ BLT(25,25),HSITE, AVTHK, SLFAC,STHK,BLGRX,BLGRY
           COMMON /CSFC/ SFCHT(25,25),SIGMA(6)
           COMMON /UARS/U(25,25,6),UA(25,25,6),V(25,25,6),VA(25,25,6)
           DATA RHSLO,CMPRES /6*0.0,0.5/
C
C  GETTING RMS AVERAGE WIND SPEED OVER LOW TERRAIN GRIDS & LOWEST PT.
C
           IF (DBUG(5)) PRINT *, 'START RESIG'
           LX=LOWIX(1,IG)
           LY=LOWIY(1,IG)
           SFCMIN=SFCHT(LX,LY)
           HIRISE=SFCMAX-SFCMIN
           DO 100 I=1,6
             RMSSPD=0.0
             DO 50 J=1,5
               JX=LOWIX(J,IG)
               JY=LOWIY(J,IG)
               RMSSPD=RMSSPD+U(JX,JY,I)**2+V(JX,JY,I)**2
   50        CONTINUE
             RHSLO(I)=RHS(LX,LY,I)
             SPD=SQRT(RMSSPD/5.0)
             IF (DBUG(5)) PRINT *,'RMS SPEED AT LEV',I,SPD
             DTHETA=PTLAPS(I)
             IF (DTHETA.LT.1.E-20) DTHETA=1.E-20
             DZMAX(I)=SPD/SQRT(9.8*DTHETA/TO(I))
             IF(DBUG(5)) PRINT*,'DZMAX=',DZMAX(I),'AT LEV',I
  100      CONTINUE
C
C    FLOW AMPLITUDES ARE LIMITED TO TERRAIN AMPLITUDE ON FIRST PASS
C
           IF (DZMAX(NLVL).GT.HIRISE) DZMAX(NLVL)=HIRISE
C
C  GETTING 1/2 THE SIGMA SFC SEPARATIONS OVER THE LOW SFC POINT.
```

```
C
      DO 125 L=1,NLVL-1
         COMPDZ(L)=CMPRES*(RHSLO(L+1)-RHSLO(L))
 125  CONTINUE
C
C  DO NOT LET SEPARATION BETWEEN SFCS COMPRESS BY MORE THAN CMPRES FACTOR
C
      DO 150 L=NLVL-1,1,-1
         IF (DZMAX(L).GT.(DZMAX(L+1)+COMPDZ(L))) DZMAX(L)=DZMAX(L+1)
     $                                                 +COMPDZ(L)
         IF (DZMAX(L).GT. HIRISE) DZMAX(L)=HIRISE
         IF(DBUG(5)) PRINT*,'DZMAX=',DZMAX(L),'AT LEV',L
 150  CONTINUE
C
C  NOW, GO BACK & MAKE SURE THAT HIGHER SURFACES DO NOT RISE MORE THAN
C  SURFACE DIRECTLY BELOW, IF THE SFC BELOW IS ABOVE THE TERRAIN HEIGHT
C  --SIMILAR TO THE CONSTRAINT THAT THE GREATEST ALLOWABLE DEVIATION IS
C  TO PARALLEL THE TERRAIN.
C
      DO 165 L=3,NLVL
         IF ( (RHSLO(L-1)+DZMAX(L-1)) .LT. SFCMAX ) GO TO 165
         IF (DZMAX(L).GT.DZMAX(L-1)) DZMAX(L)=DZMAX(L-1)
 165  CONTINUE
      DO 200 IX=1,NCOL
      DO 200 IY=1,NROW
C
C  LOCAL RISE OF SIGMA SFC WILL BE PROPORTIONAL TO THE MAXIMUM RISE (WHICH
C  OCCURS OVER HIGHEST TERRAIN POINT) AND THE RATIO OF THE RISE OF THE
C  LOCAL GROUND SURFACE TO THE MAXIMUM TERRAIN ELEVATION DIFFERENCE.
C
         HERE=SFCHT(IX,IY)
         ZRATIO=(HERE-SFCMIN)/HIRISE
         DO 175 L=1,NLVL
            RISE=ZRATIO*DZMAX(L)
            RHS(IX,IY,L)=RHSLO(L)+SFCMIN+RISE-HERE
 175     CONTINUE
C
C  DEFINE LOCAL BOUNDARY LAYER THICKNESS
C
         BLT(IX,IY)=RHS(IX,IY,NLVL)+HERE
 200  CONTINUE
      IF (DBUG(5)) THEN
         DO 300 L=1,NLVL
            PRINT 6000,L
            DO 250 IY=NROW,1,-1
              PRINT 6001, IY,(RHS(IX,IY,L),IX=1,NCOL)
              WRITE (15,6003) (RHS(IX,IY,L)+SFCHT(IX,IY),IX=1,NCOL)
 250        CONTINUE
            PRINT 6002,(IX,IX=1,NCOL)
 300     CONTINUE
      END IF
 6000 FORMAT(1H1,'LEVEL=',I2)
 6001 FORMAT(1H0,I2,25F5.0)
 6002 FORMAT(1X,'COL',1X,25(I2,3X))
 6003 FORMAT(1X,25F5.0)
      IF (DBUG(5)) PRINT *,'END RESIG'
      RETURN
      END
C
C*******************************************************************************
C
      SUBROUTINE SETBLT(DBUG)
C** THIS SUBROUTINE SETS THE HEIGHT OF THE BNDY LAYER TOP.  AVTHK IS
C  AVER. BL THICKNESS OVER AREA. SLFAC CONTROLS THE SLOPE, IF 0 THE
C  TOP IS FLAT, IF 1 THE BL TOP FOLLOWS THE TERRAIN.  HSITE IS HT OF
C  THE ANCHOR POINT (SITE), STHK IS THE SMALLEST BL THICK ALLOWED.
```

```
C  BLGRX IS B LYR HT GRADIENT TO E.
C  BY R. M. ENDLICH SRI INTNL
C  LAST REVISION JUNE '84
      LOGICAL DBUG(15)
     DIMENSION B(25,25),IB(25,25)
     COMMON /LIMITS/NCOL,NROW,NLVL,NCOLM1,NROWM1,
    $                LOWIX(5,3),LOWIY(5,3),SFCMAX
     COMMON/CVOS/ RCM,RMF,IV,DSCRS,IXCRS,JYCRS,IXMED,JYMED,
    $            IXFIN,JYFIN
     COMMON /SITE/ IXS, JYS, THSITE, IGRID
     COMMON /BLHT/ BLT(25,25),HSITE, AVTHK, SLFAC,STHK,BLGRX,BLGRY
     COMMON/CSFC/ SFCHT(25,25), SIGMA(6)
     COMMON /PRLIM/ I1, I2
     IF(DBUG(6)) PRINT 9001
     THK=AVTHK
     IF (IGRID.GT.1) THK=THSITE
       IF (IGRID .NE.1) GO TO 5
        BLX=BLGRX
        BLY=BLGRY
        IX=IXCRS
        JY=JYCRS
 5     CONTINUE
       IF (IGRID .NE. 2) GO TO 6
        BLX= BLGRX/(RCM)
        BLY=BLGRY/(RCM)
        IX=IXMED
        JY=JYMED
 6     CONTINUE
       IF (IGRID .NE.3) GO TO 7
        BLX=BLGRX/(RCM*RMF)
        BLY=BLGRY/(RCM*RMF)
        IX=IXFIN
        JY=JYFIN
 7     CONTINUE
       ITER=0
10    ITER=ITER+1
       SUM1=0.0
        Q1=0.0
      DO 50  I=1,NCOL
      DO 50 J=1,NROW
        BLT(I,J)=THK+(SLFAC*SFCHT(I,J))+(1.0-SLFAC)*HSITE
C ADD EASTWARD GRADIENT TO BLT FROM COL.  OF ANCHOR POINT
        BLT(I,J)=BLT(I,J)+ (I-IX)*(BLX/FLOATJ(NCOL))
C ADD NORTHWARD GRADIENT FROM ROW  OF ANCHOR POINT
        BLT(I,J)=BLT(I,J)+(J-JY)*(BLY/FLOATJ(NROW))
        IF (SFCHT(I,J).GT.(BLT(I,J)-  STHK)) BLT(I,J)=SFCHT(I,J)
     +       +STHK
      SUM1=SUM1+(BLT(I,J)-SFCHT(I,J))
       Q1=Q1+1.0
50    CONTINUE
       IF(IGRID.GT.1) GO TO 51
      ATH=SUM1/Q1
      THK=THK+(AVTHK-ATH)
      THSITE=BLT(IXS,JYS)-SFCHT(IXS,JYS)
      IF(DBUG(6)) PRINT 9010, AVTHK,ATH, THSITE
       DIFF=ABS(AVTHK-ATH)
       IF (ITER.GT. 9) GO TO 52
       IF (IGRID .EQ. 1 .AND. DIFF.GT.1.0) GO TO 10
51     CONTINUE
       IF(IGRID.EQ.1) GO TO 52
C  MAKE BL THICKNESS AT ANCHOR POINT (THSITE) THE SAME FOR
C  MED AND FINE GRIDS AS IT WAS FOR COARSE GRID
       ATH=SUM1/Q1
       THSITE2=BLT(IXS,JYS)-SFCHT(IXS,JYS)
       THK=THK+(THSITE-THSITE2)
       DIFF2=ABS(THSITE-THSITE2)
```

```
      IF(DBUG(6)) PRINT 9010, AVTHK,ATH,THSITE2
      IF(ITER.GT.9) GO TO 52
      IF(DIFF2.GT.1.0) GO TO 10
 52   CONTINUE
      DO 55  JP=1,NROW
      DO 55  IP=1,NCOL
        B(IP,JP)= BLT(IP,JP)
        IB(IP,JP)=JNINT(B(IP,JP))
 55   CONTINUE
      IF(DBUG(6)) PRINT 9115,IGRID
      DO 60  JP=1,NROW
      JR=NROW+ 1 -JP
 60   IF(DBUG(6)) PRINT 9105, (IB(IP,JR),IP=I1,I2)
      DO 65 JP=1,NROW
      DO 65 IP=1,NCOL
        B(IP,JP)=(BLT(IP,JP)-SFCHT(IP,JP))
        IB(IP,JP)=JNINT(B(IP,JP))
 65    CONTINUE
      IF(DBUG(6)) PRINT 9020
      DO 70 JP=1,NROW
       JR=NROW +1-JP
 70    IF(DBUG(6)) PRINT 9105, (IB(IP,JR),IP=I1,I2)
     IF(DBUG(6)) PRINT 9002
9001 FORMAT (1H1,'    BEGIN SUBROUTINE SETBLT'/)
9002 FORMAT (//'    END OF SUBROUTINE SETBLT'/)
9010 FORMAT ('  INITIAL AV. THICKNESS, M='F10.1,
    +  '   ACTUAL AV. THICKNESS ='F10.1,
    +  '   SITE THICKNESS ='F10.1/)
9020 FORMAT(1H1,'BNDY LAYER THICKNESS IN M'/)
9105 FORMAT (/1X,25I5)
9115 FORMAT (1H1,'   HEIGHT OF BNDY LAYER TOP, M, GRID ='I3)
       RETURN
       END
C
C*************************************************************************
C
      SUBROUTINE SETMAT(VALUE,ARRAY,NUM1,NUM2)
C
C     INITIALIZES ALL ELEMENTS OF ARRAY TO VALUE
C     REVISON SEPT. 1978
C
      DIMENSION ARRAY(NUM1,NUM2)
      DO 10 I=1,NUM1
      DO 10 J=1,NUM2
            ARRAY(I,J)=VALUE
 10   CONTINUE
      RETURN
      END
C
C*************************************************************************
C
      SUBROUTINE STRAT(DBUG,IG)
C
C  READS SOUNDING INFORMATION,CALCULATES LAPSE RATES & OTHER PARAM-
C  ETERS FOR VARIOUS SIGMA LEVELS
C
      LOGICAL DBUG(15)
      DIMENSION Z(50),T(50),P(50),DPTDZ(49),ZMID(49)
      COMMON /RARS/RHS(25,25,6)
      COMMON /LIMITS/NCOL,NROW,NLVL,NCOLM1,NROWM1,
     $                LOWIX(5,3),LOWIY(5,3),SFCMAX
      COMMON /SOUND/ PTLAPS(6),TO(6)
C
C  STATEMENT FUNCTION FOR POTENTIAL TEMPERATURE
C
      THETA(P,T)=(T+273.13)*((1000./P)**0.288)
```

```
C
C  READ NO. OF HEIGHTS IN SOUNDING & DATA INPUT FORM:
C       ITYP=1--
C               HEIGHT,POT TEMP LAPSE RATE
C       ITYP=2--
C               HEIGHT, TEMP & PRESSURE
C
C               READ(13,6001) NHITES,ITYP
C               READ(13,6002)(Z(I),T(I),P(I),I=1,NHITES)
C
        IF (DBUG(8)) PRINT *,'START STRAT'
        READ(13,*) NHITES,ITYP
        IF (DBUG(8)) PRINT *,'NHITES,ITYP', NHITES,ITYP
        DO 10 I=1,NHITES
           READ(13,*) Z(I),T(I),P(I)
           IF (DBUG(8)) PRINT *, Z(I),T(I),P(I)
 10     CONTINUE
        IF(ITYP.EQ.1) THEN
           DO 20 I=1,NHITES-1
                DPTDZ(I)=P(I)
                ZMID(I)=Z(I)
 20        CONTINUE
        ELSE
           DO 30 I=1,NHITES-1
                DPTDZ(I)=(THETA(P(I+1),T(I+1))-THETA(P(I),T(I)))/
     $                   (Z(I+1)-Z(I))
                ZMID(I)=0.5*(Z(I)+Z(I+1))
 30        CONTINUE
        END IF
C
C  GETTING AVERAGE HEIGHT OF LOWEST SIGMA SFCS
C
        DO 100 I=1,6
           ZBAR=0.0
C
C  GET AVERAGE HT. ABOVE LOW SPOTS FOR SIG SURFACES
C
           DO 40 J=1,5
              ZBAR=ZBAR+RHS(LOWIX(J,IG),LOWIY(J,IG),I)
 40        CONTINUE
           ZBAR=ZBAR/5.0
           DO 50 J=2,NHITES
              IF(ZMID(J).GE.ZBAR.OR.J.EQ.NHITES) THEN
                 PTLAPS(I)=DPTDZ(J-1)+(ZBAR-ZMID(J-1))*
     $              (DPTDZ(J)-DPTDZ(J-1))/(ZMID(J)-ZMID(J-1))
                 TO(I)=T(J-1)+(ZBAR-ZMID(J-1))*
     $                 (T(J)-T(J-1))/(ZMID(J)-ZMID(J-1))
                 TO(I)=TO(I)+273.13
                 GO TO 75
              END IF
 50        CONTINUE
 75        IF (DBUG(8)) PRINT*,'PTLAPS AT LEV',I,'=',PTLAPS(I)
 100    CONTINUE
        IF (DBUG(8)) PRINT*,'END STRAT'
 6001   FORMAT (2I3)
 6002   FORMAT (3F10.3)
        RETURN
        END
C
C*******************************************************************************
C
      SUBROUTINE TOPO(NUM,DBUG)
C
C   READ  AND  COMPUTE TOPOGRAPHY AT GRID POINTS
C  LAST REVISION OCTOBER '84.
C  IF NUM=0 READS TERRAIN HEIGHTS FOR ALL GRIDS.
```

```
C  IF NUM .GT. 0 PICKS TERRAIN HTS , CALLS SETBLT TO ESTABLISH
C  BNDY LYR TOP, AND COMPUTES RELATIVE HTS (RHS) FOR PROPER GRID.
C
      LOGICAL DBUG(15)
      COMMON /LIMITS/NCOL,NROW,NLVL,NCOLM1,NROWM1,
     $                LOWIX(5,3),LOWIY(5,3),SFCMAX
      COMMON/CTOP/ MCRS,NCRS,MMED,NMED,MFIN,NFIN,NGRID
      COMMON/RARS/RHS(25,25,6)
      COMMON/CSFC/SFCHT(25,25),SIGMA(6)
      COMMON /BLHT/ BLT(25,25),HSITE, AVTHK, SLFAC,STHK,BLGRX,BLGRY
      COMMON /PRLIM/ I1, I2
      DIMENSION HTCRS(25,25), HTMED(25,25), HTFIN(25,25)
C  TO ACCOUNT FOR STABLE FLOWS, THE LOWEST SIGMA SFCS SHOULD
C   INTERSECT HIGH TERRAIN. THE LIMIT FOR THIS INTERSECTION IS
C   TERLIM (IN M).
      IF(DBUG(9)) PRINT 9001,NUM
      IF (NUM.GT.0) GO TO 10
C  READ TERRAIN HEIGHT VALUES AT GRID POINTS IN METERS, ALL GRIDS
       IF(DBUG(9)) PRINT 9006
       IF(DBUG(9)) PRINT 9003
C  IN HEIGHT DATA FILE NORTHERN ROW IS FIRST, SO INVERT ORDER.
C  READ AND PRINT HEIGHTS AT COARSE GRID POINTS
      DO 8 J=1,NCRS
       JR=NCRS+1-J
      READ(11,*) (HTCRS(I,JR),I=1,MCRS)
    8 CONTINUE
        IG=1
        IF (DBUG(9)) THEN
          DO 118 J=1,NCRS
            JR=NCRS+1-J
            PRINT 4, (HTCRS(I,JR),I=I1,I2)
  118     CONTINUE
        END IF
C READ AND PRINT MEDIUM GRID HEIGHTS
       IF (NGRID.LT.2) GO TO 120
       IF(DBUG(9)) PRINT 9004
      DO 9 J=1,NMED
        JR=NMED+1-J
        READ(11,*) (HTMED(I,JR),I=1,MMED)
    9 CONTINUE
        IG=2
        IF (DBUG(9)) THEN
          DO 119 J=1,NMED
            JR=NMED+1-J
            PRINT 4, (HTMED(I,JR),I=1,MMED)
  119     CONTINUE
        END IF
  120  CONTINUE
C  READ AND PRINT FINE GRID HEIGHTS
       IF (NGRID .NE. 3) GO TO 214
       DO 210 J=1,NFIN
        JR=NFIN +1-J
       READ(11,*) (HTFIN(I,JR),I=1,MFIN)
  210  CONTINUE
       IF(DBUG(9)) PRINT 9005
        IG=3
        IF (DBUG(9)) THEN
           DO 212 J=1,NFIN
             JR=NFIN+1-J
             PRINT 4, (HTFIN(I,JR),I=1,MFIN)
  212        CONTINUE
        END IF
  214   CONTINUE
       GO TO 150
    10 CONTINUE
       DO 15 J=1,NROW
```

```
      DO 15 I=1,NCOL
      IF (NUM .NE. 1) GO TO 11
      SFCHT(I,J)=HTCRS(I,J)
   11 CONTINUE
      IF (NUM .NE. 2) GO TO 12
      SFCHT(I,J)=HTMED(I,J)
   12 CONTINUE
      IF (NUM .NE.3) GO TO 13
      SFCHT(I,J)=HTFIN(I,J)
   13 CONTINUE
   15 CONTINUE
C
C  FIND HIGHEST & LOWEST TERRAIN POINTS
C
      CALLXTREM(NUM,DBUG)
C** SET BNDY LAYER TOP (ARRAY BLT).
      CALL SETBLT(DBUG)
C DENOTE GEOMETRIC HEIGHT ABOVE TERRAIN BY RHS
      DO 67 J=1,NROW
      DO 67 I=1,NCOL
         ZVAR=BLT(I,J)-SFCHT(I,J)
         DO 67 K=1,NLVL
            RHS(I,J,K)=SIGMA(K)*ZVAR
   67 CONTINUE
  150 IF(DBUG(9)) PRINT 9002
    2 FORMAT(8F10.2)
    4 FORMAT(/,5X,21F5.0)
 9001 FORMAT (/' BEGIN SUBROUTINE TOPO, NUM='I3)
 9002 FORMAT (/' END OF SUBROUTINE TOPO'/)
 9003 FORMAT (1H1,' TERRAIN HTS, COARSE GRID, METERS'/)
 9004 FORMAT (1H1,' TERRAIN HTS, MEDIUM GRID, METERS'/)
 9005 FORMAT (1H1,'  TERRAIN HTS, FINE GRID, METERS')
 9006 FORMAT (/'   PRINTOUT IS REVERSE OF INPUT - HAS NORTH ROW 1ST'/)
      RETURN
      END
C
C*******************************************************************************
C
      SUBROUTINE WXANAL(NUM,DBUG)
C  THIS SUBROUTINE DOES THE FOLLOWING.  WHEN NUM=IGRID=1 IT
C  READS IN DATA FROM WIND PROFILES AND ASSIGNS WINDS TO
C  SIGMA LEVELS; READS  NWS STATIONS, COMPUTES THE GEOSTROPHIC
C  WIND AND ASSIGNS WINDS TO SIGMA LEVELS, COMBINES SOUNDINGS AND
C  HOURLY DATA, AND MAKES INITIAL OBJECTIVE WIND ANALYSIS USING
C  A WT FACTOR INVERSELY PROPORTIONAL TO DISTANCE SQUARED.
C  WHEN NUM .GT. 1 (IGRID=1 OR 2) IT SELECTS INITIAL WINDS FROM
C  THE NEXT COARSER GRID.
C  BY RM ENDLICH,SRI INTN'L, JAN '85
C -------------------------------
      LOGICAL DBUG(15),KEY
      COMMON /LIMITS/NCOL,NROW,NLVL,NCOLM1,NROWM1,
     $                LOWIX(5,3),LOWIY(5,3),SFCMAX
      COMMON /CVOS/ RCM,RMF,IV,DSCRS,IXCRS,JYCRS,IXMED,JYMED,
     +   IXFIN,JYFIN
      COMMON/RARS/RHS(25,25,6)
      COMMON /SITE/ IXS, JYS, THSITE, IGRID
      COMMON/UARS/U(25,25,6),UA(25,25,6),V(25,25,6),VA(25,25,6)
      COMMON /NUMOBS/ NUMDOP, NUMNWS, NUMTOT
      DIMENSION UTEMP(25,25), VTEMP(25,25)
      IF(DBUG(10)) PRINT 9001, NUM
C
C  LINES TO STATEMENT 300 ARE USED TO READ SOUNDINGS ONLY FOR COARSE
C  GRID--NUM=1.
C
      IF (NUM.GT.1)  GO TO 200
      KEY=.TRUE.
```

```
C  READ WIND SOUNDINGS AND ASSIGN TO SIGMA LEVELS
       CALL DOPSIG(DBUG,KEY)
C  READ NWS REPORTS AND INTERPOLATE TO SIGMA SFCS
C              READ(12,9014) NUMNWS
       READ(12,*) NUMNWS
       IF(DBUG(10)) PRINT 9027, NUMNWS
       IF (NUMNWS.GE.1)  CALL GEOSIG(DBUG)
C  TOTAL NUMBER OF STATIONS (NUMTOT)=NUMDOP+NUMNWS
       NUMTOT=NUMDOP+NUMNWS
C  MAKE GRID POINT ANALYSIS OF DATA
       CALL GPAN(DBUG)
C              READ (12,9014) NTSOND
        READ (12,*) NTSOND
        IF (DBUG(10)) PRINT *, 'NO.OF TSONDE=',NTSOND
        IF (NTSOND .EQ.1) THEN
           IF (DBUG(10)) PRINT*, 'WXANAL CALL STRAT,IGRID=',IGRID
           CALL STRAT (DBUG,IGRID)
           CALL RESIG(DBUG,IGRID)
           KEY=.FALSE.
           CALL DOPSIG(DBUG,KEY)
           CALL GPAN(DBUG)
        END IF
      DO 50 J=1, NROW
      DO 50 I=1, NCOL
      DO 40 LV=2,NLVL
C  TO USE RHS NEGATIVE (BELOW TERRAIN) MAKE WINDS 0.
      IF (RHS(I,J,LV).GE.0.0) GO TO 40
         U(I,J,LV)=0.0
         V(I,J,LV)=0.0
   40 CONTINUE
   50 CONTINUE
      GO TO 300
  200 CONTINUE
C  SELECT WINDS FOR SMALLER GRID FROM LARGER GRID
C  ASSIGN WINDS TO MED. GRID FROM COARSE GRID
        IF (NUM .NE. 2) GO TO 216
        DO 215 K=2,NLVL
        DO 210 I=1,NCOL
        DO 210 J=1,NROW
         IC=IXCRS+JNINT(FLOAT(I-IXMED)/RCM)
         JC=JYCRS+JNINT(FLOAT(J-JYMED)/RCM)
C  FILL IN NONZERO WINDS FROM NEAREST POINTS
       IF (U(IC,JC,K) .EQ. 0. .AND. V(IC,JC,K) .EQ. 0.) IC=IC+1
       IF (U(IC,JC,K) .EQ. 0. .AND. V(IC,JC,K) .EQ. 0.) IC=IC-2
       IF (U(IC,JC,K) .EQ. 0. .AND. V(IC,JC,K) .EQ. 0.) JC=JC+1
       IF (U(IC,JC,K) .EQ. 0. .AND. V(IC,JC,K) .EQ. 0.) JC=JC-2
         UTEMP(I,J)=U(IC,JC,K)
         VTEMP(I,J)=V(IC,JC,K)
  210    CONTINUE
        DO 212 I=1,NCOL
        DO 212 J=1,NROW
         U(I,J,K)=UTEMP(I,J)
         V(I,J,K)=VTEMP(I,J)
         IF (RHS(I,J,K).LE.0.0) U(I,J,K)=0.0
         IF (RHS(I,J,K).LE.0.0) V(I,J,K)=0.0
  212   CONTINUE
  215   CONTINUE
  216  CONTINUE
C  SELECT FINE GRID WINDS FROM MEDIUM GRID WINDS
        IF (NUM .NE. 3) GO TO 300
        DO 230 K=2,NLVL
        DO 225 I=1,NCOL
        DO 225 J=1,NROW
         IC=IXMED+JNINT(FLOAT(I-IXFIN)/RMF)
         JC=JYMED+JNINT(FLOAT(J-JYFIN)/RMF)
C  FILL IN NONZERO WINDS FROM NEAREST POINTS
```

```
      IF (U(IC,JC,K) .EQ. 0. .AND. V(IC,JC,K) .EQ. 0.) IC=IC+1
      IF (U(IC,JC,K) .EQ. 0. .AND. V(IC,JC,K) .EQ. 0.) IC=IC-2
      IF (U(IC,JC,K) .EQ. 0. .AND. V(IC,JC,K) .EQ. 0.) JC=JC+1
      IF (U(IC,JC,K) .EQ. 0. .AND. V(IC,JC,K) .EQ. 0.) JC=JC-2
        UTEMP(I,J)=U(IC,JC,K)
        VTEMP(I,J)=V(IC,JC,K)
225    CONTINUE
      DO 227 I=1,NCOL
      DO 227 J=1,NROW
       U(I,J,K)=UTEMP(I,J)
       V(I,J,K)=VTEMP(I,J)
       IF (RHS(I,J,K).LE.0.0) U(I,J,K)=0.0
       IF (RHS(I,J,K).LE.0.0) V(I,J,K)=0.0
227   CONTINUE
230   CONTINUE
300   CONTINUE
      IF(DBUG(10)) PRINT 9002
9001  FORMAT (/' BEGIN SUBROUTINE WXANAL, NUM='I3/)
9002  FORMAT (/' END OF SUBROUTINE WXANAL'/)
9014  FORMAT (3X,I5,2F8.2)
9027  FORMAT (/'  NUMBER OF HOURLY SURFACE REPORTS ='I3/)
       RETURN
        END
C
C*****************************************************************************
C
      SUBROUTINE XTREM (IG,DBUG)
C
C  FINDS 5 LOWEST SFC ELEVATIONS & GRID PT. WITH HIGHEST ELEVATION
C
      LOGICAL DBUG(15)
      DIMENSION ZLOW(5)
      COMMON/CSFC/SFCHT(25,25),SIGMA(6)
      COMMON /LIMITS/NCOL,NROW,NLVL,NCOLM1,NROWM1,
     $                LOWIX(5,3),LOWIY(5,3),SFCMAX
      DO 10 I=1,5
         ZLOW(I)=99999.
10    CONTINUE
      SFCMAX=-999999.
      DO 100 IY=1,NROW
      DO 100 IX=1,NCOL
         IF(SFCHT(IX,IY).LT.ZLOW(5)) THEN
            DO 50 I=1,5
               IF(SFCHT(IX,IY).LT.ZLOW(I)) THEN
                  IF(I.LT.5) THEN
                     DO 45 J=5,I+1,-1
                       ZLOW(J)=ZLOW(J-1)
                       LOWIX(J,IG)=LOWIX(J-1,IG)
                       LOWIY(J,IG)=LOWIY(J-1,IG)
45                   CONTINUE
                   END IF
                   ZLOW(I)=SFCHT(IX,IY)
                   LOWIX(I,IG)=IX
                   LOWIY(I,IG)=IY
                   GO TO 75
                 END IF
50           CONTINUE
           END IF
75         IF(SFCHT(IX,IY).GT.SFCMAX) SFCMAX=SFCHT(IX,IY)
100   CONTINUE
      IF (DBUG(11)) PRINT 6000, IG,(LOWIX(I,IG),LOWIY(I,IG),
     $          ZLOW(I),I=1,5)
      IF (DBUG(11)) PRINT *,'HIGHEST ELEVATION=',SFCMAX
6000  FORMAT (1X,'IN XTREM, GRID=',I2,' LOWEST COL,ROW HTS',
     $  5(/,2I4,F8.1))
      RETURN
      END
```

Appendix D

A REVIEW OF THE APPLICATION OF FRACTALS AND RELATED CONCEPTS TO ATMOSPHERIC STUDIES (with Bibliography)

CONTENTS

ILLUSTRATIONS

I INTRODUCTION

The intent of this appendix is to provide a review of some recent developments in the mathematical description of the state of the atmosphere, and of atmospheric processes. The emphasis is on physical interpretation of the mathematical concepts. Originally, the review was to be limited to fractals and fractal dimension. The emphasis remains there, but the concept of fractal dimension appears not only in connection with direct description of spatial and temporal distributions of atmospheric parameters, but also as a descriptor of equations used to describe atmospheric processes. It is in connection with the latter application that the concept of "strange attractor" enters the picture. This concept will be discussed, but not emphasized.

To date, most studies have focused on descriptive and interpretative applications of the concepts. Very little has been done toward incorporating the concepts into atmospheric modeling. This is not surprising because it is little more than a decade ago that the terms "fractal" and "fractal dimension" were coined (Mandelbrot, 1975). This neologism arose when it was recognized that what had appeared to be a very abstract branch of mathematics could serve as an analog for many natural phenomena. One of the natural phenomena to which the concept seemed most applicable was atmospheric turbulence. With this relatively short history, it is not surprising that the concepts have yet to be incorporated into fluid flow modeling. I have attempted to go somewhat beyond the usual bounds of a literature review and have made some tentative suggestions about how these new concepts might be incorporated into the flow modeling process.

II BACKGROUND

A. "Unpredictable" Determinism

Lorenz (1963) observed:

> "certain hydrodynamical systems exhibit steady-state flow patterns, while others oscillate in a regular periodic fashion. Still others vary in an irregular, seemingly haphazard manner, and, even when observed for long periods of time do not appear to repeat their previous history..."
>
> "Lack of periodicity is very common in natural systems and is one of the distinguishing features of turbulent flow. Because instantaneous turbulent flow patterns are so irregular, attention is often confined to the statistics of turbulence which, in contrast to details of turbulence, often behave in a regular well-organized manner. The short-range weather forecast, however, is forced willy-nilly to predict the details of the large scale turbulent eddies--cyclones and anticyclones--which continually arrange themselves into new

patterns. Thus, there are occasions when more than the statistics of irregular flow are a very real concern."

Lorenz (1963) then went on to show that a system could be fully deterministic in the sense that its state at one step fully determined its state at the next step, but would still be essentially unpredictable beyond a few steps, because of extreme sensitivity of the system to initial conditions. Effectively, these sensitivities make it impossible to specify the state of such a system sufficiently well that its future state can be predicted. The Navier-Stokes equations are such a system. By extension, those fluid systems such as the atmosphere that can be described by the Navier-Stokes equations will be generally unpredictable in their details and even in their major features beyond some limited time in the future. The deterministic nature of the equations and pictures of turbulent flows suggest that although future states of the system are not predictable, they may not be wholly without order. Thus, one is encouraged to seek descriptions of the system that do not obscure the order and organization that is present. The concepts of fractal dimension and strange attractors seem to provide improvements on conventional statistical measures. They augment the statistical measures rather than replace them.

B. Physical Space and Phase Space

In order to illustrate his point, Lorenz (1963) used a simple set of equations to describe a particle trajectory governed by processes closely related to those causing thermally driven convection. Those equations are

$$X' = -\sigma X + \sigma Y$$

$$Y' = -XZ + rX - Y$$

$$Z' = XY - bZ \quad . \qquad \text{(II-1)}$$

Here, $(\ )'$ represents a rate of change with respect to a dimensionless time; X, Y and Z are locations and the other parameters are constants that can be related to thermodynamic properties. The above set of equations has come to be called the "Lorenz attractor." Lorenz (1963) analyzes the properties of the equations to show that certain choices of constant values and initial conditions lead to steady-state or periodic trajectories. However, the most interesting cases are those that are neither stationary nor periodic. He used numerical integration to study the subspace in which such trajectories are ultimately confined. Lorenz' analysis indicates that the trajectories become confined to a convoluted surface that has zero volume. If the trajectories were periodic (i.e. they passed more than once through the same point, and because of the deterministic nature of the system, they repeated their passage through all subsequent points), then the solutions would be confined to a closed, distorted curve that had neither volume nor area.

The Lorenz trajectories will often tend to cluster around a limited number of points, referred to as attractors. The trajectory may stay for a number of steps in the vicinity of one of the attractors and then make a relatively rapid leap into the domain of another, stay there for awhile and then return. The nature of the trajectory-containing surfaces, and the factors that govern shifts from one attractor to another are of considerable interest because of their relevance to our understanding of the solutions to these systems.

In the case of the Lorenz attractor, the motion of the point described by the equations takes place in three-dimensional physical space. The x, y, z coordinates and the u, v, w components of motion could be considered to be descriptors of the "state" of the particle. It is common to represent the state of a fluid system by the values of relevant parameters (e.g. wind components, temperature) at a number of grid points. Then, the evolution of the fluid flow can be considered as a trajectory in this high-dimensional state (or phase) space.* The subspace occupied by the trajectory will generally be of lower topological dimension than the state space itself. The degree to which this subspace fills the complete space is determined by the nature of the equations. In many cases there will preferred regions of the phase space, i.e. attractors.

At least intuitively, the above discussion suggests that it may be possible to approximate fluid flows with fewer descriptors, and that descriptions of the shapes of the subspaces containing the solutions might provide a basis for statistical descriptions of the flow. Fractal dimension, as will be discussed later, provides a measure of the degree to which the phase space is filled by the solutions. It is this fact that has provided one of the motivations for applying the concept of fractal dimension to the study of turbulence. The hope prevails that fractals will provide a means for deriving statistical properties of turbulent fields, especially those associated with the observed intermittency of most turbulence.

There are other reasons, based on physical arguments, for believing that fractal concepts show promise for providing quantitative descriptions of turbulent fields. These other reasons will be discussed later, but it is worth noting here that the physically descriptive part of the theory can be used directly to generate "realistic" distributions of parameter values in physical space, e.g. the shapes of surfaces of constant value (iso-surfaces) can be generated. Through appropriate transformations, it is also possible to estimate fractal dimension from a time series of parameter values at a single point.

This review emphasizes applications of fractals to distributions in physical space, because the ultimate objective is to use the concepts to

---

*The terms "state space" and "phase space" are both found in the literature, but the latter seems more common.

simulate small scale distributions from information contained in larger scale distributions. In principle at least, there is potential for providing a means of closure for the large scale fluid flow equations.

C. Statistical Descriptions

It is natural to invoke statistical descriptions when trying to describe some deterministically unpredictable behavior. One of the more common statistical descriptors of turbulent behavior is the probability distribution associated with differences in parameter value over a specified distance, i.e.

$$F(q,\Delta r) = Pr[\Delta c(\Delta r) > q] \qquad \text{(II-2)}$$

where $Pr[r > s]$ is the probability that the argument inequality is true; $\Delta c(x)$ is the absolute value of the difference in c at two points separated by a distance x. If the variable c is uniformly distributed, then Δc will always be zero as will $Pr[\Delta c > 0]$.

For many practical purposes, it is the tail of the distribution that is of greatest interest. The tail involves the large, infrequent fluctuations. The nature of the tail of the distribution will have important effects on the higher moments of the probability function. Probability distributions will vary according to the separation distance between points. For example, it is natural to assume that the likelihood of exceeding some specified difference value increases as the separation between the points increases. The next section describes a simple functional relationship between the probability distributions for different separations that has been found to be applicable to many natural phenomena.

D. Scaling

Qualitatively, the fluctuations in a field that is "scaling" look the same regardless of magnification. That is, the large scale fluctuations are qualitatively the same as the middle scale fluctuations embedded within them. Those middle scale features are in turn similar to the still smaller fluctuations superimposed upon them. For a scaling field of the parameter c, this can be quantitatively defined as follows. First,

$$\Delta c(\Delta z) = c(z_o + \Delta z) - c(z_o) \quad , \qquad \text{(II-3)}$$

i.e. Δc is the change in c between z_o and $z_o + \Delta z$. If the field is scaling, then the relationship between the probability distributions for the large scales and those for the smaller scales is defined as follows:

$$Pr[\Delta c(\lambda \Delta z) > q] = Pr[\lambda^{n} \Delta c(\Delta z) > q] \quad . \qquad \text{(II-4)}$$

Scaling fields are fractals.

The potential importance of fractals arises from two facts. First, many natural phenomenon have been found to be scaling over large ranges of sizes. Second, the use of probability distributions to describe the likelihood of observing specified differences in value has proven to be a useful tool in the analysis of diffusing scalars and turbulence.

E. Relevance to Conventional Fluid Flow Modeling

Typically, numerical modeling of fluid flow involves processes that will affect the larger scale features of the flow, but are too small to be resolved by the grid that is used. Even the vortex methods (e.g. Leonard, 1985) which provide more detail in areas with the most fine structure face computational limitations that force approximations for small scale features. In general, the problem is to define either the small scale features, or their effects, in terms of those features that are resolved by the modeling. Fractals have promise for providing descriptions of small scale processes, but to date there does not seem to have been any practical application described in the literature. There have been methods described for generating fields with the appropriate fractal dimension (e.g. Lovejoy and Mandelbrot, 1985). If fields generated in this way were realistic they could presumably provide a basis for developing empirical parameterizations. Another possible avenue can be found in the spectral representations of scaling fields (e.g. Pentland, 1984). In principle, scaling allows the spectral density functions to be extrapolated to higher wave numbers (smaller scales), but it is not clear whether computationally efficient methods can be developed for taking advantage of this, or whether the effects of cross-product terms (those involving more than one parameter) can be treated realistically.

III FRACTALS, TURBULENCE, AND PHYSICAL SPACE

A. Discussion of Fractal Dimension

1. Definitions and Hypotheses

This section will discuss isotropic fractals. Later, the concept will be extended to the anisotropic case which seems more applicable to processes in the atmosphere.

Schertzer and Lovejoy (1983) show that for many atmospheric properties (e.g. kinetic energy, the logarithm of the potential temperature), the upper tail of the probability distribution discussed earlier falls

off algebraically, rather than exponentially. That is, it can be represented by:

$$Pr(\Delta c > q) = k\ \Delta c\ q^{-\alpha} \qquad \text{(III-1)}$$

The above relationship means that the probability of a random fluctuation Δc exceeding a fixed value q is proportional to that fixed value raised to the $-\alpha$ power, i.e. $q^{-\alpha}$. The exponent, $-\alpha$ is a measure of the intermittency of the distribution.

We can examine how the moments behave as a function of α. Recalling the definition of the rth moment, ν_r

$$\nu_r = \int_0^\infty c^r\ f(c)dc \qquad \text{(III-2)}$$

where f(c) is the probability density function, i.e. the derivative with respect to c of the cumulative probability function discussed earlier. When $Pr(c > q) = kq^{-\alpha}$, f(c) is given by

$$f(c) = k\alpha c^{-(\alpha+1)} \qquad \text{(III-3)}$$

substituting the definition for the rth moment gives

$$\upsilon_r = k\alpha\int_0^\infty c^{r-\alpha-1}dc \quad . \qquad \text{(III-4)}$$

A consequence of this distribution is that there will be a problem in defining moments higher than α. According to Schertzer and Lovejoy (1983), the higher moments will diverge so that the experimental estimation will increase without limit as the sample size increases.

There is an interesting conjecture that can be made in connection with the divergence of the higher moments. I have not seen the following line of reasoning spelled out in the literature, but it is relevant to the feasibility of the higher order turbulent closure schemes that are included in some fluid models. Higher order closure schemes require a parameterization of cross-product terms whose order may be the same as, or greater than the order at which the moments begin to diverge. It seems reasonable to assume that if the "self-products" involved in calculating the moments do not converge, there may be problems with the convergence of the cross-products. As noted, this is purely a conjecture, but it seems prudent to investigate it further before elaborate higher-order turbulent closures are developed.

2. Methods for Determining Fractal Dimension

Several different approaches have been developed for calculating fractal dimension. One of these follows more or less directly from the fact that fractal dimension is a measure of the space-filling properties of a curve or a higher dimensional surface. Another approach estimates the parameters of the probability distributions, which are directly related to the fractal dimension. The fractal dimension can also be derived from the spectral density function and one method is based on this approach. Finally, it is possible to estimate the fractal dimension of the attractor for a given system from a time series at a single point. The applicability of this latter method to fluid flow modeling applications is not clear, but for the sake of completeness a brief description of the approach is included.

a. Subcell counting methods

Mandelbrot (1975) used a discussion like that which follows to define fractal dimension and its relation to the "space filling" concept. If the distribution of some parameter is continuous, then there are iso-surfaces containing all the points that have the same value. In order to determine the fractal dimension of one of these iso-surfaces, we select a large cube in space that contains at least a part of that surface. We then define the length of the side of that cube as an external scale, L, and subdivide the cube into smaller cells with sides of length, ℓ. We then count the number of these smaller cells that contain at least one point on the iso-surface. If our "surface" is a straight line, then the number of small cells through which it passes will be proportional to $(L/\ell)^1$. If the surface is a flat plane, then the number of small cells through which it passes will be approximately proportional to $(L/\ell)^2$. Finally, if the distribution of the parameter in space is such that every point has the same value, then the "iso-surface" will be solid and the number of cells intercepted will be proportional to $(L/\ell)^3$: In all these examples, the exponent of the term (L/ℓ) is simply the Euclidian dimension of the "surface."

The concept of dimension outlined in the preceding paragraph can be extended to fractional dimensions, if we imagine a line with many "wiggles", and with wiggles upon those wiggles and so on and on. In such a case, the number of small cells (n) through which the line passes will be approximated by

$$n = k\,(L/\ell)^D \quad , \qquad \text{(III-5)}$$

where D is a number larger than one, but less than two. Similarly, a plane might have roughness elements with smaller roughness elements upon them and so on, in that case, the exponent D would be larger than two but less than three. The exponent D in these cases is analogous to the Euclidian dimension, except that it need not be an integer. Mandelbrot coined the term fractal (from "fractional dimension") for geometric

shapes (lines, surfaces, etc.) that have this property. Fractals are self-similar in that the fluctuations at a small scale are related to those at a larger scale by a constant power of the scale ratio over a wide range of scales. Lovejoy and Schertzer (1986) have pointed out that there are good physical reasons for the exponent for vertically oriented features to differ from that from those for the horizontal features in the atmosphere. This will be discussed further in a subsequent section.

According to Greenside et al (1982), Takens (1981), suggested an algorithm for computing fractal dimension based on Mandelbrot's (1975) definition outlined above. Greenside et al (1982) concluded that this approach was impractical for systems with dimensions greater than 2, because of convergence problems. These findings do not seem to preclude the use of the method for finding the fractal dimension for isopleths of a scalar in a plane, although the convergence may be slow. The method should probably not be applied to problems involving high-dimensional phase spaces. When the definition is reduced to two dimensions, a square and smaller squares replace the cube and subcubes, so it can be used to examine isopleths of a scalar in a plane intersecting an isosurface.

The cell counting concept is reasonably direct, and easily applied to an array of discrete numbers such as a digitized image. This makes it particularly useful for the analysis of cloud photos, or backscatter cross-sections through smoke plumes, as are obtained with mobile lidar systems. Another potential application would be to digitized images of the markers in laboratory turbulence experiments. One interesting feature of the technique, as it is applied to smoke plume cross-sections arises from the fact that the isopleths tend to be concentric (Ludwig and Nitz, 1986), so the fractal dimension obtained for low-value isopleths are applicable at the edges of the plume, while those for the higher values will be characteristic of the center.

Personal experience has shown that one does not have complete freedom in the choice of the area over which an algorithm based on the cell counting method can be applied, especially in the case of arrays of discrete values. The method uses linear regression to find the constants for the logrithmic form of Equation III-5, i.e.

$$\log(n) = \log(k) + D \log(L/\ell). \qquad \text{(III-6)}$$

In practice, we want as many values of N as possible. For a discrete array, each N must correspond to an integer value of (L/ℓ). This means that we must select the large squares so that they have a side length L that has many divisors. For example, if we choose a large square whose side L is a prime number of grid points, then we will only get two points from which to calculate the regression constants in Equation III-6. It turns out that a wide choice of values can be achieved by judicious use of products of powers of two, three and five. Using this approach, it is possible to limit the analysis to a region which

encompasses that part of the image which is of interest, but does not extend very far into background areas.

b. A Method Based on Spatial Variation Probability Distributions

We have already noted that spatially varying fields are frequently characterized by the probability distributions for the difference between values at two points separated by a specified distance, and that there is a functional relationship for the probability distributions for different separation distances. Schertzer and Lovejoy (1983) presented the following approach that makes use of these definitions to determine fractal dimension. Starting with the definition of a fractal (scaling) pattern, i.e.

$$Pr[\Delta c(\lambda Y) > q] = Pr[\lambda^H \Delta c(Y) > q] \qquad \text{(III-7)}$$

As before, $\Delta c(x)$ is a change in value of the variable c over the distance x. In practice, Y will generally be the smallest separation between points in the available data set. Equation (III-7) can be used to estimate the exponent H if one determines various quantile values as a function of the separation distance (λY) and then determines the best fit value for H.

If we accept the hypothesis of Schertzer and Lovejoy (1983) that the upper tail of the distribution has a hyperbolic form for large q

$$Pr(\Delta c > q) = kq^{-\alpha} \quad , \qquad \text{(III-8)}$$

then the constants H and α can be estimated from the data as the best fit values for the following relationship--again, for large values of q:

$$Pr[\Delta c(\lambda Y) > q] = k\, \lambda^H q^{-\alpha} \qquad \text{(III-9)}$$

The steps necessary to apply this method are as follows:

(1) Determine λ^H and α at different separations for upper tail percentiles less than a few percent.

(2) Determine the average value of α, providing that the individual values of α are sufficiently similar.

(3) Find H by a log-linear regression of λ^H values.

The scaling parameter H is related to fractal dimension as follows (Pentland, 1984):

$$D = 2 - H, \qquad \text{(III-10)}$$

Schertzer and Lovejoy (1983) analyzed distributions of several different atmospheric parameters by the above method and found that the data

support the hypothesis of a hyperbolic upper tail for the probability distribution. They also found that the data showed that the distributions are anisotropic with vertical fractal dimensions that are different from those in the horizontal. The importance of this fact will be discussed later.

c. Spectral Analysis Methods

The method described in the preceding section, based on the probabilities of finding differences of a specified magnitude as a function of separation distance, is closely related to the estimation of spatial autocorrelation. Therefore, we might expect that there would be spectral analysis methods that could be used to estimate fractal dimensions. For a variable that satisfies the scaling relationship presented above, the exponent of the corresponding power spectrum ($-\beta$) is related to the scaling exponent H as follows:

$$\beta = 2H + 1 \quad . \tag{III-11}$$

Combining Equations III-10 and III-11 gives

$$\beta = 5 - 2D \quad . \tag{III-12}$$

Thus, the power spectrum P(f) of a scaling field will be proportional to f^{2D-5}, where P is the spectral density as a function of wave number f. This relationship can be used as the basis of a method for estimating the fractal dimension of a field, where fast Fourier Transform (FFT) methods are used to generate the amplitudes of the Fourier terms in wave number space. The power spectrum is then fit without regard to direction. In essence, the procedure averages the amplitudes around circles of constant wave number radius. If anisotropic effects are to be included, the power spectra along different axes would be examined. Pentland (1984) has shown that the spectral method can be applied to fairly small subsections of an image. He used the method to characterize the fractal dimensions of 16 x 16 pixel subsections of photographs. The fractal analysis provided a basis for distinguishing the inhomogeneities in the areas of the picture that had similar texture. The method is efficient because it uses FFT algorithms and simple linear regression, but substantial changes would be needed to address anisotropic effects.

d. Estimation of Fractal Dimensions from Time Series

As we noted earlier, the time evolution of some system can be fully described by a trajectory in an n-dimensional phase space. Trajectories for atmospheric systems are often contained within "surfaces" whose dimension d is smaller than that of the complete phase space, i.e. $d < n$. Measurements are more commonly available for a long period of time at a few individual locations than at enough points to describe the

state of the system. Therefore, it is be desirable to have a method that can use time series data to estimate fractal dimension of the surface containing the state trajectories. Fraedrich (1986) presents a discussion of how this is done. This discussion and that of Packard et al (1980) form the basis for the following description. If the dynamics of the system are described by a set of n ordinary differential equations

$$\dot{x}_j = f_j(x_1, x_2, \ldots, x_n); \quad j = 1, \ldots, n \quad , \qquad \text{(III-13)}$$

then the phase space is described by the n coordinates x_j, (j=1, ..., n). These are the dependent dynamical variables. The symbol (·) indicates differentiation with respect to time; the time evolution of the system can be written as an n-dimensional vector function of time $[x_1(t), \ldots, x_n(t)]$, defining the trajectory in phase space. The differential Equations (III-13) can be reduced to a single (albeit highly nonlinear) differential equation involving only one of the variables, if all the others are eliminated by differentiation. This nth order equation will be of the form

$$x^{(n)} = f[x, x', \ldots, x^{(n-1)}] \quad . \qquad \text{(III-14)}$$

This is equivalent to n equations describing the time series of the variable x(t) and its first n-1 derivatives, $x'(t), \ldots, x^{(n-1)}(t)$. The Equations (III-14) are equivalent to the original set of differential Equations (III-13), but with the important difference that all the variables can be determined from measurements at a single point -- if the measurements have sufficient temporal resolution to obtain the necessary higher-order derivatives.

According to Fraedrich (1986), if the dimension d of the attractor contained within the original n-dimensional phase space is much less than n, it can then be described in the new phase space made up from the single variable and its derivatives. In fact, Fraedrich (1986) notes that the dimensionality of the new phase space can be smaller than that of the original phase space, i.e. one need not include all n-1 derivatives. In fact, 2d+1 variables (i.e. the variable and its first 2d derivatives should be sufficient).

In practice, one does not need to know the number of state variables in the original phase space, if sufficiently many derivatives are included. Also, in practice the measurements are available at discrete times, so that (2d-1) discrete time lag multiples are substituted for continuous derivatives. In this new system, we deal with the following vector

$$\underline{x}(t) = \{x(t), x(t+\tau), \ldots, x[t + (2d-1)\tau]\} \qquad \text{(III-15)}$$

In order to ensure linear independence, the time shift τ is chosen so that autocorrelations vanish.

Observed time series of a single variable describe trajectories in this new phase space, so that one of the methods discussed earlier can be used to determine the dimension of the structure formed by those trajectories. Of course, one must know that dimension first to determine how many derivatives (time shifts) must be included in the calculations. It is desirable to minimize that number because the required calculations increased dramatically with increasing numbers of dimensions. Also, as noted before, the cell counting method may not be appropriate for dimensions greater than two (Greenside et al, 1982).

Fraedrich (1986) uses an algorithm of Grassberger and Procaccia (1983) that provides an estimate for the lower limit of the fractal dimension. Fraedrich (1986) notes that in most of the cases that were analyzed, this lower limit was very close to the actual value. In order to circumvent the problems arising from a lack of foreknowledge about the fractal dimension, Fraedrich (1986) calculates fractal dimension using successively larger numbers of derivatives until he finds that the calculated dimension no longer changes with an increase in the number of dimensions in the phase space.

Obviously, methods based on time series from a single-point have considerable practical advantage over those that must analyze data from a multitude of individual points. Thus, this method deserves further exploration with regard to its application to studies of turbulence, including results obtained from numerical simulations, especially large eddy simulations (LES). To date, it appears that the applications of the technique have been much like those of Fraedrich (1986) and have involved climatic and other variabilities on time scales much longer than those appropriate to studies of turbulence and turbulent effects.

3. Generation of Fractal Fields with Specified Characteristics

One possible, practical use of the fractal concept would be to develop parameterizations for estimating fractal characteristics from large-scale flow parameters so that fields with the appropriate characteristics could be generated and used for empirical characterization of terms appearing in conventional closure schemes. This approach would require a method for generating fields with the appropriate fractal characteristics. This problem has been addressed, in large part because of its relevance to the generation of realistic looking artificial landscapes.

Probably the most efficient way of generating such fields is to use the appropriate Fourier series, but that technique may not allow introduction of randomness. Lovejoy and Mandelbrot (1985) describe a technique that they call the "fractal sums of pulses" (FSP) method for generating rainfall intensity statistics that have the appropriate fractal properties. In one dimension, i.e. a time series of rainfall intensity, R(t), the FSP method works as follows. The function R(t) is generated as a sum of randomly located rectangular pulses with random

height (rainfall intensity) and duration. The random locations of the centers are distributed according to a Poisson process with constant rate, ν. To ensure scaling, Lovejoy and Mandelbrot (1985) choose $Pr(\rho' > \rho)$ to be proportional to ρ^{-1}; ρ is the duration. Thus, the probability of a random duration ρ' exceeding ρ is proportional ρ^{-1}. The height of the rectangle (or rainfall intensity increment, ΔR) is taken to be equal to $\pm (\rho')^{1/\alpha}$. They point out that for any given duration ρ', the pulse intensity has a random sign, but a fixed absolute value.

This one dimensional model scales with an exponent $H=1/\alpha$. A change in duration scale by a factor of λ will change the intensity by a factor of $\lambda^{1/\alpha}$. The intensity probability distribution will be hyperbolic with an exponent of α, because of the rainfall duration probability distribution and choice of relationships between rainfall duration and rainfall intensity.

The pulses need not be rectangular, but can be smooth and continuous if their length scales as λ and the intensity scales as $\lambda^{1/\alpha}$. Lovejoy and Mandelbrot (1985) suggest a pulse shape with an amplitude ΔR proportional to $\Delta R \exp[-(u/\rho)^{2S}]$, where u is the distance from the pulse center. This arbitrary shape is convenient because the pulse is smooth for small values of S, becoming more discontinuous (more nearly rectangular pulses) as S becomes larger.

The method can be extended to more dimensions. For an isotropic distribution in two dimensions, the simplest pulse is a randomly placed right circular cylinder. The probability that the base area A of the cylinder exceeds a specified value is inversely proportional to the value, while cylinder height (intensity) equals $\pm A^{1/\alpha}$. It is necessary to define an intensity threshold and set values below that threshold to zero when a positive field (e.g. rainfall) is represented.

Although the rain fields constructed by the above method have the generally appropriate fractal properties, they tend to be sharp-edged and produce too few separate rain areas. Lovejoy and Mandelbrot (1985) go on to describe other models using pulses with annular bases and elliptical annuli of varying eccentricity to simulate anisotropic effects.

Medler et al (1986) have used some of the ideas presented by Lovejoy and Mandelbrot to generate reasonably realistic images of smoke plumes. However, it should be noted that their simulations are not based on observed fractal properties. They have simply chosen fractal properties to achieve a degree of visual realism in the images that they produce. Lovejoy and his coworkers (e.g. Lovejoy and Schertzer, 1985, 1986; Lovejoy and Mandelbrot, 1985; Schertzer and Lovejoy, 1983) have produced images that simulate clouds and precipitation areas using the methods described above. Unlike Medler et al (1986), they have attempted to use parameters based on observational evidence. They have also attempted to include anisotropic effects.

Although considerable progress has been made in producing scalar fields that have fractal properties similar to those observed for certain atmospheric variables, there are some very important problems which do not yet appear to have been addressed. In particular, I have found no reports where fractals have been used extend to some larger scale description to smaller scales. Medler et al (1986) and Pentland (personal communication, 1986) have superimposed fractal patterns on general Gaussian plume concentration cross sections, but have not used observed fractal parameters in the process. Furthermore, both applications have been limited to isotropic fractals.

Another area where much remains to be done with fractals is vector field simulation. This represents a formidable task, but is very important because appropriate vector fields could serve as a basis for turbulent closure or direct simulation of subscale eddy processes. Although at least one method for estimating fractal dimension can be applied to vector quantities (e.g. Pentland, 1984), it is not immediately obvious how that definition can be used to generate vector fields with appropriate fractal properties and statistical relationships between components.

B. Why Turbulence Might Be Expected to be Well Described by Fractals

To this point, the discussion has focused on definitions of fractals and related concepts without giving serious attention to the physical reasons why they may be important in the study of turbulence and turbulent diffusion of scalars. There are at least five kinds of evidence which suggest the connection:

(1) The structure of turbulent eddies observed in flow visualization experiments

(2) Similarity arguments from classical turbulence theory

(3) Detailed numerical flow simulations

(4) Characteristics of the governing equations, and

(5) detailed analysis of the spatial distribution of atmospheric scalars.

These are discussed in the following sections.

1. Shear Layer Flow Visualization

Reynolds (1985) provides a qualitative discussion of the processes and the structure in a turbulent mixing layer forming in the shear zone between fluids flowing at different velocities. The structure evident in Figure 1 occurs quite commonly. Although Reynolds does not mention fractals, his discussion provides evidence of scaling and similarities between the structure of the motion field on different scales. What follows is based on the material presented by Reynolds (1985).

Figure D-1 shows what happens in a mixing layer flow. Initially, vorticity flows from the tip of the separator that is used to generate the flow. An unstable 2-dimensional shear layer is formed. The instability can be excited by random noise or slight vibrations. Once excited, it grows rapidly so that vorticity is quickly concentrated in nearly discrete vortices, oriented generally perpendicular to the flow direction, although they may include some irregularities. It is important to note that not all the vorticity is concentrated in the major features, but some remains in "braids" that connect the major vortices, as shown in Figure D-1. As will become evident, this has important consequences.

As noted above, there may be irregularities in the spacing or orientation of the main vortices. Such irregularities can cause the vortices to move at different velocities, so that they merge and their size increases in the downstream direction. Figure D-2 (adapted from Reynolds, 1985) shows schematically how this takes place. The regularly spaced, uniform vortices at the left of the figure interact so that induced motions (e.g. the motion of vortex C caused by vortex B) are cancelled (e.g. by vortex D). Some of the irregularly spaced vortices shown at the right of the figure will move up and others will move down. Eventually some pairs move close together and orbit one another or merge.

It is in the braids between the large scale vortices where the evidence of fractal structure may be found. As noted before, some vorticity remains in the braids to be stretched as the large scale vortices "wind in" the fluid between them. Stretching intensifies the vorticity in the braids, forming new vortices with axes aligned along the principal strain direction as shown in Figure D-3. These vortices undergo the same processes described above, but on a smaller scale and with different orientation. One can expect that the new, smaller vortices also contain irregularities that cause them to merge, and that new "minibraids" form and are stretched along new strain axes. These new structures can undergo similar deformation on a still smaller scale, so that the processes are likely to continue down to the scale of viscous dissipation. Thus, qualitatively we would expect scaling and a similarity of turbulent structure to extend over a wide range of scales, from the outer scale defined by the large, merged vortices down to the scale of molecular dissipation processes. It should be noted that analogous reasoning can be applied to other flow types such as jets, boundary layers and wakes which are also characterized by regions of strong shear and concentrated vorticity.

2. Classical Theory

The term "classical theory" in this section's title refers to Kolmogorov's early deductions concerning the cascade of energy through the turbulent spectrum. However, the derivation that follows is taken from Frisch et al (1978), because their discussion provides a somewhat

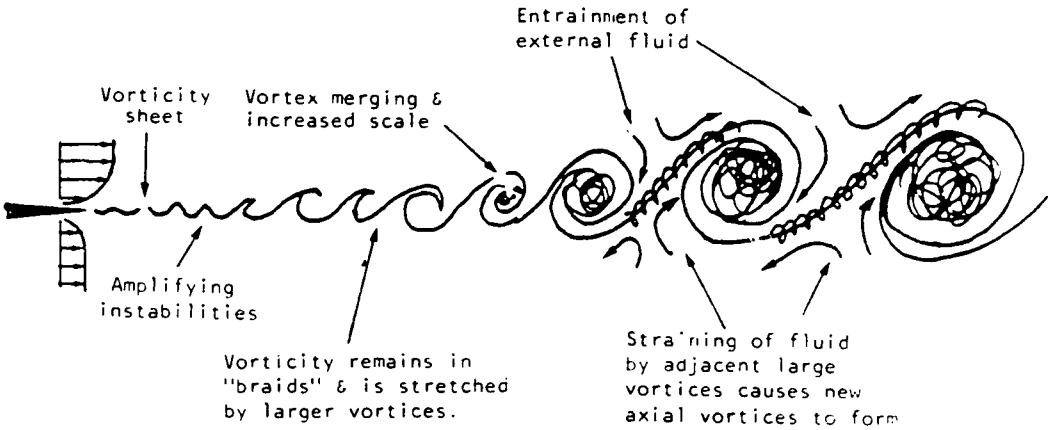

Adapted from Reynolds, 1985

FIGURE D-1 SCHEMATIC DIAGRAM OF MIXING LAYER TURBULENT BEHAVIOR

AD-A175 410 BEHAVIOR OF SMOKES AND AGENTS DURING VARIABLE METEOROLOGICAL CONDITIONS OVER COMPLEX TERRAIN(U) SRI INTERNATIONAL MENLO PARK CA F L LUDWIG SEP 86 2/2

UNCLASSIFIED ARO-19630.8-GS DAAG29-83-K-0009 F/G 4/2 NL

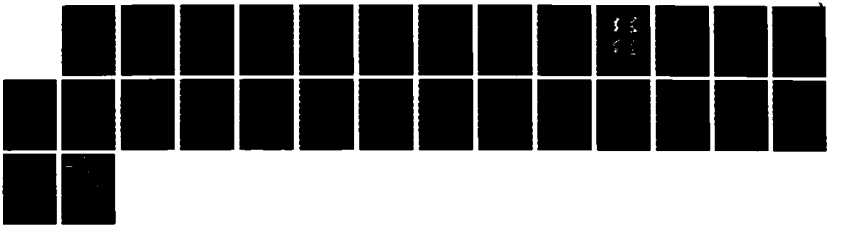

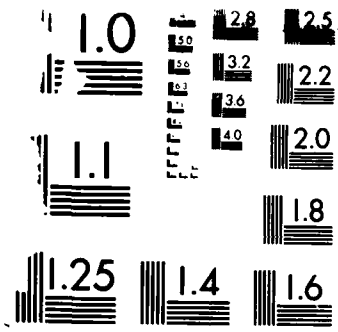

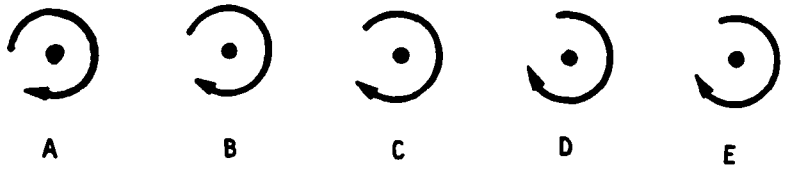

a. Regularly spaced vortices

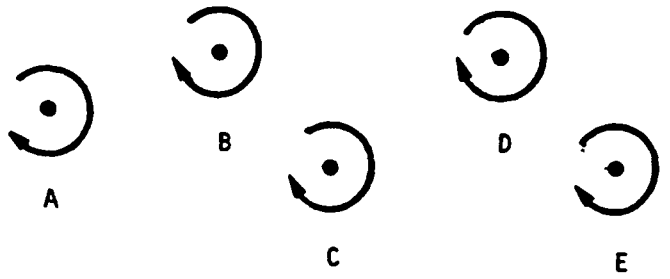

b. Irregularly spaced vortices

Adapted from Reynolds, 1985

FIGURE D-2 SCHEMATIC DIAGRAM OF VORTEX INTERACTIONS

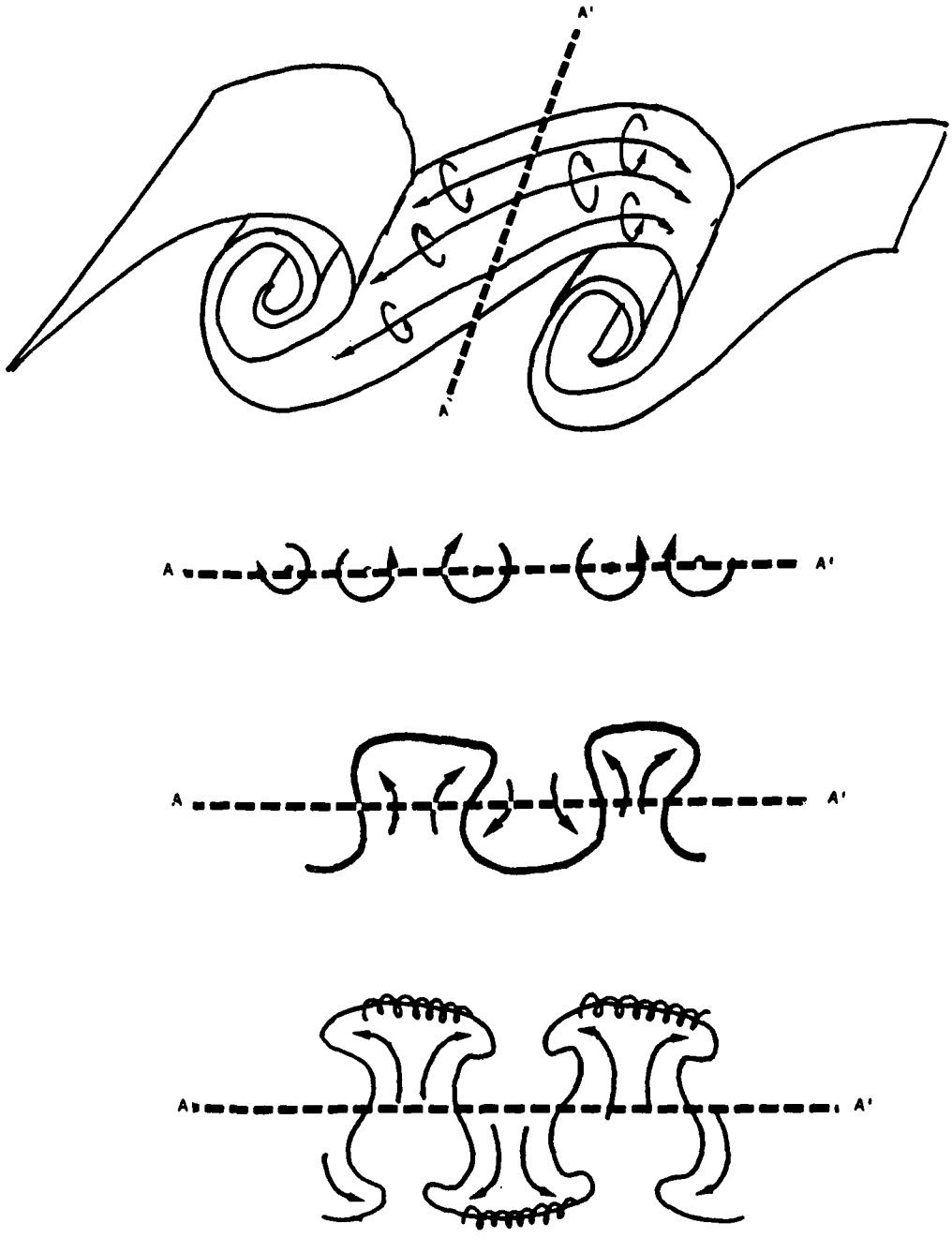

Adapted from Reynolds, 1985

FIGURE D-3 SCHEMATIC DIAGRAM OF BRAID FORMATION AND BEHAVIOR

more physical picture of the process. Similar arguments have also been given by Lovejoy and Schertzer (1986). We begin by defining the energy spectrum E(k) as the kinetic energy per unit mass per unit wave number k. For purposes of argument, Frisch et al (1978) choose to define a discrete spectrum of eddies beginning with the large scale ℓ_o where the energy is introduced and proceeding to successively smaller wave numbers according to the relationship

$$\ell_n = \ell_o 2^{-n} \quad , \qquad n=0,1,2, \ldots, \qquad \text{(III-16)}$$

the corresponding wave numbers are

$$k_n=1/\ell_n \quad . \qquad \text{(III-17)}$$

The discretized kinetic energy per unit mass in the wave numbers near ℓ_n is given by

$$E_n = \int_{k_n}^{k_{n+1}} E(k)dk \quad . \qquad \text{(III-18)}$$

If the turbulence is statistically stationary, energy introduced at large scales (ℓ_o) is transferred to successively smaller scales until the dissipation scale ℓ_d is reached. We can define a characteristic velocity v_n *in terms of* E_n *for the* k_n eddies, *i.e.*

$$E_n \sim v_n^2 \quad . \qquad \text{(III-19)}$$

It should be noted that v_n is not total velocity, but rather a velocity difference characteristic of that particular eddy size ℓ_n. With this in mind, an eddy turnover time t_n can be defined

$$t_n \sim \ell_n/v_n \quad . \qquad \text{(III-20)}$$

Frisch et al (1978) go on to argue that in the inertial subrange--where t_n is much greater than the viscous dissipation time, ℓ_n^2/ν (ν is the kinematic viscosity), and much less than the characteristic time for the larger scale motions, ℓ_o/v_o--we can define an energy (per unit mass) transfer rate from eddies of wave number k_n to k_{n+1} to be

$$\epsilon_n \sim E_n/t_n \sim v_n^3/\ell_n \quad . \qquad \text{(III-21)}$$

If the process is stationary as hypothesized, then the energy dissipation rate ϵ_n will be a constant $\bar{\epsilon}$, and we can now solve for v_n and E_n:

$$v_n \sim (\bar{\epsilon}\ell_n)^{1/3} \qquad \text{(III-22)}$$

$$E_n \sim (\bar{\epsilon}\ell_n)^{2/3} \quad , \qquad \text{(III-23)}$$

Equations (III-22) and (III-23) are the same as Kolmogorov's result for the structure functions. A Fourier transformation provides the wave number spectrum

$$E(k) \sim \bar{\varepsilon}^{2/3} k^{-5/3} \quad . \tag{III-24}$$

We can also obtain the eddy turnover time

$$t_n \sim \bar{\varepsilon}^{-1/3} \ell_n^{2/3} \quad . \tag{III-25}$$

The above results can be rewritten to show their scaling properties more clearly. For example from Equation (III-22)

$$E_n \sim \bar{\varepsilon}^{2/3} \ell_n^{2/3} = \bar{\varepsilon}^{2/3} \ell_o^{2/3} (\ell_n/\ell_o)^{2/3} \tag{III-26}$$

$$E_n = E[(\ell_n/\ell_o)\ \ell_o] \sim E_o(\ell_n/\ell_o)^{2/3} \quad . \tag{III-27}$$

Thus, the energy per unit mass per unit volume scales according to $(\ell/\ell_o)^{2/3}$. There is a tacit, but very important assumption in the above relationship, i.e. all eddy sizes are assumed to be spread more-or-less uniformly throughout the same volume.

For greater generality, Frisch et al. (1978) assume that the smaller eddies are less space filling than the larger ones. Certainly, the qualitative behavior of mixing layer turbulence described in the preceding section makes such an assumption plausible. This assumption requires that we introduce a new parameter to characterize the degree to which the cascade is space filling. If the whole volume is filled by eddies of all sizes, then the cascade we have been discussing (where $\ell_n = \ell_o^{-n}$) has 2^3 times as many eddies of size ℓ_{n+1} as it has of size ℓ_n. That is, it takes eight eddies of dimension $\ell/2$ to fill the volume occupied by one of dimension ℓ. Frisch et al (1978) define β to be the ratio of the average number of ℓ_{n+1} eddies produced by each ℓ_n eddy and the maximum possible, i.e. eight. If eddies of size ℓ_o are space filling, then eddies of size ℓ_n will fill only a fraction β_n of the total space

$$\beta_n = \beta^n = (N/2^3)^n \tag{III-28}$$

where N is the average number of eddies formed by each eddy of the preceding generation; $N \leq 8$.

Frisch et al (1978) assume that the eddies of the (n+1)th generation are positionally correlated with those of the nth generation by embedding or attachment. This seems to mean that they believe that the smaller eddies are produced in the same general area as the larger eddy

from which they arise. The discussion of mixing layer turbulence given in the preceeding section suggests that the "positional correlation" is more likely to be one of "attachment" than "embedding." Frisch et al (1978) are assuming that the region where an eddy is formed becomes an "active region" for the cascade to smaller sizes. There seems to be one other tacit assumption in the arguments of Frisch et al (1978) that they do not explicitly state. It appears that they assume that the average number of eddies formed, N, does not vary systematically according to eddy size.

Frisch et al (1978) redefine the typical velocity difference v_n in terms of active regions only, so that the kinetic energy per unit mass associated with scales on the order of ℓ_n is given by

$$E_n \sim \beta_n v_n^2 \quad . \tag{III-29}$$

The characteristic time for energy transfer from ℓ_n-scale eddies to smaller scales remains the same, i.e. $t_n = \ell_n/v_n$, assuming that the production of eddies of the next smaller scale arises from the internal dynamics of the larger eddies producing them. This seems reasonable in light of the mixing layer discussion given earlier, because smaller scale eddy generation depends on the stretching of the braids caused by the "winding up" in the larger eddies.

If, as before, we assume a steady-state condition so that the rate of energy transfer is independent of scale over the inertial range, i.e.

$$\varepsilon_n \sim E_n/t_n \sim \beta_n v_n^2/\ell_n \sim \bar{\varepsilon} \quad , \tag{III-30}$$

then, the following relationships are obtained

$$v_n \sim \bar{\varepsilon}^{1/3} \ell_n^{1/3} \ (\ell_n/\ell_o)^{-(3-D)/3} \quad , \tag{III-31}$$

$$t_n \sim \bar{\varepsilon}^{-1/3} \ell_n^{2/3} \ (\ell_n/\ell_o)^{(3-D)/3} \quad , \tag{III-32}$$

$$E_n \sim \bar{\varepsilon}^{2/3} \ell_n^{2/3} \ (\ell_n/\ell_o)^{(3-D)/3} \tag{III-33}$$

and

$$E(k) \sim \bar{\varepsilon}^{2/3} k^{-5/3} \ (k\ell_o)^{-(3-D)/3} \quad . \tag{III-34}$$

In the above expressions, D is defined by $N=2^D$. The scaling nature of the relationships becomes evident if we rewrite Equation (III-33)

$$E[(\ell_n/\ell_o)\ \ell_o] \sim \bar{\varepsilon}^{2/3} \ell_o^{2/3} \ (\ell_n/\ell_o)^{(\frac{5}{3} - \frac{D}{3})} \sim (\ell_n/\ell_o)^{(\frac{5}{3} - \frac{D}{3})} E_o \tag{III-35}$$

This is the Kolmogorov result, but with a correction of D/3 in the exponent to account for intermittency in the energy transfer to smaller scales. Finally, the relationship among N,β and D is:

$$\beta_n = (N/2^3)^n = (2^{D-3})^n \quad . \tag{III-36}$$

The above derivation demonstrates the scaling properties of important turbulent parameters. It also relates them to classical theory and some of the observed physical factors that lead to intermittency. In the process, the fractal dimension is introduced to describe the space-filling properties of the "surfaces" within which transfers of energy from larger to smaller scales take place.

It should be noted that there is a scale at which the viscous dissipation takes place, and it is different from that given by Kolmogorov. The outer scale where energy is introduced to the cascade remains the same, and defines $\bar{\varepsilon} \sim v_o^2/\ell_o$. At the other end, we can still define the scale at which the viscous dissipation takes place by equating turnover time, $t_n \sim \bar{\varepsilon}^{-1/3} \ell_n^{2/3} (\ell_n/\ell_o)^{(3-D)/3}$ to the viscous diffusion time, ℓ_n^2/ν. Solving gives

$$\ell_d \sim \ell_o \left(\frac{\nu}{\bar{\varepsilon}^{-1/3} \ell_o^{4/3}} \right)^{3/(1+D)} \tag{III-37}$$

Thus, when the intermittency effects are included, the dissipation scale ℓ_d will differ from the Kolmogorov microscale $(\nu^3/\bar{\varepsilon})^{1/4}$. They are equal only when D = 3, i.e for the space-filling case.

3. Numerical Simulation of Small Scale Structure

Most fluid simulations parameterize turbulent effects and so provide little evidence for any fractal structures related to turbulence. However, Chorin (1982) performed a very interesting numerical experiment that bears a close relationship to the formation of vortices in the braids between eddies that was discussed earlier. Chorin (1982) considered a straight vortex with a single perturbation, embedded in a 3-dimensionally periodic domain. The initial vortex ran from the center of the bottom of the box to the center of the top, with a jog like that showed schematically in Figure D-4. Thus, he began with a perturbation on a structure very much like the vortex filaments in the braids.

Chorin (1982) used a vortex element simulation technique, much like those described by Leonard (1985). The overall structure was simulated by a number of straight vortex tube segments. After the simulation

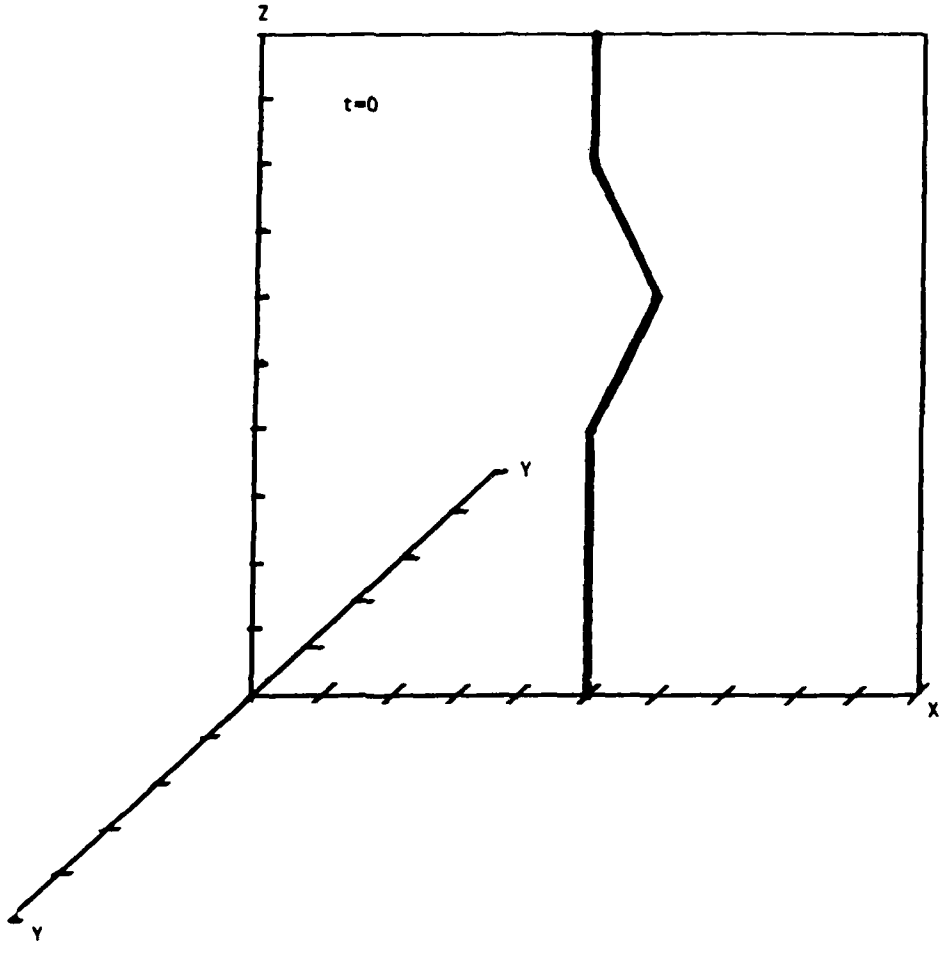

Source: Chorin (1982)

FIGURE D-4 INITIAL VORTEX USED IN CHORIN's SIMULATION

began, the vorticity stretched very rapidly and increased the number of segments that were required to approximate the distorted vortex tube. The rapid increase in the required number of vortex elements limited the time that the calculations could be continued. Figure D-5 shows the general configuration after 10, 20, 30, and 40 time steps, corresponding to elapsed times of 0.65, 0.88, 1.04, and 1.21, respectively. Presumably, though not stated, the units are seconds.

Figure D-5 shows that the general orientation of the pattern remains vertical while becoming very complex. Chorin (1982) evaluated the Hausdorff (fractal) dimension of the structure in Figure D-5 and found it to be on the order of 2.5. This is consistent with values suggested by Mandelbrot (1977) for the fractal dimension of turbulent structures.

4. The Navier-Stokes Equations

The three preceding sections show that there is a wide variety of evidence to suggest the general applicability of fractal concepts to the description of turbulence. Before proceeding to discuss some evidence gathered from atmospheric observations, it is worth noting that solution spaces for the Navier-Stokes equations are widely believed to be fractals as well. The focus of this review is not on that aspect of the problem, so it will not be reviewed in detail.

Lorenz (1963) devised a set of very simple differential equations whose trajectories in state space are contained in convoluted surfaces that seem to have many of the same characteristics that we have been describing. Furthermore, this system, which has come to be called the "Lorenz attractor" is closely related to fluid dynamic equations for convective motions in a heated fluid. Lorenz chose this system because it is simple to solve and related to more general fluid dynamic systems, such as those described by the Navier-Stokes equations.

It seems to be generally presumed that the more complicated systems (and nature itself) behave in a fashion which is at least qualitatively similar to Lorenz' (1963) simple system, which was later extended to a somewhat more realistic set of ordinary differential equations derived from the shallow-water equations with bottom topography (Lorenz, 1980). In that latter paper, Lorenz concludes with some remarks about the importance of attractors and strange attractors to fluid dynamics. Lorenz states,

> "The attractor set of a dynamical system is for practical purposes the set of points in phase space which will continue to be encountered by an arbitrary orbit after an arbitrarily long time has passed. For a large class of forced dissipative systems the attractor has zero volume, i.e., an arbitrarily selected point in phase space is almost always not on the attractor. When the general solution is aperiodic, the attractor is strange."

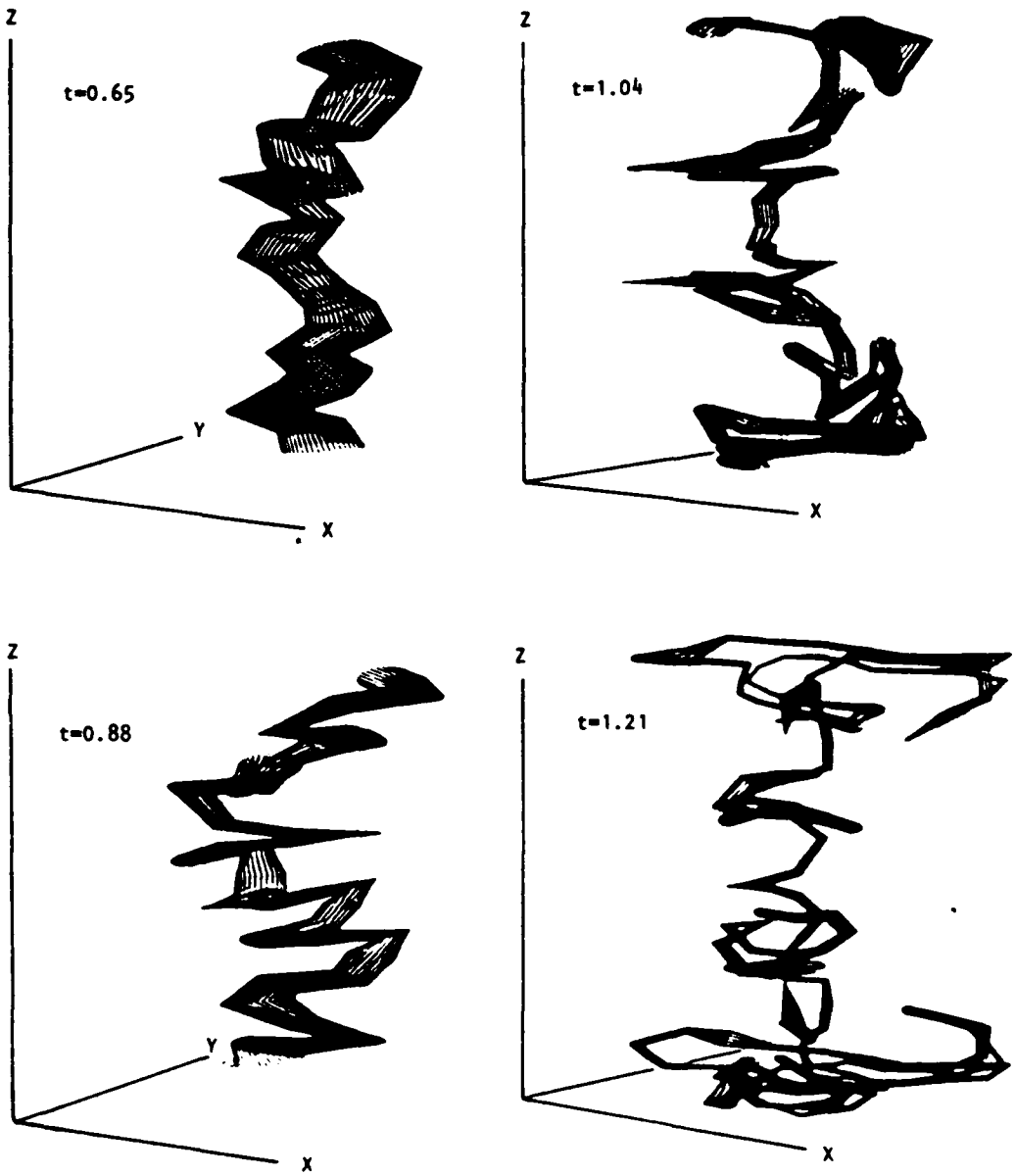

From Chorin, 1982

FIGURE D-5 VORTEX CONFIGURATIONS DURING CHORIN'S SIMULATION

Lorenz (1980) then goes on to discuss the degree to which the attractors of simpler equation sets approximate the strange attractors of a complete set. He speculates that the attractor of a global circulation model with 100,000 variables would be strange, but would have many fewer dimensions than the entire phase space, perhaps as few as several hundred dimensions.

The connection between fractals and strange attractors takes place in phase space. Mandelbrot (1983) contends "that for most purposes an attractor is strange when it is a fractal." According to Frisch (1980) one shortcoming of the strange attractor approaches is that they seem capable of describing only temporal chaos, but not the commonly observed chaotic spatial structure especially at small scales. He suggests that this shortcoming may arise from the phase limited spaces used in most studies, which represent the system on a coarse grid, or with limited spatial Fourier modes. It appears likely at this time that a focus on fractals in geometric space, rather the fractal nature of the strange attractors of fluid systems in phase space, will prove more fruitful for practical applications.

5. Observational Evidence

Procaccia (1984) gives a review of how fractal structures and turbulence might affect turbulent diffusion, fluctuations of passive scalars, electromagnetic wave propagation and the perimeters of clouds in the atmosphere. He examines two particle (relative) turbulent diffusion. He considers two particles (at $\vec{r}_1$ and $\vec{r}_2$) and the behavior of the separation distance $\vec{R} = \vec{r}_1 - \vec{r}_2$ produced by their relative velocity i.e. by $\vec{V}(t) = \vec{V}_1 - \vec{V}_2$:

$$\vec{R}(t) = \vec{R}(0) + \int_0^t \vec{V}(\tau)\, d\tau \qquad \text{(III-38)}$$

for isotropic turbulence $\langle \vec{V}(t) \rangle = 0$ so that the ensemble average separation (represented by angle brackets, $\langle \_ \rangle$) is constant and equal to the initial separation, but the variance, $\langle R^2 \rangle$ changes:

$$\frac{d}{dt} \langle R^2 \rangle = 2 \int_0^t \langle \vec{V}(t) \cdot \vec{V}(\tau) \rangle\, d\tau \qquad \text{(III-39)}$$

The above equation requires estimation of a time correlation function for velocity difference over a length scale R. Procaccia (1984) asserts that although the correlation $\langle \vec{V}(t) \cdot \vec{V}(\tau) \rangle$ is nonstationary, there is some function of scaled time variables g(x) such that

$$\langle \vec{V}(t) \cdot \vec{V}(\tau) \rangle = \langle \vec{V}(t) \cdot \vec{V}(t) \rangle\, g[(t-\tau)/t_R] \qquad \text{(III-40)}$$

where t_R is the typical decay time for velocity differences over a length scale R. Substituting in Equation (III-39) provides asymptotic predictions

$$\frac{d}{dt}\langle R^2\rangle \sim \begin{cases} \langle \vec{V}(t)\cdot\vec{V}(t)\rangle t & t \ll t_R \\ \langle \vec{V}(t)\cdot\vec{V}(t)\rangle t_R & t \gg t_R \end{cases} \qquad \text{(III-41)}$$

at extreme times. When R is in the inertial range, the diffusivity $d\langle R^2\rangle/dt$ can be determined from $\langle \vec{V}(t)\cdot\vec{V}(t)\rangle$, which is relatively easy to determine. For the "homogeneous fractal model" of turbulence described earlier,

$$\langle \vec{V}(t)\cdot\vec{V}(t)\rangle \sim \langle\varepsilon\rangle^{2/3} R^{2/3} (R/\ell_o)^{1-D/3} \qquad \text{(III-42)}$$

where ℓ_o is the outer scale of the turbulence and t_R is taken to be the ratio of the separation distance R to a typical velocity difference over that separation distance. Hentschel and Procaccia (1983) used the above assumption to derive the following expressions for $d\langle R^2\rangle/dt$

$$\frac{d}{dt}\langle R^2\rangle \sim \langle\varepsilon\rangle^{1/3} R^{4/3} (R/\ell)^{1/2-D/6} \qquad t \ll t_r \qquad \text{(III-43a)}$$

$$\frac{d}{dt}\langle R^2\rangle \sim \langle\varepsilon\rangle^{1/3} R^{4/3} (R/\ell_o)^{2-2D/3} \qquad t \gg t_r \qquad \text{(III-43b)}$$

Where R is the root-mean-square of the separation. For space filling turbulence, where D=3, the above expressions reduce to the classical "4/3 law".

Hentschel and Procaccia (1983a) examined data on 2-point diffusion published by Richardson (1926) and Gifford (1957). Their results from the Gifford data give an estimate for D between 2.5 and 2.75. The Richardson data give estimates that correspond to a value of D between 2.64 and 2.78. Hentschel and Procaccia (1983) concluded that these values were reasonable and supported the "fractally homogeneous turbulence" concept. It should be noted that they did not exhaust the available data and that further tests are possible. For example, Gifford (1977) identified 21 sources of relative diffusion data.

Procaccia (1984) also discusses Lovejoy's studies of the fractal properties of perimeters of clouds and rain areas. Lovejoy (1982) found that the perimeter P of a cloud is related to the cloud area, A, by

$$P \sim (A)^{\bar{D}/2} \qquad \text{(III-44)}$$

where $\bar{D}$ = 1.35 ±0.05. Procaccia argues that $\bar{D}$ is the fractal dimension of the perimeter, and that the fractal dimension of the cloud surface $D_c = 1+\bar{D}$, or 2.35 ±0.05, (in the isotropic case).

Lovejoy's (1982) results represented a range of six orders of magnitude in cloud area -- from about 1 kilometer to 1000 kilometers in length. Hentschel and Procaccia (1984), argue that the perimeter of the cloud is on a surface where some scalar is constant. Lovejoy (1982) defines the boundary according to its temperature. Procaccia (1984) considers a surface defining the outer boundary of the cloud, and how that surface is distorted by turbulent diffusion. He then relates the fractal dimension of the resulting surface to that associated with rate of change of separation variance, $d\langle R^2\rangle/dt$. Expressed in terms of the fractal dimension of the cloud perimeter, $\bar{D}$ the relationship is (from Procaccia, 1984:

$$\bar{D} = (11-D)/6 \quad . \qquad \text{(III-45)}$$

where D is the fractal dimension of the turbulence. Using the values for D, that Hentschel and Procaccia (1983) derived from Gifford's (1957) data gives a value of $\bar{D}$ of about 1.4 which is certainly in reasonable agreement with the value of $\bar{D}$ = 1.35 ±0.05.

From the standpoint of fluid flow modeling, one of the more interesting aspects of Hentschel and Procaccia's (1983, 1984; Procaccia, 1984) analysis is the link it provides between scalar distributions and the properties of the turbulent field. They made the connection via cloud perimeters, but there are other possibilities that deserve exploration. For example, the distribution of smokes, dyes or metal flakes in flow visualization experiments might be analyzed for fractal dimension and used to estimate turbulent properties. Ludwig (1986) has been attempting to estimate fractal dimension from lidar observations of backscatter in vertical cross sections through smoke plumes. No attempt has been made to determine turbulent properties, but that seems to be the logical next step.

D. Recent Developments in Atmospheric Applications

To this point, the discussion has centered on isotropic turbulence and its effects. However, horizontal scales of atmospheric motion extend to larger dimensions than do vertical scales, which suggests that any derivations that depend on isotropic turbulence should not be used throughout the atmosphere, at least without modification. Recent work by Lovejoy and Schertzer (1986) and Schertzer and Lovejoy (1985) has provided the basis for necessary modification. They note the following important facts regarding mesoscale processes:

(1) The energy spectrum is scaling (i.e. it is of the form $k^{-\beta_h}$ where k is wave number and β_h is the appropriate value for wave numbers in the horizontal plane, $\beta_h \sim 5/3$).

(2) The energy spectrum for wave numbers in the vertical plane is also scaling, but anisotropy makes the relevant exponent, β_v, quite different; $\beta_h \sim 11/5$.

(3) There is extreme variability, because active regions that account for most of the energy and moisture flux are very sparsely distributed.

Lovejoy and Schertzer (1986) present most of the concepts related to isotropic turbulence that have already been discussed and then extend those concepts to the anisotropic case. They make the extension by continuing to assume that there is a constant energy flux over the range of scales of interest, and that there are rules for describing how the statistical properties of eddies are transformed from one scale to another. In dealing with anisotropic eddies, their shape must be characterized along with their dimensions. Schertzer and Lovejoy choose to represent the anisotropic cascade in a manner very similar to that discussed earlier for the isotropic case, except that horizontal and vertical scaling are considered separately, i.e.

$$\Pr[\Delta c(\lambda \Delta x) > q] = \Pr[\lambda^{H_h} \Delta c(\Delta x) > q] \qquad \text{(III-45a)}$$

$$\Pr[\Delta c(\lambda \Delta y) > q] = \Pr[\lambda^{H_h} \Delta c(\Delta y) > q] \qquad \text{(III-45b)}$$

$$\Pr[\Delta c(\lambda \Delta z) > q] = \Pr[\lambda^{H_v} \Delta c(\Delta z) > q] \qquad \text{(III-45c)}$$

Equations (III-45) can be written in matrix form:

$$\Pr[\Delta c(\underline{T}\Delta\vec{r}) > \vec{q}] = \Pr[\lambda^{H_h} \Delta c(\Delta\vec{r}) > \vec{q}] \quad , \qquad \text{(III-46)}$$

The matrix $\underline{T}$ is given by:

$$\underline{T} = \begin{bmatrix} \lambda & 0 & 0 \\ 0 & \lambda & 0 \\ 0 & 0 & \lambda^{H_z} \end{bmatrix} \quad , \qquad \text{(III-47)}$$

where

$$H_z = H_v / H_h \quad , \qquad \text{(III-48)}$$

and

$$\Delta\vec{r} = \begin{bmatrix} \Delta x \\ \Delta y \\ \Delta z \end{bmatrix} \quad . \tag{III-49}$$

The matrix $\underline{T}$ produces a magnification overall, with stretching in the z direction; it transforms the probability distributions and introduces an elliptical geometry to account for the different horizontal and vertical scalings. Figure D-6 shows the how the magnification and stretching relates the small, vertically oriented eddies to the a large, horizontally oriented eddy. The transformation changes the volume of the eddy by a factor $\lambda^2 \lambda^{H_z} = \lambda^{D_{el}}$, where the "elliptical dimension" $D_{el} = 2 + H_z$. In an isotropic atmosphere, $H_z = 1$, and therefore the elliptical dimension equals 3. For 2-dimensionally isotropic turbulence $H_z = 0$ and $D_{el} = 2$. By analogy with the purely homogeneous case, Schertzer and Lovejoy (1985) regard D_{el} as a fractal dimension for the anisotropic space. Schertzer and Lovejoy (1985) show that the number of eddies of horizontal scale ℓ is proportional to $\ell^{D_{el}}$.

The reason for introducing the modification described above is apparent in Figure D-6; it provides a smooth transition from the very large, horizontally oriented, "Hadley-like" cells down to the vertically oriented convective cells. There is some scale where the eddies are--at least in the statistical sense--spherical. Lovejoy and Schertzer (1985) refer to this as the "sphero-scale." They contend that it is quite variable because it depends on both the average turbulent energy flux $\bar{\varepsilon}$ and the average flux of buoyant force variance.

The dependence on buoyant force flux variance arises, according to Schertzer and Lovejoy (1985) because the vertical structure is governed by that factor, analogous to the flux of kinetic energy $\bar{\varepsilon}$. The flux of the buoyant force variance D is given by

$$\phi(\Delta z) = \tau^{-1}(\Delta z)\, \Delta f^2\, (\Delta z) \tag{III-50}$$

where $\tau(\Delta z)$ is a characteristic time for the transfer process, and f is the buoyant force per unit mass. It follows from dimensional analysis that:

$$Pr[\Delta v(\Delta z) > q] = Pr\{[\bar{\phi}(\Delta z)]^{1/5}\, \Delta z^{3/5} > q\} \tag{III-51}$$

According to Schertzer and Lovejoy (1985), the above scaling holds in the vertical, while the Kolmogorov scaling governs the horizontal, i.e.

$$Pr[\Delta v(\Delta x) > q] = Pr\{[\bar{\varepsilon}(\Delta x)]^{1/3}\, \Delta x^{1/3} > q\} \tag{III-52}$$

The probability distributions for the two Δv's can be equated (after cubing) to give

$$Pr(\bar{\varepsilon}\Delta x > q) = Pr(\bar{\phi}^{3/5}\, \Delta z^{9/5} > q) \tag{III-53}$$

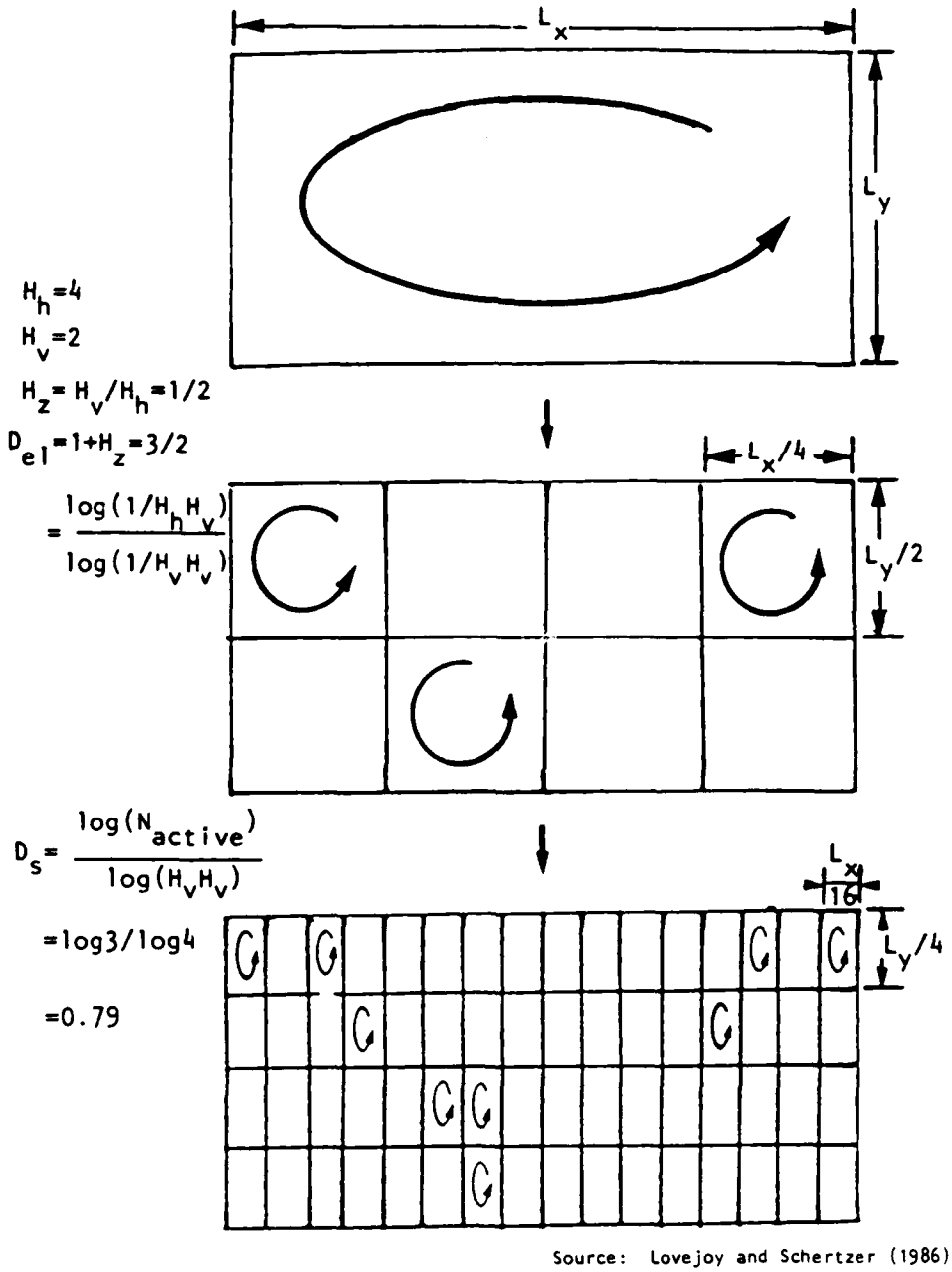

Source: Lovejoy and Schertzer (1986)

FIGURE D-6 SCHEMATIC DIAGRAM ILLUSTRATING LOVEJOY AND SCHERTZER'S CONCEPT OF THE CASCADE FROM LARGE TO SMALL SCALES

to provide an algebraic relationship between the buoyant force variance and eddy kinetic energy fluxes. For the case with hyperbolic upper tails of the probability distributions, and exponents α_ε and α_ϕ for the turbulent energy and buoyant force variance fluxes respectively, Schertzer and Lovejoy (1985) show that $\alpha_\varepsilon \sim 5\alpha_\phi/3$.

One of the more important consequences of Schertzer and Lovejoy's (1985) analysis is that it provides a bridge between the large and small scales of motion. It does not require a distinction between large scale motions which are essentially 2-dimensional, and small motions which are more 3-dimensional. They contend that there is no evidence (although it has been sought) for any transition from 2-dimensional to 3-dimensional regimes. It should be noted that their hypothesis is not necessarily relevant only to the atmosphere, but may also be relevant to other fluid systems where there are vastly different horizontal and vertical scales, and where vertical motions are largely the product of buoyancy effects.

IV APPLICATION TO CLOSURE SCHEMES AND FLOW MODELING

It is beyond the scope of this review to develop a turbulent closure scheme for flow modeling based on fractal concepts. The literature does contain some tantalizing results that appear to have the potential to solve some of closure problems. However, the whole history of turbulence modeling is characterized by promising approaches that have just one essential item beyond grasp. In essence, the problem is to determine local covariances between important hydrodynamic variables (e.g. velocity components, temperature, pressure, diffusing scalar concentrations and so forth) for volumes that are representative the model's grid dimensions. Determination of these covariances must not require information that is not generated by the model for the larger scales (i.e. it must use data available at the grid points).

The first thing that is apparent from a review of the fractal literature is that it should be possible to generate scalar and vector fields that have realistic statistical properties. However, this does not by itself solve the closure problem. Two more major requirements remain:

(1) it must be possible to infer the fractal characteristics of those smaller scale distributions from the information at model grid points.

(2) The determination of covariances between different quantities (especially anisotropic covariance) requires both that the statistics of the variable distributions in space be realistic, and that their mutual distributions be correctly related.

Is there anything in the literature that suggests that the above problems can be resolved? Until the last two or three years, the answer would have been no. However, the contention by Schertzer and Lovejoy (1985) that there is a continuous cascade from the synoptic atmospheric scales down to the viscous scale, and that the statistical properties of that cascade can be described using the concept of elliptical fractal dimension suggests that it should be possible effect a transition from the grid scale to smaller scales. Furthermore, the relationships among elliptical fractal dimension, turbulent energy flux and the flux of buoyant force variance involve major hydrodynamic variables, which gives hope that any subgrid scale fields that might be generated would have the appropriate interrelationships among velocity, temperature, pressure, and so forth.

The work of Hentschel and Procaccia (1983) attempts to relate the fractal properties of diffusing scalars to the fractal dimension of the turbulence. That work might also provide the link necessary to obtain the covariances. Certainly, it has the potential to help in the design of useful experimental studies, because it should considerably easier to measure small scale distributions of a scalar in space than to measure the distributions of velocity fluctuations.

The intermittency of turbulence means that on all scales there are "active" and "inactive" regions. It seems reasonable to presume that subgrid scale effects in regions that are active on scales resolved by the model will be different from those in areas which are inactive. We might also expect that the processes occuring in active regions will smooth out fluctuations, so that those regions become less active. The smaller velocity fluctuations characteristic of the inactive regions may allow the development of gradients that will in turn lead to greater fluctuations and cause the region to eventually become "active." Regardless of whether or not this conjecture is true, it is clear that any model should be able to deal with time variations of intermittency in the turbulent fields.

Two major components will be required for any closure scheme derived from fractal concepts. They are:

(1) A method for deriving fractal characteristics and identifying "active" areas from information at the model gridpoints.

(2) A method for determining the necessary covariance terms from the fractal characteristics, either analytically or through parameterization of numerical "experiments" using artificially generated fields based on specified fractal characteristics.

There are major unsolved problems associated with both the above components. Determining fractal characteristics requires calculations of spatial correlations over a wide range of scales. Furthermore, anisotropy requires that the correlations in the vertical and horizontal

planes be determined separately. The limited number of gridpoints available in most modeling may make this unreliable or impossible. This may not be as severe a problem as it first appears, because the literature provides, through theory or observation, estimated values for many of the scaling exponents and probability distribution parameters. It is encouraging to note that the parameters of interest in turbulence modeling such as turbulent kinetic energy, buoyant flux variance, velocity fluctuations, and so forth have generally been the focus of the studies reviewed here. Thus, the most severe problems may be limited to the determination of the degree of turbulent activity in an area which could be a much simpler task.

One final problem remains. Most of the derivations and analyses do not consider boundaries like the earth's surface or the basin and air-water interfaces of water bodies. This may limit the usefulness of much published information, at least in the vicinity of the boundaries.

V CONCLUDING REMARKS

It is clear that a great deal of effort will be required to exploit whatever potential there is for application of fractal concepts to the modeling of turbulence. Other fractal applications are much easier and have in fact been accomplished. Visual simulation of cloud and smoke plume appearance has been done (e.g. Medler et al, 1986; Lovejoy and Schertzer, 1986). It is a fairly easy step from there to the determination of concentration probability distributions, effects on optical transmission and so forth. Of course, it requires that the fractal characteristics of the temperature field, the diffusing smoke cloud or whatever scalar is of interest be known, but this should be experimentally determinable. In the case of atmospheric cloud formations and precipitation areas the fractal properties have been determined. The information is already at hand for solving many practical problems such as those related to scintillation and other optical transmission effects, and those related to variations in the visibility through fog.

The fact that Schertzer and Lovejoy (1986) have made connections between buoyant flux variance and turbulent kinetic energy lends credence to the notion that one can use fractal concepts to model correlation functions as well as variance of a single variable. It is of course the correlation functions which are the key to the modeling of turbulent effects in fluid flow.

Even the problem of boundaries may be tractable. According to Mandelbrot (1983) natural surfaces assume fractal shapes. It, therefore, seems plausible that air motions above such a surface would assume fractal properties. There remains of course the problem of transition

between those motions where the surface plays an important role and those aloft were the variations are introduced by turbulent kinetic energy cascades and buoyancy forces. Even if fractal concepts could only provide turbulence models in the free fluid, away from boundaries, that would be a major contribution.

BIBLIOGRAPHY*

Adrian, R. J., 1979: "Conditional Eddies in Isotropic Turbulence," Phys. Fluids, 22, 2065-2070.

Aizawa, J., C. Murakami, and T. Kohyama, 1984: "Statistical Mechanics of Intermittent Chaos," Prog. of Theor. Phys. Suppl., 79, 96-124.

Anselmet, F., Y. Gagne, E. J. Hopfinger, and R. A. Antonia, 1984: "High-Order Velocity Structure Functions in Turbulent Shear Flows," J. Fluid Mech., 140, 63-89.

Antonia, R. A., B. R. Satyaprakash, and A. J. Chambers, 1982: "Reynolds Number Dependence of Velocity Structure Functions in Turbulent Shear Flows," Phys. Fluids, 25, 29-37.

Antonia, R. A., B. R. Satyaprakash, and A. K. M. F. Hussain, 1982: "Statistics of Fine-Scale Velocity in Turbulent Plane and Circular Jets," J. Fluid Mech., 119, 55-89.

Basdevant, C., B. Legras, R. Sadourny, and M. Beland, 1981: "A Study of Barotropic Model Flows: Intermittency, Waves and Predictability," J. Atmos. Sci., 38, 2305-2326.

Benzi, R., G. Paladin, G. Parisi, and A. Vulpiani, 1984: "On The Multifractal Nature of Fully Developed Turbulence and Chaotic Systems," J. Phys. A: Math. Gen., 17, 3521-3531.

Benzi, R. and A. Vulpiani, 1980: "Small-Scale Intermittency of Turbulent Flows," J. Phys. A: Math. Gen., 13, 3319-3324.

Bernard, P. S., 1983: "Kinematics of Velocity and Vorticity Correlations in Turbulent Flow," Phys. Fluids, 26, 2080-2087.

Bradshaw, P., 1978: "Introduction (to Physical Processes that Govern Turbulence)," Chapter 1, Topics in Appl. Phys., 12, 1-44.

Cederwall, R. T., 1983: "Review of Algebraic Stress Models for Simulating Atmospheric Turbulence in a Three-Dimensional Sea-Breeze Model," Final Report, Stanford University Civil Eng. 399, 20 pp.

Champagne, F. H., 1978: "The Fine-Scale Structure of the Turbulent Velocity Field," J. Fluid Mech., 86, 67-108.

*Not all the references in this bibliography were cited in the review.

Chatwin, P. C., 1982: "The Use of Statistics in Describing and Predicting the Effects of Dispersing Gas Clouds," J. Hazard. Mat., 6, 213-230.

Chatwin, E. C. and P. J. Sullivan, 1979: "The Relative Diffusion of a Cloud of Passive Contaminant in Incompressible Turbulent Flow," J. Fluid Mech., 91, 337-355.

Chatwin, P. C. and P. J. Sullivan, 1979: "Measurements of Concentration Fluctuations in Relative Turbulent Diffusion," J. Fluid Mech., 94, 83-101.

Chatwin, P. C. and P. J. Sullivan, 1979: "An Interpretation of Some Turbulent Diffusion Measurements," Proc. 7th Canadian Congress of Appl. Mech., 657-658.

Chatwin, P. C. and P. J. Sullivan, 1979: "The Basic Structure of Clouds of Diffusing Contaminant," Mathematical Modeling of Turbulent Diffusion in the Environment, Academic Press, London, 3-32.

Chatwin, P. C. and P.J. Sullivan, 1979: "The Core-Bulk Structure Associated with Diffusing Clouds," Turbulent Shear Flows 2, Springer Verlag, Berlin, 379-389.

Chatwin, P. C. and P. J. Sullivan, 1980: "Some Turbulent Diffusion Invariants," J. Fluid Mech., 97, 405-416.

Chorin, A. J., 1973: "Numerical Study of Slightly Viscous Flow," J. Fluid Mech., 57, 785-796.

Chorin, A. J., 1982: "The Evolution of a Turbulent Vortex," Commun. Math. Phys., 83, 517-535.

Constantin, P., C. Foias, and O. P. Manley, 1985: "Determining Modes and Fractal Dimension of Turbulent Flows," J. Fluid Mech., 150, 427-440.

Csanady, G. T., 1967: "Concentration Fluctuations in Turbulent Diffusion," J. Atmos. Sci., 24, 21-28.

Domaradzki, J. A. and G. L. Mellor, 1984: "A Simple Turbulence Closure Hypothesis for the Triple-Velocity Correlation Functions in Homogeneous Isotropic Turbulence," J. Fluid Mech., 140, 45-61.

Eckmann, J. P., 1981: "Roads to Turbulence in Dissipative Dynamical Systems," Rev. Modern Phys., 53, 643-654.

Endlich, R. M., R. C. Singleton, and J. W. Kaufman, 1969: "Spectral Analysis of Detailed Vertical Wind Speed Profiles," J. Atmos. Sci., 26, 1030-1041.

Fackrell, J. E. and A. G. Robins, 1981: "The Effects of Source Size on Concentration Fluctuations in Plumes," Bound. Lay. Meteorol., 22, 335-350.

Fraedrich, K., 1986: "Estimating the Dimensions of Weather and Climate Attractors," J. Atmos. Sci., 43, 419-432.

Frisch, U, 1980: "Fully Developed Turbulence and Intermittency," NY Acad. Sci. Ann., 357, 359-367.

Frisch, U., P.-L. Sulem, and M. Nelkin, 1978: "A Simple Dynamical Model of Intermittent Fully Developed Turbulence," J. Fluid Mech., 87, 719-736.

Froehling, H., J. P. Crutchfield, D. Farmer, N. H. Packard, and R. Shaw, 1981: "On Determining the Dimension of Chaotic Flows," Physica, 3D, 605-617.

Gardner, M. 1978: "White and Brown Music, Fractal Curves and One-Over-f Fluctuations," Sci. Amer., 238(4), 16-32.

Gent, P. R. and J. C. McWilliams, 1982: "Intermediate Model Solutions to the Lorenz Equations: Strange Attractors and Other Phenomena," J. Atmos. Sci., 39, 3-13.

Gifford, F., Jr., 1957: "Relative Atmospheric Diffusion of Smoke Puffs," J. Meteorol., 14, 410- 414.

Gifford, F., Jr., 1977: "Tropospheric Relative Diffusion Observations," J. Appl. Meteorol., 16, 311-313.

Giglio, M., S. Musazzi, and U. Perini, 1984: "Low-Dimensionality Turbulent Convection," Phys. Rev. Let., 53, 2402-2404.

Grassberger, P. and I. Procaccia, 1983: "Characterization of Strange Attractors," Phys. Rev. Let., 50, 346-349.

Greenside, H. S., A. Wolf, J. Swift, and T. Pignataro, 1982: "Impracticality of a Box-Counting Algorithm for Calculating the Dimensionality of Strange Attractors," Phys, Rev. A, 25, 3453-3456.

Grossmann, S. and S. Thomae, 1982: "Correlation Decay of Lagrangian Velocity Differences in Locally Isotropic Turbulence," Z. Phys. B - Condensed Matter, 49, 253-261.

Hanna, S. R., 1984: "The Exponential Probability Density Function and Concentration Fluctuations in Smoke Plumes," Bound. Lay. Meteorol., 29, 361-375.

Hentschel, H. G. E. and I. Procaccia, 1982: "Intermittency Exponent in Fractally Homogeneous Turbulence," Phys. Rev. Let., 49, 1158-1161.

Hentschel, H. G. E. and I. Procaccia, 1983a: "Fractal Nature of Turbulence as Manifested in Turbulent Diffusion," Phys. Rev. A, 27, 1266-1269.

Hentschel, H. G. E. and I. Procaccia, 1983b: "Passive Scalar Fluctuations in Intermittent Turbulence with Applications to Wave Propagation," Phys. Rev. A, 28, 417-426.

Hentschel, H. G. E. and I. Procaccia, 1984: "Relative Diffusion in Turbulent Media: The Fractal Dimension of Clouds," Phys. Rev. A, 29, 1461-1470.

Hofstadter, D. R., 1981: "Strange Attractors: Mathematical Patterns Delicately Poised Between Order and Chaos," Sci. Amer., 245(5), 22-43.

Kida, S., 1982: "Statistics of Active Regions in the β-Model of Turbulence," Prog. Theor. Phys., 67, 1630-1632.

Kowe, R. and P. C. Chatwin, 1983: "On Modelling the Probability Density Function of Concentration in Turbulent Shear Flows," Proc. 8th Australasian Fluid Mech. Conf., Univ. of Newcastle, N.S.W., 3A.5-3A.8.

Kraichnan, R. H., 1974: "On Kolmogorov's Inertial-Range Theories," J. Fluid Mech., 62, 305-330.

Kraichnan, R. H., 1985: "Intermittency and Attractor Size in Isotropic Turbulence," Phys. Fluids, 28, 10-11.

Kunkel, K. E., E. W. Eloranta, and J. A. Weinman, 1980: "Remote Determination of Winds, Turbulence Spectra and Energy Dissipation Rates in the Boundary Layer from Lidar Measurements," J. Atmos. Sci., 37, 978-985.

Lamb, R. G., 1981: "A Scheme for Simulating Particle Pair Motions in Turbulent Fluid," J. Comput. Phys., 39, 329-346.

Lanford, O. E., III., 1982: "The Strange Attractor Theory of Turbulence," Ann. Rev. Fluid Mech., 14, 347-364.

Leonard, A., 1985: "Computing Three-Dimensional Incompressible Flows with Vortex Elements," Ann. Rev. Fluid Mech., 17, 523-559.

Levich, E. and A. Tsinober, 1983: "Helical Structures, Fractal Dimensions and Renormalization-Group Approach in Homogeneous Turbulence," Phys. Let., 96A, 292-298.

Lilly, D. K., 1984: "Some Facets of the Predictability Problem for Atmospheric Mesoscales," Amer. Inst. Phys. Conf. Proc. 106, 287-294.

Long, R. R., 1982: "A New Theory of the Energy Spectrum," Bound. Lay. Meteorol., 24, 137-160.

Lorenz, E. N., 1963: "Deterministic Nonperiodic Flow," J. Atmos. Sci., 20, 130-141.

Lorenz, E. N., 1980: "Attractor Sets and Quasi-Geostrophic Equilibrium," J. Atmos. Sci., 37, 1685-1699.

Lovejoy, S., 1982: "The Area-Perimeter Relationship for Rain and Cloud Areas," Science, 216, 185-187.

Lovejoy, S. and B. B. Mandelbrot, 1985: "Fractal Properties of Rain, and A Fractal Model," Tellus, 37A, 209-232.

Lovejoy, S. and D. Schertzer, 1983: "Buoyancy, Shear, Scaling and Fractals," Preprints 6th Symposium on Turbulence and Diffusion, Boston, MA, 102-105.

Lovejoy, S. and D. Schertzer, 1985: "Generalized Scale Invariance in the Atmosphere and Fractal Models of Rain," Water Resour. Res., 21, 1233-1250.

Lovejoy S. and D. Schertzer, 1986: "Scale Invariance, Symmetries, Fractals, and Stochastic Simulations of Atmospheric Phenomena," Bull. Amer. Meteorol. Soc., 67, 21-32.

Lovejoy, S., D. Schertzer, and P. Ladoy, 1986: "Fractal Characterization of inhomogeneous Geophysical Measuring Networks," Nature, 319, 43-44.

Ludwig, F. L., 1986: "Flow Simulation Using Vortex Methods," Report for Stanford University (Prof. J. Spreiter), 31 pp.

Ludwig, F. L. and K. C. Nitz, 1986: "Analysis of Lidar Cross-Sections to Determine Spatial Structure of Material in Smoke Plumes," to appear in Proc. Smoke/Obscurants Symposium X, Harry Diamond Labs., Adelphi, MD, 10 pp.

Ludwig, F. L. and K. C. Nitz, and A. Valdes, 1984: "Techniques for Studying the Spatial Distribution of Clear Patches in Smoke Plumes," Proc. Smoke/Obscurants Symposium VIII, Harry Diamond Labs., Adelphi, MD, 231-241.

Ludwig, F. L. , K. C. Nitz, and A. Valdes, 1984: "Spatial Fluctuations of Concentration in Smoke Plume Cross-Sections,"Preprints 4th Joint Conf. on Appl. of Air Pol. Meteorol. and 3rd Conf. on Mountain Meteorol., Portland, OR, 51-54.

Lundgren, T. S., 1982: "Strained Spiral Vortex Model for Turbulent Fine Structure," Phys. Fluids, 25, 2193-2203.

Mandelbrot, B. B., 1974: "Intermittent Turbulence in Self-Similar Cascades: Divergence of High Moments and Dimension of the Carrier," J. Fluid Mech., 62, 331-358.

Mandelbrot, B. B., 1975: "On the Geometry of Homogeneous Turbulence, with Stress on the Fractal Dimension of the Iso-Surfaces of Scalars," J. Fluid Mech., 72, 401-416.

Mandelbrot, B. B., 1977: "Fractals and Turbulence: Attractors and Dispersion," Lecture Notes in Mathematics, Turbulence Seminars, (ed. P. Bernard and T. Ratiu) Springer-Verlag, Berlin, 83-93.

Mandelbrot, B. B., 1977: "Intermittent Turbulence and Fractal Dimension: Kurtosis and The Spectral Exponent 5/3+β," Lecture Notes in Mathematics, Turbulence and Navier-Stokes Equations, (ed. R. Temam) Springer-Verlag, Berlin, 121-145.

Mandelbrot, B. B., 1983: The Fractal Geometry of Nature, W. H. Freeman and Co., NY, 468 pp.

May, R. M., 1976: "Simple Mathematical Models with Very Complicated Dynamics," Nature, 261,459-467.

Medler, C. L., L. M. Gelberg, and R. P. Burkhart, 1986: "Graphical Realization of Turbulent Smoke Plumes on the Pixar," to appear in Proc. Smoke/Obscurants Symposium X, Harry Diamond Labs., Adelphi, MD, 13 pp.

Moffatt, H. K., 1981: "Some Developments in the Theory of Turbulence," J. Fluid Mech., 106, 27-47.

Mori, H., 1980: "Anomalous Diffusion of Vorticity in Fully-Developed Turbulence," Suppl. Prog. Theor. Phys., 69, 111-121.

Mori, H., 1980: "Fractal Dimensions of Chaotic Flows of Autonomous Dissipative Systems," Prog. Theor. Phys., 63, 1044-1047.

Nakano, T. and M. Nelkin, 1985: "Crossover Model for The Scaling Exponents of Intermittent Fully Developed Turbulence," Phys. Rev. A, 31, 1980-1982.

Narayanan, M. A. B., S. Rajagopalan, and R. Narasimha, 1977: "Experiments on the Fine Structure of Turbulence," J. Fluid Mech., 80, 237-257.

Ott, E., 1981: "Strange Attractors and Chaotic Motions of Dynamical Systems," Rev. Mod. Phys., 53, 655-671.

Packard, N. H., J. P. Crutchfield, J. D. Farmer, and P. S. Shaw, 1980: "Geometry from a Time Series," Phys. Rev. Let., 45, 712-716.

Pentland, A. P., 1984: "Fractal-Based Description of Natural Scenes," IEEE Trans. Pat. Anal. Mach. Intel., PAMI-6, 661-674.

Phythian, R. and W. D. Curtis, 1978: "The Effective Long-Time Diffusivity for a Passive Scalar in a Gaussian Model Fluid Flow," J. Fluid Mech., 89, 241-250.

Procaccia, I., 1984: "Fractal Structures in Turbulence," J. Stat. Phys., 36, 649-663.

Raupach, M. R., 1983: "Near-Field Dispersion from Instantaneous Sources in the Surface Layer," Bound. Lay. Meteorol., 27, 105-113.

Reynolds, W. C., 1985: "Class Notes for Mechanical Engineering 261B--Turbulence Modeling," Stanford University, Stanford, California.

Richardson, L. F., 1926: "Atmospheric Diffusion Shown as a Distance-Neighbor Graph," Proc. Roy. Soc. London, Series A, 110, 709-737.*

Rollefson, J. P., 1978: "On Kolmogoroff's Theory of Turbulence and Intermittency," Canadian J. Phys., 56, 1426-1441.

Rose, H. A. and P. L. Sulem, 1978: "Fully Developed Turbulence and Statistical Mechanics," Le Journal de Physique, 39, 441-484.

Rosen, G., 1981: "Grid-Generated Isotropic Homogeneous Turbulence at High Reynolds Numbers," Lettere al Nuovo Cimento, 31, 509-512.

Ruelle, D., 1982: "Large Volume Limit of the Distribution of Characteristic Exponents in Turbulence," Commun. Math Phys., 87, 287-302.

Ruelle, D., 1984: "Conceptual Problems of Weak and Strong Turbulence," Physics Reports, 103, 81-85.

Sawford, B. L., 1983: "The Effect of Gaussian Particle-Pair Distribution Functions in the Statistical Theory of Concentration Fluctuations in Homogeneous Turbulence," Quart. J. Roy. Meteorol. Soc., 109, 339-354.

*Cited indirectly.

Scheffer, V. and M. J. Leray, 1976: "Geometrie Fractale de la Turbulence: Equations de Navier-Stokes et Dimension de Hausdorff," C. R. Acad. Sc. Paris, 282, A121-A122.

Schertzer, D. and S. Lovejoy, 1983: "The Dimension and Intermittency of Atmospheric Dynamics," Turbulent Shear Flows 4, Springer Verlag, Berlin, 7-33.

Siggia, E. D., 1978: "Model of Intermittency in Three-Dimensional Turbulence," Phy. Rev. A, 17, 1166-1176.

Siggia, E. D., 1981: "Numerical Study of Small-Scale Intermittency in Three-Dimensional Turbulence," J. Fluid Mech., 107, 375-406.

Sreenivasan, K. R., 1985: "On the Fine-Scale Intermittency of Turbulence," J. Fluid Mech., 151, 81-103.

Storebo, P. B., 1983: "Concentration Pattern During Turbulent Dispersion," Bound. Lay. Meteorol., 27, 359-370.

Takens, F., 1981: Proceedings of the Symposium on Dynamical Systems and Turbulence, (ed. D. A. Rand and L. A. Young), Springer, Berlin.

Van Dyke, M., 1982: An Album of Fluid Motion, Parabolic Press, Stanford, California, 176 pp.

Voss, R. F., 1982: "Fourier Synthesis of Gaussian Fractals: 1/f noises, landscapes, and flakes," unpublished paper from IBM Thomas J. Watson Research Center, Yorktown Heights, NY, 20 pp.

Wyngaard, J. C., 1975: "Progress in Research on Boundary Layers and Atmospheric Turbulences," Rev. Geophys. and Space Phy., 13, 716-720.

END

2-87

DTIC